Title
Holographic Entanglement Entropy in the Presence of Defects

Author
Marasinou, Chrysostomos

Publication Date
2018

Peer reviewed|Thesis/dissertation

UNIVERSITY OF CALIFORNIA

Los Angeles

Holographic Entanglement Entropy in the Presence of Defects

A dissertation submitted in partial satisfaction

of the requirements for the degree

Doctor of Philosophy in Physics

by

Chrysostomos Marasinou

2018

ABSTRACT OF THE DISSERTATION

Holographic Entanglement Entropy in the Presence of Defects

by

Chrysostomos Marasinou

Doctor of Philosophy in Physics

University of California, Los Angeles, 2018

Professor Michael Gutperle, Chair

A quantum observable which received renewed attention recently is entanglement entropy. It's application ranges over several fields in physics, from condensed matter physics to general relativity. In this dissertation we study entanglement entropy for quantum field theories in the presence of defects and singularities.

We study entanglement entropy using the framework of AdS/CFT correspondence. We focus on entangling surfaces across ball-shaped regions for systems outside their ground state. Quantum field theories in the presence of defects are considered first. These are the six-dimensional $(2, 0)$ theory in the presence of Wilson surfaces and the four-dimensional $\mathcal{N} = 4$ super-Yang-Mills theory in the presence of surface defects of the disordered type. Their holographic entanglement entropy is calculated applying the Ryu-Takayanagi prescripstion on their holographic duals, which are eleven-dimensional supergravity (M-theory) solutions for the former and ten-dimensional type IIB supergravity solutions for the latter. Other holographic observables are computed as well: the holographic stress tensor and the expectation value of the defect (operator). For the disordered defects, an alternative expression for the additional entanglement entropy due to the defect (in terms of expectation values) is derived, adapting the method of Lewkowycz and Maldacena for Wilson loops. The two entanglement entropies agree up to an additional term, the origin of which may be

attributed to the conformal anomaly of even dimensional defects as we discuss.

The holographic entanglement and free energy is computed for five-dimensional super conformal field theories, starting from their holographic supergravity duals. Although the supergravity solutions possess singularities, these do not obstruct our calculations. The expected relation between the two observables is verified. This supports the supergravity solutions as holographic duals and gives the first quantitative results for five-dimensional superconformal field theories.

The dissertation of Chrysostomos Marasinou is approved.

Chandrashekhar Khare

Eric D'Hoker

Per J. Kraus

Michael Gutperle, Committee Chair

University of California, Los Angeles

2018

Στην οικογένεια μου

Contents

List of Figures

Acknowledgements

Firstly, I would like to thank my advisor Michael Gutperle for his strong and continuous support, during my time at UCLA. He has been the greatest teacher and mentor I ever had, providing me with invaluable lessons on the research in physics and motivation to keep going through difficult times.

I would also like to thank Simon Gentle, Andrea Trivella and Christoph Uhlemann, who I worked in collaboration with here at UCLA. Without them my time here would have not been so fruitful and exciting.

I am very grateful for the excellent professors in my department. Especially, I want to thank Eric D'Hoker and Per Kraus for their amazing and very influential teaching which motivated me in pursuing this degree.

Next, I want to express my gratitude to the many people who have contributed to the research presented in this dissertation. This includes Xi Dong, Matthew Headrick, Bruno Le Floch, Edgar Shaghoulian, Oren Bergman and Diego Rodriguez-Gomez.

I could not forget to thank my friends and especially the friends I made here in Los Angeles, who are always there for me. Their love and devotion made my life balanced, made me a better person and helped me through the most difficult times.

Last but not least I would like to thank my family; My parents and sisters and brother. Without their love and support, this journey would have been impossible.

Contribution of authors

Chapters 2 and 3 are based on [2, 3] in collaboration with Michael Gutperle and Simon Gentle. Chapter 4 is based on [4] in collaboration with Michael Gutperle, Andrea Trivella and Christoph F. Uhlemann.

Vita

2012	B.A. (Physics), University of Cyprus
2012 – 2018	Teaching Assistant, Department of Physics and Astronomy, UCLA
2016, 2017	GSR, Department of Physics and Astronomy, UCLA

Publications

"Entanglement entropy of Wilson surfaces from bubbling geometries in M-theory,"
S. A. Gentle, M. Gutperle, and C. Marasinou, JHEP 08 (2015) 019
arXiv:1506.00052 [hep-th]

"Holographic entanglement entropy of surface defects,"
S. A. Gentle, M. Gutperle, and C. Marasinou, JHEP 04 (2016) 067
arXiv:1512.04953 [hep-th]

"Entanglement entropy vs. free energy in IIB supergravity duals for 5d SCFTs,"
M. Gutperle, C. Marasinou, A. Trivella, and C. F. Uhlemann, JHEP 09 (2017) 125
arXiv:1705.01561 [hep-th]

Chapter 1

Introduction

1.1 The AdS/CFT correspondence

1.1.1 The importance of holography

The holographic principle was introduced in the context of string theories by Susskind [5]. In semi-classical considerations of quantum gravity, in $(d+1)$-dimensions, it states that all the information contained in a volume V_{d+1} is encoded on the surface of it's boundary ∂V_{d+1}. An explicit realization of the holographic principle is the AdS/CFT correspondence [1] [6]. This is a duality relating a quantum gravity theory on a certain spacetime to a non-gravitational quantum theory on a spacetime of one dimension lower. The gravity theory is a string theory on Anti-de Sitter (AdS) spacetime in $(d+1)$-dimensions and the non-gravitational theory is a conformal field theory (CFT) living on the d-dimensional boundary of AdS_{d+1}. The AdS/CFT correspondence is sometimes called gauge/gravity duality since it's relating gauge theories to theories with gravity. In fact, the argument was initially introduced by t'Hooft for the case of the large N limit of gauge theories (or t'Hooft limit), where N is the dimension of the gauge group [7]. In particular, he showed that the gauge theory Feynman diagrams at $N \to \infty$ organize themselves with topology matching that of a dual string ending on quarks.

[1] We postpone the exact statement of the AdS/CFT correspondence until section 1.1.3

The AdS/CFT correspondence extends this approach, to conjecture that the dynamics of a gauge and a string theory are equivalent in general.

The correspondence has proven proven to be very useful. On one side, intractable field theory calculations of strongly coupled quantum systems were worked out on the gravity side. Some of the most important results involve correlators of 1/2 BPS operators in $\mathcal{N} = 4$ SYM. Examples are the computation of three-point functions, check of non-renormalization theorems for two- and three- point functions, study of four-point functions and extremal correlators. Another important result is the computation of the conformal anomaly for various CFTs, e.g. the holographic calculation of the conformal anomaly of 2d CFT, which resulted to the anticipated Brown-Henneaux formula [8]. On the other side, known quantum field theory quantities and properties gave a new approach in the interpretation of gravity. A long standing open problem which is targeted is the black hole information paradox. A CFT at finite temperature T corresponds to a dual black hole in AdS with T being the Hawking temperature. The unitarity of the CFT suggests that the information of the initial state of the black hole should be preserved. This means that during the evaporation of the black hole, the emitted Hawking radiation should carry all the information [9]. Although for the region outside the horizon encoding of the information on the dual CFT is well understood, a similar encoding for the inner region remains subtle. An effort to explain it was proposed by the introduction of the so-called "firewall" [10]. This is a region very close to the horizon, where the local effective field theory breaks down. A resolution whether this is a valid mechanism to explain the information paradox has not been achieved to this date. More on tests and breakthroughs of the AdS/CFT correspondence, are being discussed in the lectures by D'Hoker and Freedman [11].

The biggest unresolved problem in theoretical physics is finding a quantum theory of gravity (usually called quantum gravity). The quantization of all other interactions is possible using the framework of quantum field theory (QFT). In fact, the electromagnetic and nuclear interactions are described by the Standard Model of particle physics, many aspects

of which have been studied and confirmed experimentally. However, gravity does not admit such a description. Trying to consider gravity as a QFT we get a nonrenormalizable theory. This means that infinite number of counterterms have to be added to the Lagrangian in order to render observable quantities (calculated perturbatively) finite. The nonrenormalizability of gravity as a QFT can be understood from black hole considerations. At high energies black holes are created. The Bekenstein-Hawking formula says that black hole entropy is proportional to the area of the black hole horizon [12, 13], which scales in a certain way with energy given the dimensionality, d. However, interpreting gravity as a QFT, in the extremely high energy range, we would expect it to lie on a UV fixed point (CFT). Following this expectation, one computes the entropy of the CFT in d-dimensions and how it scales with the energy. It turns out that the entropy here scales differently compared to the case of the black hole. This is a contradiction and therefore if we choose to trust the Bekenstein-Hawking formula we have that gravity is non-renormalizable.

There are different approaches to quantum gravity. The main focus of this dissertation is on one of them which is string theory. The fact that the gravity side of AdS/CFT consists of a string theory makes it a promising tool in the efforts of trying to "solve" quantum gravity. In particular, one avenue that is being explored a lot lately is the connection between quantum entanglement and geometry. The connection is manifested in the proposal for the holographic entanglement entropy [14, 15], where a minimal surface in the bulk AdS gives the entanglement entropy of the CFT. In the same direction, it was proposed that entanglement actually creates geometry [16–18] and also that any EPR pair is associated by an 'Einstein-Rosen bridge' in spacetime, a claim known as "ER=EPR" [19]. Further information, on recent developments on the interpretation of quantum information theory quantities in the AdS/CFT framework, can be found in [20].

Although the motivation which led to AdS/CFT was the exploration of quantum gravity, the duality contributed to the understanding of various topics in physics. In particular, guided by the main attribute of relating a strongly coupled theory to a dual weakly

coupled theory, various generalizations of the duality were launched. One of them is the AdS/QCD program, which applies the same philosophy to geometrize quantum chromodynamics (QCD), the theory of the strong interactions. The program led to synthesis of lattice QCD and heavy ion phenomenology. It further aims to shed more light in the most important open problem of QCD, which is, understanding confinement. For a review on the AdS/QCD program see e.g. [21]. Another program inspired by AdS/CFT is AdS/CMT. This is the application of the duality in condensed matter physics systems. The program creates the possibility for experimentally accessible systems. In fact, amongst others novel phases of matter were explored, cold atom systems with specified properties were designed, a holographic model for superconductors was constructed [22]. Extensive lectures on holographic methods for many-body systems can be found in [23].

1.1.2 The extra dimension

There are different approaches in motivating the presence of one extra dimension in the gravity side of the AdS/CFT correspondence. One of them is the Kadanoff-Wilson renormalization group (RG). To examine this approach, let us consider a non-gravitational quantum system living on a lattice with spacing a. The system has the following Hamiltonian:

$$H = \sum_{x,i} J_i(x,a)\mathcal{O}^i(x) \tag{1.1.1}$$

where x are the site locations, $\mathcal{O}^i$ are the different local operators of the system and J_i their coupling constants. Notice that the coupling constants depend on the lattice size. In the RG approach we coarsegrain the lattice. To apply this let us successively double the lattice site. The resulting coupling constants are the averages of the neighboring J_i before doubling.

$$\text{coarsegraining:} \quad J_i(x,a) \to J_i(x,2a) \to J_i(x,4a) \to \cdots$$

The form of the Hamiltonian stays the same as in (1.1.1) whereas the couplings change as a function of the current lattice size. Thus, we can interpret the lattice size as a length scale we can use to probe the system. Let us name this length scale u. The coupling constants are now given by $J_i(x,u)$, where $u \geq 0$. The flow of the couplings when we allow u to run is described by the so-called RG equations

$$u\frac{\partial}{\partial u}J_i(x,u) = \beta_i(J_j(x,u)) \tag{1.1.2}$$

which are local in the scale u. The functions β_i are the so called beta-functions describing the dependence of couplings J_i upon the energy scale in consideration. In the AdS/CFT framework at strong coupling, we can interpret u as the extra dimension, i.e. the radial dimension of AdS. Based on this argument, the sources $J_i(x,u)$ are mapped to the bulk fields $\phi_i(x,u)$:

$$J_i(x,u) = \phi_i(x,u)$$

The dynamics of ϕ_i admit an action of a gravitational theory on AdS spacetime. This illustrates that the AdS/CFT correspondence is a concrete way to geometrize the RG. Moreover, we see that the microscopic couplings in the UV are identified with the bulk fields at the boundary of the AdS spacetime. Therefore, we could say that the quantum system lives on the boundary of the gravity theory's spacetime.

A different approach in motivating the duality is matching the degrees of freedom on the two sides. Let us consider a d-dimensional QFT. A measure of it's degrees of freedom is entropy which is extensive in this case. This means that considering a spatial region R_{d-1} in the QFT the associated entropy is proportional to it's volume.

$$S_{\text{QFT}} \propto \text{Vol}(R_{d-1})$$

On the other side, in a gravitational theory entropy is subextensive. In particular, there is

a maximum threshold on the value of entropy for a certain spatial region. The threshold is defined by the entropy of a black hole, same in size as the region [24]. The black hole entropy is given by the Bekenstein-Hawking (BH) formula [12, 13]

$$S_{\rm BH} = \frac{A_H}{4G_N} \tag{1.1.3}$$

where A_H is the area of the black hole horizon and G_N the Newton's constant. Let us consider a $(d+1)$-dimensional gravity theory and a spatial region R_d which is bounded by R_{d-1}. Then, employing the BH formula (1.1.3) we get that

$$S_{\rm GR} \propto \text{Area}(R_d) \propto \text{Vol}(R_{d-1})$$

Therefore, assuming that the boundary of R_d matches the spatial region we considered for the QFT, we have that the degrees of freedom in both cases scale identically. This is another hint supporting the correspondence.

Investigating the statement of the AdS/CFT correspondence further, one can ask: "Why don't we study the connection of any QFT to a gravity theory?" The main reason is that geometrizing any QFT is a difficult task. Instead the attention is being drawn to CFTs. These are theories that lie at a fixed point of the RG flow and therefore enjoy conformal invariance. The latter is the reason making the geometrization of CFTs more accessible compare to the case of other more general QFTs.

To illustrate this, let us consider a CFT living in d spacetime dimensions $(t, x^1, x^2, \cdots, x^{d-1})$. We want to associate it with a $(d+1)$-dimensional spacetime. The conformal group consists of the Poincaré group, dilatations and special conformal transformations. We begin by writing the most general $(d+1)$-dimensional metric with Poincaré invariance in d-dimensions:

$$ds^2_{d+1} = \Omega^2(z)\left(-dt^2 + dx_i dx_i + dz^2\right) \tag{1.1.4}$$

with z being the extra dimension, $\Omega(z)$ a metric factor to be determined and x_i spatial directions with $i = 1, 2, \cdots, d-1$.

We further assume that z is a length scale and require the metric to be invariant under scalings. Including the d-dimensional dilatations we can write the overall scaling transformations as

$$z \to \lambda z, \quad (t, x_i) \to (\lambda t, \lambda x_i) \tag{1.1.5}$$

Requiring scale invariance the metric factor gets the form

$$\Omega(z) = L/z \tag{1.1.6}$$

where L is an arbitrary constant. Therefore, the final form of the $(d+1)$-dimensional metric is given by

$$ds^2_{d+1} = \frac{L^2}{z^2}\left(-dt^2 + dx_i dx_i + dz^2\right) \tag{1.1.7}$$

This is AdS_{d+1} spacetime in Poincaré coordinates, if we identify L with the AdS radius of curvature.

Summarizing, we used the conformal symmetry $SO(d, 2)$ and found the geometric analog. The latter is the AdS_{d+1} spacetime and it has isometries same as the conformal group $SO(d, 2)$. This justifies the preference towards investigating CFTs rather than more general QFTs and provides a heuristic argument supporting AdS/CFT.

1.1.3 The original AdS/CFT statement

The AdS/CFT correspondence was conjectured in 1998 by Maldacena [6]. The conjecture takes the form $\mathrm{AdS}_{d+1}/\mathrm{CFT}_d$, identifying a string theory on AdS_{d+1} with a CFT in d-dimensions. The most prominent example given in his paper is the $\mathrm{AdS}_5/\mathrm{CFT}_4$ correspondence which states that "type IIB string theory with string length $l_s = \sqrt{\alpha'}$ and coupling constant g_s living on $AdS_5 \times S^5$ with radius of curvature L and having N $F_{(5)}$ flux units

on the S^5 is equivalent to $\mathcal{N}=4$ $d=3+1$ $SU(N)$ super-Yang-Mills (SYM) with coupling constant $g_{\rm YM}$", when the parameters of the two theories are identified in the following way:

$$g^2_{\rm YM}=2\pi g_s \quad \text{and} \quad 2g^2_{\rm YM}N=L^4/\alpha'^2 \tag{1.1.8}$$

Next, we briefly introduce the two sides of the correspondence.

1.1.4 $\mathcal{N}=4$ Super-Yang-Mills

The Lagrangian of $\mathcal{N}=4$ $d=3+1$ $SU(N)$ super-Yang-Mills theory is given by [25]

$$\begin{aligned}\mathcal{L}_{\rm SYM}=\mathrm{tr}\Big\{&-\frac{1}{2g^2_{\rm YM}}F_{\mu\nu}F^{\mu\nu}+\frac{\theta_I}{8\pi^2}F_{\mu\nu}\tilde{F}^{\mu\nu}-\sum_a i\bar{\lambda}^a\bar{\sigma}^\mu D_\mu\lambda_a-\sum_i D_\mu X^i D^\mu X^i\\&+\sum_{a,b,i}g_{\rm YM}C_i^{ab}\lambda_a[X^i,\lambda_b]+\sum_{a,b,i}g_{\rm YM}\bar{C}_{iab}\bar{\lambda}^a[X^i,\bar{\lambda}^b]+\frac{g^2_{\rm YM}}{2}\sum_{i,j}[X^i,X^j]^2\Big\}\end{aligned} \tag{1.1.9}$$

which contains the $\mathcal{N}=4$ multiplet, i.e. six real scalars X^i, one real vector A^a_μ with field strength $F_{\mu\nu}$ and four Weyl spinors λ_a, all of them transforming in the adjoint representation of the gauge group $SU(N)$. The theory is exactly invariant under the superconformal group $SU(2,2|4)$ at the quantum level. The bosonic part of the group is given by the conformal symmetry in $(3+1)$ spacetime dimensions, $SO(4,2)$, and the R-symmetry, $SO(6)_R\sim SU(4)_R$. In particular, under the $SU(4)_R$ the vector field A^a_μ is a singlet whereas the scalars X^i and the spinors λ_a are a rank 2 anti-symmetric **6** and a **4** respectively. The fermionic part of the symmetry is given by $\mathcal{N}=4$ conformal supersymmetry, which includes in total 32 real supercharges. The supercharges are organized in terms of Weyl spinors which transform in **4** of $SU(4)_R$.

1.1.5 Type IIB Supergravity

It is useful to introduce the low energy limit of type IIB string theory, the $\mathcal{N}=2$ $(9+1)$-dimensional type IIB supergravity theory. The theory has the following field contents: the

metric $G_{\mu\nu}$, the axion-dilaton complex field $C + i\Phi$, a complex antisymmetric rank 2 tensor $B_{2\mu\nu} + iA_{2\mu\nu}$, a real antisymmetric rank 4 tensor $A_{4\mu\nu\rho\sigma}$ with a self-dual field strength, two Majorana-Weyl gravitinos $\psi^I_{\mu\alpha}$ of the same chirality and two Majorana-Weyl dilatinos λ^I_α of the opposite chirality compare to the gravitinos.

Due to the self-dual nature of the five-form field strength we cannot write a satisfactory action producing all field equations including self-duality. Instead, we can write a Lagrangian which reproduces all field equations of type IIB supergravity and impose self-duality as a separate equation. Doing this yields the following Lagrangian

$$\begin{aligned} S_{\text{IIB}} = &+ \frac{1}{4\kappa_{10}^2}\int \sqrt{G}e^{-2\Phi}(2R + 8\partial_\mu\Phi\partial^\mu\Phi - |H_3|^2) \\ &- \frac{1}{4\kappa_{10}^2}\int\left[\sqrt{G}(|F_1|^2 + |\tilde{F}_3|^2 + \frac{1}{2}|\tilde{F}_5|^2) + A_4 \wedge H_3 \wedge F_3\right] + \text{fermions} \end{aligned} \tag{1.1.10}$$

where the different field strengths are given by

$$\begin{cases} F_1 = dC \\ H_3 = dB_2 \\ F_3 = dA_2 \\ F_5 = dA_4 \end{cases} \qquad \begin{cases} \tilde{F}_3 = F_3 - CH_3 \\ \tilde{F}_5 = F_5 - \frac{1}{2}A_2 \wedge H_3 + \frac{1}{2}B_2 \wedge F_3 \end{cases} \tag{1.1.11}$$

supplemented by the self duality condition $\tilde{F}_5 = *\tilde{F}_5$. The gravitational coupling in 10 dimensions is related to the string scale α' and the string coupling g_s of the type IIB superstring theory by

$$\kappa_{10}^2 = 8\pi G_{10} = 64\pi^7 g_s^2 \alpha'^4 \tag{1.1.12}$$

where G_{10} is the 10-dimensional Newton's constant.

1.1.6 AdS/CFT from branes

An argument supporting the AdS_5/CFT_4 correspondence comes from geometric realization of gauge theories in superstring theory. Other than the fundamental strings, superstring theory contains also higher dimensional objects called Dirichlet branes (D-branes). They are denoted as Dp-branes and extend in $(p+1)$ spacetime dimensions. D-branes can be described using two different viewpoints: the open string and closed string perspectives. In the open string perspective, we consider small string coupling constant g_s and the approach is perturbative. D-branes here are described as hyperplanes where open strings can end. In the closed string perspective, D-branes are viewed as non-perturbative massive charged solitons sourcing the superstring theory fields.

To arrive at the desired argument for AdS_5/CFT_4 we need to apply the two perspectives on a stack of N coincident $D3$-branes. The underlying theory is type IIB superstring theory in $\mathbb{R}^{9,1}$ and the brane-configuration retains only half of the 32 supercharges of the theory. The argument concerns the weak form of the correspondence at low energy, $E \ll \alpha'^{-1/2}$.

We start with the open string perspective where we consider our setup in the weak coupling limit $g_s N \ll 1$. In this perturbative limit, our background is described in terms of open and closed string excitations. The former are modes of the $(3+1)$-dimensional hypersurface, whereas the latter are modes propagating in the bulk $(9+1)$-dimensional spacetime.

We apply the low energy limit to our setup in two steps. The first step is integrating out the massive degrees of freedom. This gives an effective action containing only the massless string modes,

$$S = S_{\text{closed}} + S_{\text{open}} + S_{\text{int}} \tag{1.1.13}$$

with S_{closed} (S_{open}) containing the modes of closed (open) strings and S_{int} the interactions between open and closed string modes. S_{closed} is the ten-dimensional type IIB supergravity action plus higher derivative terms. S_{open} can be derived from the Dirac-Born-Infeld (DBI)

action for D3-branes with the Wess-Zumino term added. The open massless modes give the $\mathcal{N}=4$ SYM action with higher derivative corrections. Schematically, so far we have:

$$\begin{aligned} S_{\text{closed}} &= \frac{1}{2\kappa_{10}^2}\int d^{10}x\sqrt{-g}e^{-2\phi}(R+4\partial_M\phi\partial^M\phi)) + \cdots \\ &\approx -\frac{1}{2}\int d^{10}x\ \partial_M h\partial^M h + O(\kappa_{10}) \\ S_{\text{DBI}} + \cdots &= -\frac{1}{(2\pi)^3\alpha'^2 g_s}\int d^4x e^{-\phi}\sqrt{-\det(\mathcal{P}[g]+2\pi\alpha' F)} + \cdots \\ \to S_{\text{open}} &= -\frac{1}{2\pi g_s}\int d^4x\left(\frac{1}{4}F_{\mu\nu}F^{\mu\nu} + \frac{1}{2}\eta^{\mu\nu}\partial_\mu X^i\partial_\nu X^i + O(\alpha')\right) \end{aligned}$$

where we represent the closed sector schematically with the graviton and dilaton only and the open sector with the DBI term for one D3-brane. The metric is given by $g=\eta+\kappa h$, with h being the metric fluctuation (graviton) and $2\kappa^2=(2\pi)^7\alpha'^4 g_s^2$. In the open sector we end up with a gauge field with field strength F and six real scalars ϕ^i. Generalizing to the case of N coincident branes the open sector fields are in the adjoint representation of $U(N)$. Notice that we expand either in κ_{10} or α'.

The second step of taking the low energy limit is to ignore the stringy excitations. This can be achieved by sending $\alpha'\to 0$ keeping all dimensionless parameters fixed. Therefore, we can take either limit $\alpha'\to 0$ or $\kappa_{10}\to 0$. Applying this limit, S_{closed} becomes the type IIB supergravity action in $(9+1)$-dimensional Minkowski spacetime. On the other side, S_{open} becomes the bosonic part of $N=4$ $d=3+1$ $SU(N)$ SYM action (1.1.9). We should mention that the $U(1)\subset U(N)$ degrees of freedom decouple from the rest, leaving $SU(N)$ as the gauge group. Also, S_{int} vanishes and open and closed strings decouple. For this reason the limit we just applied is called the "decoupling limit", indicating the decoupling between open and closed string sectors.

Next, we study the closed string perspective where we consider our setup in the strong coupling limit $g_sN\gg 1$. Since now the D3-branes are viewed as massive charged solitons they source the superstring theory fields, deforming the spacetime and generating flux. There

are only closed strings propagating in this background. We work in type IIB supergravity in $\mathbb{R}^{9,1}$ since it is the low energy limit of type IIB superstring theory in $\mathbb{R}^{9,1}$. The supergravity solution of N coincident D3-branes is given by

$$\begin{aligned} ds^2 &= H(r)^{-1/2}\eta_{\mu\nu}dx^\mu dx^\nu + H(r)^{1/2}\delta_{ij}dx^i dx^j, \\ e^{2\phi(r)} &= g_s^2, \\ A_{(4)} &= (1 - H(r)^{-1})dx^0 \wedge dx^1 \wedge dx^2 \wedge dx^3 + \cdots \\ H(r) &= 1 + \left(\frac{L}{r}\right)^4 \end{aligned}$$

where $\mu, \nu = 0, 1, 2, 3$ and $i, j = 4, 5, \cdots, 9$. The D3-branes extend in the x^μ directions, r is the radial coordinate in the x^i directions, the ellipses in $A_{(4)}$ ensure that $F_{(5)} = dA_{(4)}$ is self-dual and L is a constant which can be fixed by applying flux quantization. In particular, we have N units of flux corresponding to the number of branes which gives

$$L^4 = 4\pi g_s N \alpha'^2 \tag{1.1.14}$$

We proceed with splitting spacetime into two regions: the large radial distance ($r \gg L$) and the small radial distance ($r \ll L$). In the former limit, $H(r) \approx 1$ and the metric reduces to $\mathbb{R}^{9,1}$. In the latter limit, we have that $H(r) \approx L^4/r^4$ which corresponds to the near-horizon limit where the metric gets

$$\begin{aligned} ds^2 &= \frac{r^2}{L^2}\eta_{\mu\nu}dx^\mu dx^\nu + \frac{L^2}{r^2}\delta_{ij}dx^i dx^j \\ &= \frac{L^2}{z^2}\left(\eta_{\mu\nu}dx^\mu dx^\nu + dz^2\right) + L^2 ds^2_{S^5} \end{aligned}$$

where we mapped x^i to spherical coordinates and performed a coordinate transformation, $z = L^2/r$. This is $AdS_5 \times S^5$ with the AdS factor in Poincaré coordinates and both factors

having radius of curvature L.

To apply the low energy limit we should integrate out the massive degrees of freedom. But, since the geometry is curved, the energies (or masses) are measured with a redshift factor depending on our location. However, what matters in our case is measurements of an observer at infinity, i.e. at $r \to \infty$. For a string excitation at fixed location r the energy observed at infinity is given by

$$E_\infty = H(r)^{-1/4} E_r \tag{1.1.15}$$

where E_r is the energy measured at radial distance r. In the asymptotically flat region $r \gg L$, $E_\infty \approx E_r$ which vanishes as we approach infinity. In the near-horizon region $r \ll L$, $E_\infty \approx (r/L)E_r$ which vanishes as we go closer to $r = 0$. Hence, the massless closed string modes exist only in these two regions which are spatially separated. Therefore, there are two types of closed strings belonging to the two regions which decouple in the low energy limit.

The dynamics of the closed string massless fields in the two regions are different. The backgrounds are: in the asymptotically flat region type IIB supergravity in $\mathbb{R}^{9,1}$ and in the near-horizon region type IIB supergravity in $AdS_5 \times S^5$.

A pictorial visualization of the open and closed string perspectives is given in figure 1.1.6. Working in the low energy limit in both cases we find two decoupled effective theories one of which is the type IIB supergravity in $\mathbb{R}^{9,1}$. It is then natural to identify the remaining systems in the two sides. Then, $\mathcal{N} = 4$ SYM theory in four dimensions is equivalent to type IIB supergravity on $AdS_5 \times S^5$. Relaxing the low energy limit we are led to the conjecture that $\mathcal{N} = 4$ SYM theory in four dimensions is equivalent to type IIB superstring theory on $AdS_5 \times S^5$, which was conjectured by Maldacena in [6].

A first test of the correspondence is to check whether the dual theories possess the same symmetries. As a maximally supersymmetric solution of 10-dimensional supergravity, $AdS_5 \times S^5$ has 32 Killing spinors. These correspond to the 32 supercharges of $\mathcal{N} = 4$ SYM. It's isometry groups are $SO(4, 2)$ and $SO(6)$ for the AdS_5 and the S^5 factor respectively. The former is the conformal group in $3 + 1$ dimensions and the latter the R-symmetry of

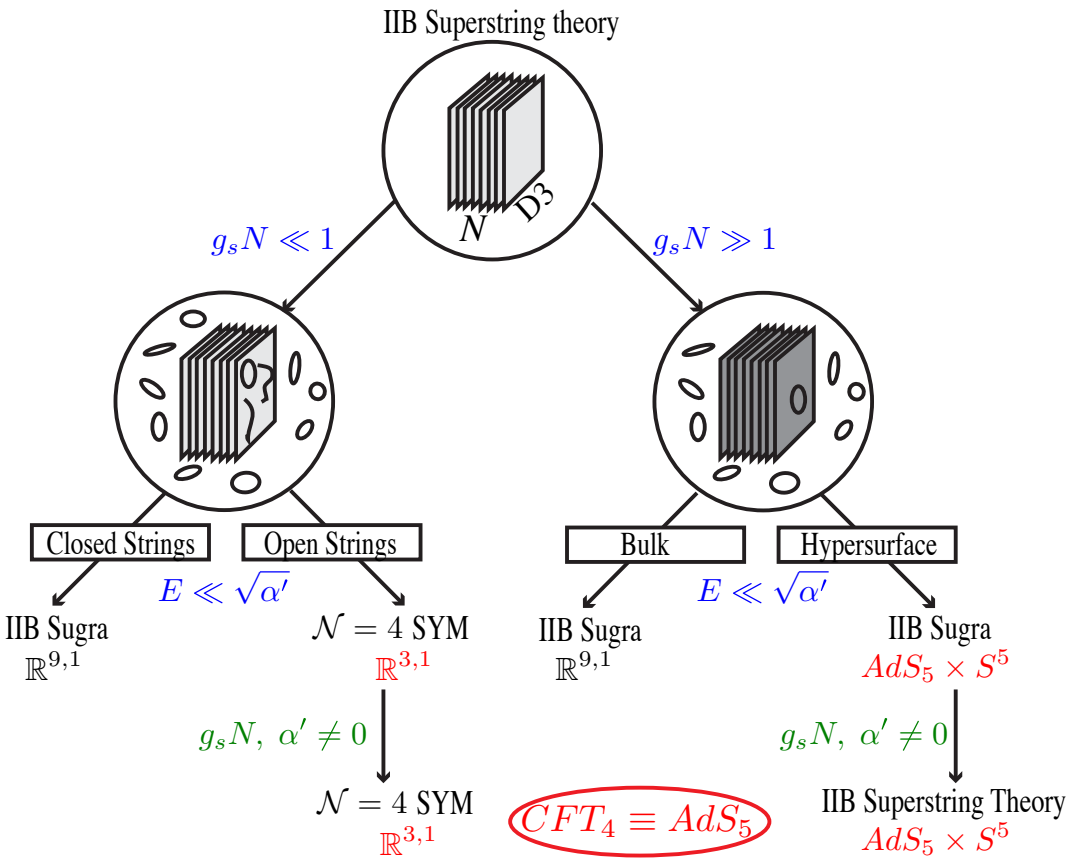

Figure 1.1: N D3-branes are inserted in type IIB superstring theory. The open string perspective ($g_sN \ll 1$) is showed on the left branch. Here, the D3-branes are the hypersurfaces where open strings end and the treatment is perturbative. In the low energy limit open and closed strings decouple (decoupling limit) describing a bulk and a brane worldvolume theory. The closed string perspective ($g_sN \gg 1$) is showed on the right branch. Here, the D3-branes are soliton-like objects, open strings are absent and the treatment is non-perturbative (back-reacted supergravity solution). The bulk and brane closed strings decouple leading to two bulk theories. Matching the two perspectives and lifting the low energy limit restriction, we are led to the $\mathrm{AdS}_5/\mathrm{CFT}_4$ correspondence.

$\mathcal{N} = 4$ SYM. Hence, there is symmetry matching between the two sides in $\mathrm{AdS}_5/\mathrm{CFT}_4$.

Following the geometric argument for the validity of $\mathrm{AdS}_5/\mathrm{CFT}_4$ above, we can predict the existence of the correspondence in other dimensions. We begin by using M-theory in the place of superstring theory and consider stacks of N coincident branes in the low energy limit. The low energy effective action of M-theory is 11-dimensional supergravity, which contains M2- and M5-branes. We consider both. In the near horizon limit we get the geometries: $AdS_4 \times S^7$ with curvature radii $2R_{AdS_4} = R_{S^7}$ for the M2-branes and $AdS_7 \times S^4$

with curvature radii $R_{AdS_7} = 2R_{S^4}$ for the M5-branes. The corresponding worldvolume theories at low energy are the 3-dimensional SCFT (or ABJM theory [26]) for the M2-branes and 6-dimensional (2,0) SCFT for the M5-branes. Lifting the low-energy limit one arrives to the conjectures for $\mathrm{AdS}_4/\mathrm{CFT}_3$ and $\mathrm{AdS}_7/\mathrm{CFT}_6$, which were also introduced in [6].

1.1.7 AdS/CFT made precise

The advantage of having AdS/CFT at our disposal is to be able to compute observables. Usually, with observables in field theory, we refer to correlation functions of the form $\langle \mathcal{O}_1(x_1)\mathcal{O}_2(x_2)\cdots\mathcal{O}_n(x_n)\rangle$, where the $\mathcal{O}$s are local composite operators. Let us assume that S is the action of a CFT in the Euclidean signature and we are interested to find correlation functions of a single local composite operator $\mathcal{O}$. Formally we can calculate correlation functions setting up the corresponding generating functional. First, we add the associated source term to the action

$$S' = S - \int d^d x\, \phi_0(x)\mathcal{O}(x) \tag{1.1.16}$$

where ϕ_0 is a field sourcing the operator $\mathcal{O}$. Then, we compute the partition function $Z[\phi_0]$ for the new action S'. Hence, the generating functional is given by

$$W[\phi_0] = -\ln Z[\phi_0] \tag{1.1.17}$$

where

$$Z[\phi_0] = \left\langle \exp\left(\int d^d x\, \phi_0(x)\mathcal{O}(x)\right)\right\rangle \tag{1.1.18}$$

is the partition function. The correlation functions are obtained from functional derivatives on the generating functional $W[\phi_0]$ with respect to the source field ϕ_0. The above arguments generalize to the case of correlation functions between multiple operators. This is done by adding extra source terms in S'.

The AdS/CFT conjecture states that the CFT generating functional $W[\phi_0]$ is identified

with the on-shell supergravity action S_{SUGRA}, with the corresponding solutions being subject to boundary conditions on the AdS boundary. More precisely,

$$W[\phi_0] = S_{\text{SUGRA}}[\phi]\Big|_{\lim_{z\to 0} z^{\Delta-d}\phi(z,x)=\phi_0(x)} \tag{1.1.19}$$

where Δ is the conformal dimension of $\mathcal{O}$ and z the radial dimension of AdS_{d+1}. This is the precise mathematical formulation of AdS/CFT introduced in [27, 28]. However, the on-shell $S_{\text{SUGRA}}[\phi]$ suffers from infrared divergences arising when integrating over the Anti-de Sitter spacetime. Therefore the right-hand side appearing in (1.1.19) does not make sense. We need to consider a renormalized version of it. To do this, we apply a systematic procedure called holographic renormalization [29, 30] (a review can be found in [31]), which replaces the on-shell supergravity action with a renormalized version, eliminating the IR divergences. Looking at the duality, we can interpret these gravity IR divergences as analogs to the UV divergences appearing in the field theory side before the usual QFT renormalization.

In the strong form of AdS/CFT, which as described above is found after relaxing the low energy limit, the argument follows the above logic and we arrive to the identification

$$\left\langle \exp\left(\int d^d x\, \phi_0(x)\mathcal{O}(x)\right)\right\rangle = Z_{\text{string}}\Big|_{\lim_{z\to 0} z^{\Delta-d}\phi(z,x)=\phi_0(x)} \tag{1.1.20}$$

in the Euclidean signature. The right hand side is now the partition function of the dual string theory with specific boundary conditions on the bulk fields ϕ on the boundary, whereas the left hand side is the CFT generating functional at arbitrary energy level.

1.2 Holography in the presence of conformal defects

AdS/CFT can be generalized by introducing additional structure to both sides. Spatial probes or defects may be introduced in CFTs, preserving a large subgroup of the conformal symmetry. The most basic example is that of a conformal boundary condition [32, 33]. For

a CFT in d-dimensions, the boundary condition fixes the location of the CFT boundary, being invariant under a $SO(d-1,2)$ subgroup of the $SO(d,2)$ conformal group. In general, one can consider a n-dimensional conformal defect, wrapping a n-dimensional hyperplane inside the CFT. In this case, the defect preserves a $SO(n,2) \times SO(d-n)$ subgroup of the $SO(d,2)$ conformal group, where scale invariance survives and some translations, rotations and special conformal transformations of the ambient conformal group are lost.

When supersymmetric theories are concerned, the introduction of a conformal defect breaks in general more symmetries, besides the conformal. In particular, the fermionic and the R-symmetries may get reduced as well. Such defects are called superconformal and can be classified as follows. First, we consider the superalgebra of the original superconformal field theory (SCFT). Then, we find all it's sub-superalgebras containing a bosonic factor of the form $SO(n,2)$. All such subalgebras correspond to SCFTs in the presence of a n-dimensional superconformal defect. A complete analysis for defects preserving 16 out of the 32 original supercharges, in maximally supersymmetric theories, was performed in [34]. Also, a concrete example was examined in [35], where $\mathcal{N} = 4$ SYM in $3+1$ spacetime dimensions was concerned. In particular the authors showed that the introduction of a codimension one defect is reducing the number of supersymmetries from 32 down to 0, 4, 8 or 16 with a corresponding reduction of the R-symmetry to $SO(6)$, $SU(3)$, $SU(2) \times U(1)$ and $SO(3) \times SO(3)$ respectively.

Conformal defects can be realized using holography. One can proceed using two different approaches. The first one, is a geometric realization similar to the one described in section 1.1.6. In this approach, we consider intersecting brane configurations in superstring theory. In addition to the case in section 1.1.6, here we have probe branes, i.e. branes that do not backreact on the geometry (and all the other bulk fields). The configurations are chosen such that the desired symmetries are preserved. Then, taking the open string perspective ($g_s N \ll 1$) we end up with a CFT in the presence of a conformal defect. The dynamics of the defect arise from the modes of open strings spanning intersecting branes. These modes

are interpreted in the field theory side as an interacting multiplet localized on the defect. The closed string perspective leads to gravity on AdS as before, but now in the presence of a probe brane. The geometry of the probe brane is of the form $AdS \times M$ with the AdS factor having the same isometry as the unbroken part of the conformal group. An example of such a defect, is the codimension one defect found by Karch and Randall [36]. The defect is engineered in string theory by a certain D3-D5 brane configuration, which corresponds to $AdS_5 \times S^5$ bisected by a $AdS_4 \times S^2$ brane [37,38]. The dual field theory is $\mathcal{N} = 4$ SYM in $\mathbb{R}^4$ in the presence of a $\mathbb{R}^3$ defect. In particular, we have N D3-branes and a D5-brane spanning the (9+1)-dimensional flat coordinates as in the following table:

	x^0	x^1	x^2	x^3	x^4	x^5	x^6	x^7	x^8	x^9
D5	x	x	x	x	x	x	o	o	o	o
D3	x	x	x	o	o	o	x	o	o	o

The longitudinal coordinates of each brane are denoted by "x" and the transeverse by "o". The branes sit on the origin of their transverse directions. Following Maldacena [6], in the absence of the D5-brane we get AdS/CFT as visualized in figure 1.1.6. Turning on the D5 brane though, we further break supersymmetry down to 8 supercharges, reduce conformal symmetry/AdS isometry to $SO(3,2)$ acting on the common directions x^0, x^1, x^2 and also the R-symmetry/five-sphere isometry to $SO(3) \times SO(3)$ which acts on x^3, x^4, x^5 and x^7, x^8, x^9 directions respectively.

In this dissertation, we study holographic conformal defects constructed using a second approach, where the holographic duals are supergravity solutions. In this approach we constraint the geometry (and all other supergravity fields) using an Ansatz. The form of the Ansatz is dictated by the desired unbroken symmetries, i.e. the symmetries preserved by the conformal defect, which are adopted as isometries of the geometry. Then, the appropriate BPS equations are solved, after being reduced by the Ansatz, giving rise to local solutions. Global solutions can be found by applying regularity and topology conditions. One simple and concrete example is that of the 1/2 BPS Janus solutions [39, 40], which are dual to the

maximally supersymmetric Yang-Mills interface theory [35]. In order to highlight this second approach to constructing defects holographically, we present the above example in detail in the next section.

1.2.1 Supersymmetric Janus solution

The dual field theory of the Janus Solutions exhibits an interface preserving in total the $OSp(2,2|4)$ supergroup (subgroup of $PSU(2,2|4)$) with the following bosonic subgroup:

$$SO(3,2) \times SO(3) \times SO(3) \tag{1.2.1}$$

Also, it contains six scalars in groups of three. The conformal factor $SO(3,2)$ requires the appearance of AdS_4 in our geometry, whereas the behavior of the scalars suggests an additional $S^2 \times S^2$ factor. Therefore, since we are working in type IIB supergravity, we should have a geometry of this form

$$AdS_4 \times S_1^2 \times S_2^2 \times \Sigma \tag{1.2.2}$$

with Σ being a Riemann surface over which the product $AdS_4 \times S_1^2 \times S_2^2$ is warped. These considerations constrain the supergravity solutions to the following form (used as Ansatz):

$$\begin{aligned} ds^2 &= f_4^2 ds^2_{AdS_4} + f_1^2 ds^2_{S_1^2} + f_2^2 ds^2_{S_2^2} + ds^2_\Sigma \\ P &= p_a e^a \qquad G_{(3)} = g_a e^{45a} + i h_a e^{67a} \\ Q &= q_a e^a \qquad F_{(5)} = f_a(-e^{0123a} + \epsilon^{ab} e^{4567b}) \end{aligned}$$

where ds^2 is the $(9+1)$-dimensional metric, P and Q represent the axion-dilaton field, $G_{(3)}$ is the complex 3-form field strength and $F_{(5)}$ the 5-form field strength whereas the fermionic fields are set to vanish. Also, $ds^2_{AdS_4}$, $ds^2_{S_1^2}$, $ds^2_{S_2^2}$ are the metrics of AdS_4, S_1^2, S_2^2 with unit radii respectively and ds^2_Σ a Riemannian metric on Σ. The frame e^μ is set for $\mu = 0,1,2,3$

on AdS_4, $\mu = 4, 5$ on S_1^2, $\mu = 6, 7$ on S_2^2 and $\mu = a = 8, 9$ on Σ. The vectors f_a, q_a, p_a, h_a, g_a live on Σ and f_1, f_2, f_4 are functions on Σ.

Solving the BPS equations the authors in [39] found all 1/2 BPS type IIB supergravity solutions, of the above form, in terms of two harmonic functions on Σ. The solutions demonstrate a varying dilaton and non-vanishing 3-form field strengths whereas the 5-form field strength vanishes. Some of the solutions were found to be regular, upon application of the corresponding conditions. A subclass of the non-singular solutions was derived as a simple deformation of the vacuum solution. These solutions are of the Janus type, i.e. they have two asymptotic regions where the dilaton tends to different constant values $\phi_\pm$ approaching the boundary. In the dual field theory this is interpreted as a domain-wall type defect or interface since the gauge coupling, represented by the dilaton in the gravity side, jumps across it.

1.2.2 Surface Conformal Defects

In this section, we briefly present conformal defects we study in subsequent chapters. These are two-dimensional 1/2 BPS defects with known holographic duals as bubbling solutions.

Disordered Surface Defects: As can be found in the classification of 1/2 BPS defects in [34], within the $PSU(2,2|4)$ supergroup of $\mathcal{N} = 4$ SYM theory there is a $PSU(1,1|2) \times PSU(1,1|2) \times U(1)$ maximal subgroup. The corresponding bosonic subgroup is given by $SO(2,2) \times SO(4) \times SO(2)$ and is associated to a two-dimensional conformal defect on a plane $\mathbb{R}^{1,1}$. The $SO(2,2) \times SO(2)$ factor is the preserved part of the conformal group, with $SO(2,2)$ representing the conformal group on the plane and $SO(2)$ rotations in the transverse directions. The $SO(2)$ factor represents also the remaining R-symmetry along with the $SO(4)$ factor. These defects are the so-called surface defects of the disorder type and were first obtained in [41]. They are characterized by singularities of the gauge and scalar fields in the original theory. Also, they include holonomies along cycles in the directions transverse

to the defect. Their holographic duals are supergravity solutions with geometry of the form

$$AdS_3 \times S^3 \times S^1 \times X_3$$

where X_3 is a 3-dimensional space with boundary. The solutions were found in [42] as a double analytic continuation of the LLM bubbling solutions [43]. They have a non-trivial metric and a non-vanishing five-form field strength. They are locally asymptotic to $AdS_5 \times S^5$. Also, they are expressed in terms of a function on X_3, satisfying a linear partial differential equation in the presence of sources. A more extended review of these solutions is presented in chapter 3 where we study them.

Wilson Surfaces: We are interested also in defects within the $(5+1)$-dimensional $(2,0)$ SCFT associated to the $OSp(8^*|4)$ supergroup. Referring to the classification in [34] we can find that within $OSp(8^*|4)$ there is a $OSp(4^*|2) \times OSp(4^*|2)$ maximal subgroup. This possesses a bosonic subgroup given by $SO(2,2) \times SO(4) \times SO(4)$ associated to a two-dimensional conformal defect on a plane $\mathbb{R}^{1,1}$. The $SO(2,2)$ factor corresponds to the conformal group associated with the surface, one of the $SO(4)$ factors is the rotational symmetry in the directions transverse to the surface and the other $SO(4)$ factor is the remaining R-symmetry. These defects are the so-called Wilson surfaces, first found in [44]. They are defects of the ordered-type as they can be expressed as operator insertions in terms of the fundamental fields of the theory. Their holographic duals are solutions to the eleven-dimensional supergravity with geometry of the form

$$AdS_3 \times S^3 \times S^3 \times \Sigma_2$$

where Σ_2 is a 2-dimensional Riemann surface with boundary. The solutions were found in [45, 46]. They have a non-trivial metric and a non-trivial four-form field strength and they are locally asymptotic to $AdS_7 \times S^4$. Also, they are expressed in terms of a harmonic function on Σ_2, in addition to a complex function satisfying a first order differential equation

on the Riemann surface. Further details about the solutions are presented in chapter 2 where we study them.

The solutions in this section are studied in subsequent chapters from the point of view of quantum entanglement. In the next section, we introduce entanglement entropy which is the main measure of entanglement we investigate in this dissertation.

1.3 Entanglement Entropy

The distinction between classical systems and quantum systems can be realized using the concept of entanglement. Entanglement is the non-local correlation between degrees of freedom in a quantum system. A measure of entanglement called entanglement entropy has received a lot of attention recently, with applications in many areas of physics. The renewed interest stems mainly from the holographic proposal for entanglement entropy given by Ryu and Takayanagi [14, 15]. Some active areas where entanglement entropy is being studied include: condensed matter physics, general relativity, quantum information theory and high energy theory. For example, in condensed matter physics entanglement entropy is used to characterize quantum phases of matter and phase transitions, identify quantum critical phenomena and reveal the dynamics of strongly-correlated many body systems. Also, in general relativity, entanglement entropy is considered central to the recent efforts to explore the relation between quantum entanglement and geometry.

1.3.1 Definition

In this section, we define entanglement entropy. Let us consider a quantum system with Hilbert space $\mathcal{H}$ in a state with density matrix ρ_{tot}. We divide the system into two subsystems A and $B = \bar{A}$, complementary to each other (for an example see figure 1.2). Also, let us assume that $\mathcal{H}$ can be written in a direct product form

$$\mathcal{H} = \mathcal{H}_A \otimes \mathcal{H}_B \tag{1.3.1}$$

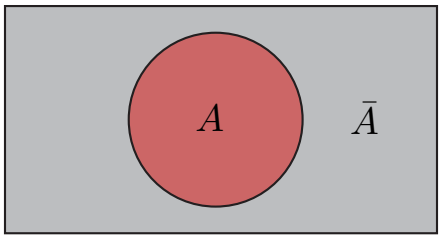

Figure 1.2: The entanglement entropy setup in a QFT constitutes a time slice of the space-time divided into two regions (subsystems): The entangling region A colored in red and the complementary region $\bar{A}$ in grey.

where the factors $\mathcal{H}_A$ and $\mathcal{H}_B$ correspond to Hilbert spaces of the subsystems. For an observer with access only in subsystem A the state looks as follows

$$\rho_A = \mathrm{tr}_B(\rho_{\mathrm{tot}}) \tag{1.3.2}$$

This is the reduced density matrix for subsystem A, found by tracing over all the degrees of freedom in subsystem B. The reduced density matrix ρ_A has enough information for $\mathcal{H}_A$ to be able to reconstruct all correlation functions in subregion A. Then, the entanglement entropy is defined simply as the Von Neumann entropy for the state ρ_A:

$$S_A = -\,\mathrm{tr}_A(\rho_A \log \rho_A) \tag{1.3.3}$$

When finite dimensional quantum systems are considered, entanglement entropy yields finite results. Conversely, for infinite dimensional systems, such as QFTs, entanglement entropy is divergent. The divergence arises mainly from the correlation of degrees of freedom close to the boundary ∂A, also called entangling surface. Introducing a UV cutoff a (lattice spacing) to regulate the divergence, it turns out that the leading divergent term is proportional to the area of the entangling surface:

$$S_A = \gamma \frac{\mathrm{Area}(\partial A)}{a^{d-1}} + \text{subleading terms} \tag{1.3.4}$$

with γ depending on the exact system. In this sense, we say that entanglement entropy follows an area law.

In the case the total state of the system is separable, i.e. it can be written in product form as $|\Psi\rangle = |\Psi_A\rangle \otimes |\Psi_B\rangle$, the reduced density matrix (1.3.2) is pure and therefore S_A vanishes. In the case the total state is inseparable (or entangled) the resulting ρ_A corresponds to a mixed state giving a non-vanishing S_A. In this sense, entanglement entropy measures how far a given state is from a separable state.

Entanglement entropy is not the only measure of quantum entanglement. There are other measures with different defining properties and purpose. Relative entropy measures the "distance" between two states of the system. Mutual information measures the correlation between two subsystems in the same total state. Rènyi entropy, an one-parameter generalization of entanglement entropy, provides more information on the spectrum of ρ_A than the entanglement entropy. However, for the purpose of this dissertation we emphasize only on entanglement entropy.

1.3.2 The replica method

A useful approach for performing analytical computations of entanglement entropy in QFTs was introduced by Calabrese and Cardy in [47]. In this method we use an alternative definition for the entanglement entropy

$$S_A = -\lim_{n\to 1} \frac{\log \mathrm{tr}_A(\rho_A^n)}{n-1} = -\lim_{n\to 1} \partial_n \log \mathrm{tr}_A(\rho_A^n) \tag{1.3.5}$$

where the expression inside the limit gives the Rényi entropies when n integer. Instead, n is analytically continued and the limit $n \to 1$ is taken. The total density matrix ρ_{tot} of the QFT state $|\Psi\rangle$ is given by $\rho = |\Psi\rangle\langle\Psi|/Z$, where the state can be represented by a wave functional as $(\langle\phi^A| \otimes \langle\phi^B|)|\Psi\rangle$. To get the reduced density matrix at the time slice $t = 0$,

we integrate over all states $\phi^B(t=0,\mathbf{x})$ supported only in $\mathbf{x}\in B$:

$$(\rho_A)_{ab}=\frac{1}{Z}\int\left[\mathcal{D}\phi^B(t=0,\mathbf{x}\in B)\right]\left(\langle\phi_a^A|\otimes\langle\phi^B|\right)|\Psi\rangle\langle\Psi|\left(|\phi_b^A\rangle\otimes|\phi^B\rangle\right) \tag{1.3.6}$$

Notice that ρ_A has two indices corresponding to two states ϕ_a^A,ϕ_b^A in region A. Employing the Euclidean path integral formulation the state is represented as

$$\Psi\left[\phi_0(\mathbf{x})\right]=\langle\phi_0\ (\mathbf{x})|\Psi\rangle=\int_{t=-\infty}^{t=0,\phi(t=0,\mathbf{x})=\phi_0(\mathbf{x})}\left[\mathcal{D}\phi(t,\mathbf{x})\right]e^{-I_E[\phi]} \tag{1.3.7}$$

defined by the boundary condition on the field(s) ϕ at $t=0$. Similarly, the conjugate is given by

$$\Psi^*\left[\phi_0(\mathbf{x})\right]=\langle\Psi|\phi_0(\mathbf{x})\rangle=\int_{t=0}^{t=\infty,\phi(t=0,\mathbf{x})=\phi_0(\mathbf{x})}\left[\mathcal{D}\phi(t,\mathbf{x})\right]e^{-I_E[\phi]} \tag{1.3.8}$$

Applying into the reduced density matrix we get

$$(\rho_A)_{ab}=\frac{1}{Z}\int\left[\mathcal{D}\phi(t,\mathbf{x})\right]e^{-I_E[\phi]}\prod_{\mathbf{x}\in A}\delta(\phi(0^+,\mathbf{x})-\phi_b^A(\mathbf{x}))\delta(\phi(0^-,\mathbf{x})-\phi_a^A(\mathbf{x})) \tag{1.3.9}$$

where the integral over $\phi^B(t=0,\mathbf{x})$ was carried out. The result is a path integral on a Euclidean space with a cut along region A. The cut is defined by the boundary conditions at $t=0^{\pm}$. In our case, we are interested in obtaining the trace of the reduced density matrix to the n^{th} power, i.e. $\mathrm{tr}(\rho_A^n)=(\rho_A)_{a_1a_2}(\rho_A)_{a_2a_3}\cdots(\rho_A)_{a_na_1}$. This is given by gluing n replicas of the Euclidean space along the cut matching the edges of the cuts alternately. The outcome is the partition function on the glued n-fold cover which we denote as Z_n. Thus, the entanglement entropy is given by

$$S_{\mathcal{A}}=-\lim_{n\to1}\partial_n\left(\log Z_n-n\log Z\right) \tag{1.3.10}$$

where Z is the partition function on the original space. The n-fold cover has a conical singularity with a deficit angle $2\pi(1-n)$ along the entangling surface ∂A. The singularity

is absent in the limit of the entanglement entropy, $n \to 1$.

1.3.3 Holographic Entanglement Entropy

The problem posed using the replica method (computing the partition function Z_n) is not necessarily a simple task. An alternative way of computing entanglement entropy is through the AdS/CFT correspondence when a gravity AdS dual exists. A prescription of how to do so was initially proposed by Ryu and Takayanagi [14, 15]. Following their proposal, the entanglement entropy of a region A on a spatial slice of a CFT_d is given by the area of a co-dimension two minimal surface γ_A in the bulk that is anchored on the AdS boundary at ∂A as

$$S_A = \frac{\text{Area}(\gamma_A)}{4G_N^{d+1}} \tag{1.3.11}$$

where G_N^{d+1} is the $(d+1)$-dimensional bulk Newton's constant. Further, γ_A needs to be homologous to A and in case the area functional has multiple extrema the one with the least area should be chosen. The setup is represented in figure 1.3.

The formula (1.3.11) applies for the case of holographic duals which are asymptotically AdS (with time-reflection symmetry about time slice). It was originally used to calculate the entanglement entropy for theories in their vacuum state, but was quickly generalized to include more general settings, such as finite temperature and time-dependent states (see e.g. [48,49] for reviews on the topic). It can be considered a generalization of the Bekenstein-Hawking formula (1.1.3), since in an asymptotically AdS spacetime in the presence of an event horizon the minimal surface tends to wrap the horizon. In fact, for spherical entangling surfaces it was observed by Casini, Huerta and Myers (CHM) [50] that the holographic entanglement entropy can be mapped to the thermal entropy of a hyperbolic black hole. In the field theory, the corresponding entanglement entropy is mapped to the thermal entropy on a hyperbolic space. Additionally, the proposal (1.3.11) follows the expected area law (1.3.4). This is derived simply by regulating the AdS radial direction with a cutoff a and computing

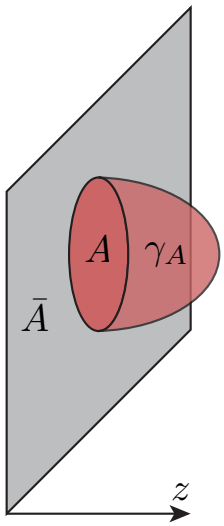

Figure 1.3: The holographic entanglement entropy setup. The AdS boundary, where the CFT lives, is represented by the gray slice at $z = 0$ with z being the radial AdS coordinate. There, the entangling region A colored in red and the complementary region $\bar{A}$ in grey. To calculate entanglement entropy we need to find the minimal surface in the bulk which is anchored at ∂A.

the leading divergence of the minimal area functional. The Ryu-Takayanagi proposal was extended to a covariant version by Hubeny, Rangamani and Takayanagi in [51]. Although, for the purpose of this dissertation we focus on the non-covariant formulation (1.3.11), since the solutions we investigate possess time-reflection symmetry.

1.3.4 Entanglement entropy in the presence of defects

Another generalization, of the Ryu-Takayanagi proposal, (1.3.11) concerns entanglement entropy in the presence of extended conformal defects (reviewed in section 1.2). A concrete example, where the proposal was verified, is that of a Wilson loop in $\mathcal{N} = 4$ $SU(N)$ SYM. The holographic description of a Wilson loop in $SU(N)$ $\mathcal{N} = 4$ SYM in the fundamental representation is given by a fundamental string in $AdS_5 \times S^5$ [52,53], whereas higher dimensional representations can be described by D3- (D5-) branes with $AdS_2 \times S^2(S^4)$ worldvolume in $AdS_5 \times S^5$ [54,55]. These representations reside in the probe brane approximation where the backreaction is neglected. For spherical entangling surfaces, the probe brane entanglement

entropy can be found applying the CHM method. The vacuum is promoted to a thermal background (black brane) at arbitrary temperature on which the brane on-shell action is computed. The on-shell action (multiplied by the temperature) corresponds to the defect free energy of the corresponding CFT. It's temperature derivative gives the thermal entropy, which at zero temperature is the entanglement entropy. This is actually the additional entanglement entropy due to the presence of the defect (see [56–58] for a discussion on this topic).

When the dimension of the representation increases and becomes of order N^2, the back-reaction cannot be neglected and the probe is replaced by a new bubbling geometry with flux. The bubbling holographic solutions corresponding to half-BPS Wilson loops in $\mathcal{N} = 4$ SYM were found in [59–61]. In [62], Lewkowycz and Maldacena applied the CHM mapping to the calculation of the entanglement entropy in the presence of Wilson loops in $\mathcal{N} = 4$ SYM theory and ABJM theories [26]. They showed that the entanglement entropy can be calculated from the expectation value of the Wilson loop operator as well as the one point function of the stress tensor in the presence of the Wilson loop. For BPS Wilson loops these quantities can be evaluated using localization and reduced to matrix models [63, 64]. In [65] the holographic entanglement entropy, (1.3.11), was calculated using the bubbling solution dual to half-BPS Wilson loops. It was shown that the result agrees with [62] when the exact map between matrix model quantities and the supergravity solution, found in [66, 67], is applied.

Chapter 2

Entanglement entropy of Wilson surfaces

In this chapter we generalize the holographic calculation of the entanglement entropy to the case of six-dimensional $(2,0)$ theory with half-BPS Wilson surfaces present. The $(2,0)$ theory can be defined either by a low-energy limit of type IIB string theory on an A_{N-1} singularity [68] or by a decoupling limit of N coincident M5 branes [69]. While there exists no simple Lagrangian description of this theory due to the presence of tensor fields B^+ with self-dual field strength, the holographic dual [6] is given by M-theory on $AdS_7 \times S^4$. In analogy with the Wilson loop (see section 1.3.4) one expects that the six-dimensional theory has extended Wilson surface operators [44] of the form

$$W_\Gamma \sim \mathrm{tr}\exp\left(\int_\Gamma B^+\right)$$

In the probe approximation the Wilson surface operators can be described by embedding M2-branes [70, 71] or M5-branes [72–74] on various submanifolds inside the $AdS_7 \times S^4$. It is an interesting open question whether the expectation value of Wilson surface operators can be calculated by localization in the $(2,0)$ theory . As mentioned in the introduction, bubbling solutions corresponding to half-BPS Wilson surfaces were found in [45, 46] (see [75]

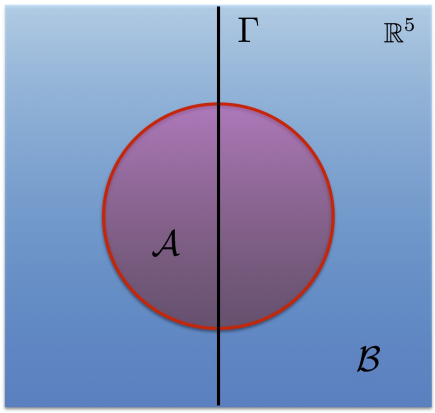

Figure 2.1: The spherical entangling surface $\partial\mathcal{A}$ is the boundary of a region $\mathcal{A}$ on a constant time slice of the $(2,0)$ theory on $\mathbb{R}^6$. The Wilson surface Γ intersects this surface twice.

for earlier work in this direction). In this chapter we use these solutions of eleven-dimensional supergravity to calculate the entanglement entropy as well as other holographic observables.

The solutions are locally asymptotic to $AdS_7 \times S^4$ and the six-dimensional asymptotic metric on the AdS_7 boundary is naturally $AdS_3 \times S^3$. It is convenient to describe the Wilson surface on this space by imposing boundary conditions at the boundary of AdS_3 and choosing Poincaré coordinates for the AdS_3 factor describes a planar Wilson surface. However, as we discuss in section 2.2.3, this metric on $AdS_3 \times S^3$ can be related to the more familiar flat metric on $\mathbb{R}^6$ by a conformal transformation. It is easier to visualize the geometry of our setup on $\mathbb{R}^6$: the entangling surface at constant time is a four-sphere of radius R and the Wilson surface is a line (also filling out the time direction) that intersects the four-sphere at two points, as illustrated in figure 2.1.

The chapter is structured as follows: In section 2.1 we review the bubbling half-BPS solutions of M-theory originally obtained in [45, 46] and work out the behavior of the solution near the asymptotic boundary. In particular, we determine the Fefferman-Graham map for an asymptotic $AdS_3 \times S^3$ boundary metric. In section 2.2 we calculate the entanglement entropy for a spherical entangling surface following the Ryu-Takayanagi prescription for the bubbling solution. In section 2.3 we use the methods of Kaluza-Klein holography and holographic renormalization to calculate the one point function of the stress tensor for

the bubbling solution. In section 2.4 we evaluate the on-shell action of eleven-dimensional supergravity to determine the expectation value of the Wilson surface. We show that the bulk part of the action is given by a total derivative and evaluate the integral as well as the Gibbons-Hawking term.[1]

2.1 Review of bubbling M-theory solutions

In this section we will review the construction of half-BPS M-theory solutions found in [45] that are locally asymptotic to $AdS_7 \times S^4$. These solutions generalize the construction of Janus solutions [39, 76] in type IIB to M-theory. They correspond to the holographic description of Wilson surface defects in the six-dimensional $(2, 0)$ theory, where the Wilson surface is 'heavy' and the backreaction on the geometry is taken into account.

One demands that these solutions preserve an $OSp(4^*|2) \oplus OSp(4^*|2)$ sub-superalgebra of the $OSp(8^*|4)$ superalgebra of the $AdS_7 \times S^4$ vacuum. This form of the preserved superalgebra is uniquely determined by demanding that the solution has sixteen unbroken supersymmetries and preserves $so(2, 2|\mathbb{R})$ associated with conformal symmetry on the worldvolume of the Wilson surface, $so(4|\mathbb{R})$ corresponding to rotational symmetry in the space transverse to the Wilson surface and an unbroken $so(4|\mathbb{R})$ R-symmetry [34]. Note that a generalization was recently analyzed in [77] in which the preserved superalgebra is $D(2|1, \gamma) \oplus D(2|1, \gamma)$, but we will not discuss this case here.

It follows from these superalgebra considerations that the bubbling BPS solution has an $so(2, 2|\mathbb{R}) \oplus so(4|\mathbb{R}) \oplus so(4|\mathbb{R})$ algebra of isometries. Furthermore, the solution preserves sixteen of the thirty-two supersymmetries. The BPS equations were solved in [45] and the global regular solutions were found in [46]. The ansatz for the eleven-dimensional metric is

[1] Notation: To avoid conflict in notation, in this chapter we denote the Ryu-Takayanagi minimal surface as $\mathcal{M}$.

given by an $AdS_3 \times S^3 \times S^3$ fibration over a Riemann surface Σ with boundary:

$$ds^2 = f_1^2\, ds^2_{AdS_3} + f_2^2\, ds^2_{S^3} + f_3^2\, ds^2_{\tilde{S}^3} + 4\rho^2\, |dv|^2 \tag{2.1.1}$$

where we denote the complex coordinate of the two-dimensional Riemann surface by v. In addition, $ds^2_{S^3}$ and $ds^2_{\tilde{S}^3}$ are the metrics on the unit-radius three-spheres and the metric on the unit-radius Euclidean AdS_3 in Poincaré half-plane coordinates is given by

$$ds^2_{AdS_3} = \frac{dz^2 + dt^2 + dl^2}{z^2} \tag{2.1.2}$$

The Wilson surface on the boundary $AdS_3 \times S^3$ fills the t, l directions and is located at $z = 0$.

These solutions are parametrized by a harmonic function h and a complex function $G(v, \bar{v})$ that satisfies a first order differential equation:

$$\partial_v G = \frac{1}{2}\left(G + \bar{G}\right) \partial_v \ln h \tag{2.1.3}$$

It is useful to introduce the combinations[2]

$$W_+ = |G - \bar{G}| + 2|G|^2, \quad W_- = |G - \bar{G}| - 2|G|^2 \tag{2.1.4}$$

in terms of which the metric functions in (2.1.1) are given by

$$\begin{aligned} f_1^6 &= 4h^2(1 - |G|^2)\, \frac{W_+}{W_-^2}, \quad f_2^6 = 4h^2(1 - |G|^2)\, \frac{W_-}{W_+^2} \\ f_3^6 &= \frac{h^2 W_+ W_-}{16(1 - |G|^2)^2}, \quad \rho^6 = \frac{(\partial_v h \partial_{\bar{v}} h)^3}{16h^4}\, (1 - |G|^2)\, W_+ W_- \end{aligned} \tag{2.1.5}$$

It was shown in [46] that for a solution to be regular the functions h and G must satisfy the

[2]Note that there is a typo in eq (2.5) of [46]: it should read $W^2 = -4|G|^2 - (G - \bar{G})^2$.

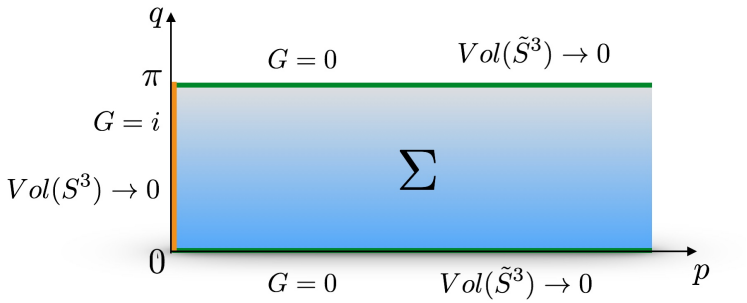

Figure 2.2: $AdS_7 \times S^4$ parameterized on the half strip.

following conditions on the Riemann surface Σ and its boundary:

$$\begin{aligned} &h = 0, \quad G = 0, +i, \qquad v \in \partial\Sigma \\ &h > 0, \quad |G|^2 < 1 \qquad\quad v \in \Sigma \end{aligned} \tag{2.1.6}$$

First we consider the simplest example: the $AdS_7 \times S^4$ vacuum solution. This can be obtained by choosing Σ to be the half strip $\Sigma = \{v = p + iq/2, p > 0, q \in [0, \pi]\}$ with

$$h = -iL^3 \left(\cosh(2v) - \cosh(2\bar{v})\right), \quad G = -i\,\frac{\sinh(v - \bar{v})}{\sinh 2\bar{v}} \tag{2.1.7}$$

which produces

$$f_1 = 2L\cosh p, \quad f_2 = 2L\sinh p, \quad f_3 = L\sin q, \quad \rho = L \tag{2.1.8}$$

Hence the $AdS_7 \times S^4$ metric is given by

$$ds^2 = 4L^2\left(dp^2 + \cosh^2 p\, ds^2_{AdS_3} + \sinh^2 p\, ds^2_{S^3}\right) + L^2\left(dq^2 + \sin^2 q\, ds^2_{\tilde{S}^3}\right) \tag{2.1.9}$$

This geometry is represented in figure 2.2. More general bubbling solutions can be constructed once we realize that the $AdS_7 \times S^4$ solution can be mapped from the half strip to

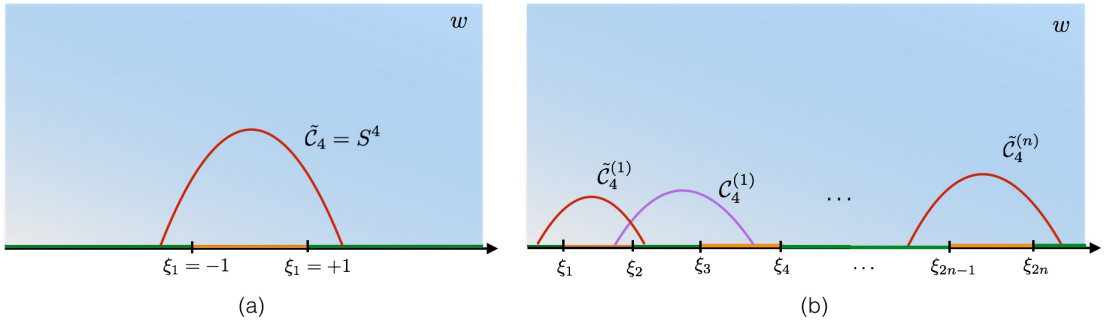

Figure 2.3: (a) $AdS_7 \times S^4$ on the upper half-plane. (b) General bubbling solution with n four-cycles $\tilde{\mathcal{C}}_4^{(i)}$, $i = 1, \ldots, n$ and $n-1$ four-cycles $\mathcal{C}_4^{(i)}$, $i = 1, \ldots, n-1$.

the upper half-plane via

$$w = \cosh(2v) \tag{2.1.10}$$

The functions h and G then take the form

$$h = -iL^3(w - \bar{w}), \qquad G = \frac{i}{2}\left(\frac{w+1}{\sqrt{(w+1)(\bar{w}+1)}} - \frac{w-1}{\sqrt{(w-1)(\bar{w}-1)}}\right) \tag{2.1.11}$$

Note that the boundary of Σ is now located at the real line and that on the real line the function $G = +i$ when $\mathrm{Re}\, w \in [-1, 1]$ and $G = 0$ when $\mathrm{Re}\, w > 1$ or $\mathrm{Re}\, w < -1$.

A general bubbling solution is constructed by choosing a simple form for h and the following linear superposition for G:

$$h = -iL^3(w - \bar{w}), \qquad G = \sum_{i=1}^{2n}(-1)^i g(\xi_i), \qquad g(\xi) \equiv -\frac{i}{2}\frac{w-\xi}{\sqrt{(w-\xi)(\bar{w}-\xi)}} \tag{2.1.12}$$

where w is now a general coordinate on the upper half-plane. The solution is completely characterized by the choice of $2n$ real numbers ξ_i with $i = 1, 2, \ldots, 2n$ that are ordered

$$-\infty = \xi_0 < \xi_1 < \xi_2 < \cdots < \xi_{2n} < \xi_{2n+1} = +\infty \tag{2.1.13}$$

We have introduced ξ_0 and ξ_{2n+1} to simplify the expression for the boundary condition that the function G satisfies on the real line:

$$G|_{\mathrm{Im}\, w=0} = \begin{cases} 0 & \mathrm{Re}\, w \in [\xi_{2k}, \xi_{2k+1}] \\ +i & \mathrm{Re}\, w \in [\xi_{2k+1}, \xi_{2k+2}] \end{cases}, \qquad \begin{matrix} k = 0, 1, 2, \ldots, n \\ k = 0, 1, 2, \ldots, n-1 \end{matrix} \tag{2.1.14}$$

A general bubbling solution is characterized by the appearance of new nontrivial four-cycles (see figure 2.3). The n four-cycles $\tilde{\mathcal{C}}_4^{(i)}$ are constructed by connecting two boundary points on different intervals where the volume of the three-sphere $\tilde{S}^3$ shrinks to zero. This generalizes the construction of the four-sphere in the $AdS_7 \times S^4$ vacuum solution. In addition, the geometry also has $n-1$ four-cycles $\mathcal{C}_4^{(i)}$ that are constructed by connecting points on different intervals where the three-sphere S^3 shrinks to zero size. In the bubbling solution these cycles carry nontrivial four-form flux and are the remnants of M5-branes wrapping $AdS_3 \times S^3$ and $AdS_3 \times \tilde{S}^3$, respectively.

2.1.1 Asymptotic behaviour and regularization

In this section we study the asymptotic behaviour of a general bubbling solution. We will see later that the area integral and the action integral both diverge, so we need to regulate the integrals and map the regulator to the Fefferman-Graham (FG) UV cut-off.

It is convenient to choose the following coordinates on Σ: $w = r\, e^{i\theta}$. The boundary of $AdS_7 \times S^4$ is located at $r \to \infty$. The expressions for G and $\bar{G}$ given in (2.1.12) can be expanded at large r in terms of the generating function of the Legendre polynomials

$$\frac{1}{\sqrt{1-2xt+t^2}} = \sum_{k=0}^{\infty} P_k(x)\, t^k \tag{2.1.15}$$

with the result

$$G = \frac{i}{2} \sum_{k=1}^{\infty} \frac{a_k(\theta)\, m_k}{r^k}, \quad \bar{G} = -\frac{i}{2} \sum_{k=1}^{\infty} \frac{\bar{a}_k(\theta)\, m_k}{r^k} \tag{2.1.16}$$

where the dependence on the angular coordinate θ is given by

$$\begin{aligned} a_k(\theta) &\equiv P_{k-1}(\cos\theta) - e^{i\theta} P_k(\cos\theta) \\ \bar{a}_k(\theta) &\equiv P_{k-1}(\cos\theta) - e^{-i\theta} P_k(\cos\theta) \end{aligned} \tag{2.1.17}$$

The moments m_k are defined via

$$m_k \equiv \sum_{i=1}^{2n} (-1)^i \xi_i^k \tag{2.1.18}$$

To ensure that a general bubbling solution is asymptotic to $AdS_7 \times S^4$ with radii

$$R_{S^4} = \frac{R_{AdS_7}}{2} = L \tag{2.1.19}$$

we must identify $m_1 \equiv 2$. This provides a constraint on the ξ_i. Also, for the $AdS_7 \times S^4$ solution ($n = 1$) we note here that all even moments vanish and all odd moments equal 2.

The metric functions take the following forms as power series in large r:

$$\begin{aligned} \frac{f_1^2}{L^2} &= 2r + \frac{4 - m_2 \cos\theta}{2} + \frac{3(8 + m_2^2 - 2m_3) + (8 + 3m_2^2 - 10m_3)\cos 2\theta}{24\, r} + O\left(\frac{1}{r^2}\right) \\ \frac{f_2^2}{L^2} &= 2r - \frac{4 + m_2 \cos\theta}{2} + \frac{3(8 + m_2^2 - 2m_3) + (8 + 3m_2^2 - 10m_3)\cos 2\theta}{24\, r} + O\left(\frac{1}{r^2}\right) \\ \frac{f_3^2}{L^2 \sin^2\theta} &= 1 + \frac{m_2 \cos\theta}{2\, r} - \frac{3(m_2^2 - 8m_3) + (32 + 3m_2^2 - 40m_3)\cos 2\theta}{96\, r^2} + O\left(\frac{1}{r^3}\right) \\ \frac{\rho^2}{L^2} &= \frac{1}{4\, r^2} + \frac{m_2 \cos\theta}{8\, r^3} + \frac{-3(16 + m_2^2 - 8m_3) + (16 - 3m_2^2 + 40m_3)\cos 2\theta}{384\, r^4} + O\left(\frac{1}{r^5}\right) \end{aligned} \tag{2.1.20}$$

Next we present the mapping of the (r, θ) coordinates for large values of r to an FG coordinate system $(u, \tilde{\theta})$ for a general bubbling solution. We need this map to define the large r cut-off function as well as to perform the Kaluza-Klein (KK) reduction in the calculation of the expectation value of the stress tensor in section 2.3.

It is natural to consider a Wilson surface living on $AdS_3 \times S^3$. This space is related to $\mathbb{R}^6$ by a Weyl rescaling. We can choose to adapt our FG chart to either space; here we choose the former. The general FG metric that preserves the $AdS_3 \times S^3 \times S^3$ isometry of a bubbling solution is given by

$$ds^2 = L^2 \left[\frac{4}{u^2} \left(du^2 + \alpha_1 ds^2_{AdS_3} + \alpha_2 ds^2_{S^3} \right) + \alpha_3 d\tilde{\theta}^2 + \alpha_4 ds^2_{\tilde{S}^3} \right] \tag{2.1.21}$$

Equating this metric with the bubbling metric (2.1.1) we find

$$\begin{aligned} f_1^2 = \frac{4L^2\alpha_1}{u^2}, \quad f_2^2 = \frac{4L^2\alpha_2}{u^2}, \quad f_3^2 = L^2\alpha_4 \\ 4\rho^2 \left(dr^2 + r^2 d\theta^2 \right) = \frac{4L^2 du^2}{u^2} + L^2 \alpha_3 d\tilde{\theta}^2 \end{aligned} \tag{2.1.22}$$

We regulate the spacetime at a small value of u and identify this with ε: the (dimensionless) UV cut-off on $AdS_3 \times S^3$. The boundary conditions on the coordinate map and the functions $\alpha_i(u, \tilde{\theta})$ at small u must be chosen to ensure that the boundary metric is $ds^2_{AdS_3} + ds^2_{S^3}$ and the transverse S^4 is recovered. We find

$$\begin{aligned} r = \frac{2}{u^2} + \ldots, \quad \theta = \tilde{\theta} + \ldots \\ \alpha_1 = 1 + \ldots, \quad \alpha_2 = 1 + \ldots, \quad \alpha_3 = 1 + \ldots, \quad \alpha_4 = \sin^2 \tilde{\theta} + \ldots \end{aligned} \tag{2.1.23}$$

Whilst we have not been able to solve (2.1.22) in closed form, we can build the coordinate map as an asymptotic expansion in u. The mapping is given by

$$\begin{aligned} r = \frac{2}{u^2} + \frac{m_2 \cos\tilde{\theta}}{4} + \frac{3(-16 - m_2^2 + 8m_3) + (16 - 21m_2^2 + 40m_3)\cos 2\tilde{\theta}}{768} u^2 \\ + \frac{\cos\tilde{\theta}}{18432} \left(48m_2 - 43m_2^3 + 40m_2 m_3 + 80m_4 \right. \\ \left. - \left(48m_2 - 203m_2^3 + 680m_2 m_3 - 560m_4 \right) \cos 2\tilde{\theta} \right) u^4 + O(u^6) \end{aligned} \tag{2.1.24}$$

and

$$\theta = \tilde{\theta} - \frac{m_2 \sin\tilde{\theta}}{8}\, u^2 - \frac{(16 - 27m_2^2 + 40m_3)\cos\tilde{\theta}\sin\tilde{\theta}}{768}\, u^4 + \frac{\sin\tilde{\theta}}{18432}\Big(296m_2m_3 - 48m_2 - 98m_2^3 - 200m_4 + \big(48m_2 - 139m_2^3 + 400m_2m_3 - 280m_4\big)\cos 2\tilde{\theta}\Big)\, u^6 + O(u^8) \tag{2.1.25}$$

The area integral and action integral both diverge at large r. It is useful to express the coordinate map as a cut-off relation $r_c = r_c(\theta, \varepsilon)$. This is found by first inverting the relation (2.1.25) in the small u limit and then eliminating $\tilde{\theta}$ from (2.1.24). The result is

$$r_c(\theta,\varepsilon) = \frac{2}{\varepsilon^2} + \frac{m_2\cos\theta}{4} + \frac{-3(16 + 5m_2^2 - 8m_3) + (16 - 9m_2^2 + 40m_3)\cos 2\theta}{768}\,\varepsilon^2 + \frac{\cos\theta}{9216}\big(-48m_2 + 55m_2^3 - 160m_2m_3 + 40m_4 + \big(48m_2 + 25m_2^3 - 160m_2m_3 + 280m_4\big)\cos 2\theta\big)\,\varepsilon^4 + O(\varepsilon^6) \tag{2.1.26}$$

2.2 Holographic entanglement entropy

The Ryu-Takayanagi prescription for the holographic entanglement entropy is given by (1.3.11). Since we are dealing with static states of our CFT, it is applicable here. In the following section we derive the minimal surface $\mathcal{M}$ for a general bubbling solution and show that its restriction to the boundary maps to a four-sphere in $\mathbb{R}^6$. We then evaluate its regulated area and compare with our expectations from $\mathbb{R}^6$.

2.2.1 Minimal surface geometry

A bubbling geometry is an $AdS_3 \times S^3 \times S^3$ fibration over Σ. We consider a surface $\mathcal{M}$ at constant t that fills the $S^3 \times S^3$ and has profile $z = z(w, \bar{w}, l)$, where z is the AdS_3 radial

coordinate defined in (2.1.2). The area functional becomes

$$A(\mathcal{M}) = 2\,\mathrm{Vol}(S^3)^2 \int dl \int_\Sigma d^2w\, \frac{f_1 f_2^3 f_3^3 \rho^2}{z} \sqrt{1 + \frac{f_1^2}{z^2\rho^2}\frac{\partial z}{\partial w}\frac{\partial z}{\partial \bar{w}} + \left(\frac{\partial z}{\partial l}\right)^2} \tag{2.2.1}$$

The equations of motion derived from this functional are solved by

$$z(w, \bar{w}, l)^2 + l^2 = R^2 \tag{2.2.2}$$

This semicircle is simply a co-dimension two minimal surface in AdS_3. Following [57, 58] it is straightforward to see that this is in fact the surface of minimal area (within this ansatz).

The surface (2.2.2) is independent of the AdS_7 radial coordinate. Thus, the boundary $\partial\mathcal{A}$ of the entangling region on $AdS_3 \times S^3$ is given by the same formula. To understand this, let us consider two coordinate charts on $\mathbb{R}^6$:

$$ds^2_{\mathbb{R}^6} = z^2\left(\frac{dz^2 + dt^2 + dl^2}{z^2} + ds^2_{S^3}\right) = dt^2 + d\bar{r}^2 + \bar{r}^2\left(d\chi^2 + \sin^2\chi\, ds^2_{S^3}\right) \tag{2.2.3}$$

The map between these two charts is given by

$$z = \bar{r}\,\sin\chi, \qquad l = \bar{r}\,\cos\chi \tag{2.2.4}$$

Thus, our $\partial\mathcal{A}$ on $AdS_3 \times S^3$ can be written as a four-sphere of radius R on $\mathbb{R}^6$ (given by $\bar{r} = R$) after a Weyl rescaling.

2.2.2 Evaluating the area integral

The combination of metric factors that appears in the area integral (2.2.1) can be written

$$f_1 f_2^3 f_3^3 \rho^2 = \frac{1}{4}\,|\partial_w h|^2\, h\, W_- \tag{2.2.5}$$

The entanglement entropy is proportional to the area evaluated on the surface (2.2.2):

$$S_{\mathcal{A}} = \frac{\mathrm{Vol}(S^3)^2}{8G_N^{(11)}} \int dl \, \frac{R}{R^2 - l^2} \, (J_1 + J_2) \tag{2.2.6}$$

where we have defined

$$\begin{aligned} J_1 &\equiv \int_\Sigma d^2w \, |\partial_w h|^2 \, h \, |G - \bar{G}| \\ J_2 &\equiv -2 \int_\Sigma d^2w \, |\partial_w h|^2 \, h \, |G|^2 \end{aligned} \tag{2.2.7}$$

Substituting $w = r\, e^{i\theta}$ into (2.1.12) we find for J_1

$$J_1 = -4L^9 \sum_{i=1}^{2n} (-1)^i \int_0^\pi d\theta \, \sin\theta \int_0^{r_c(\theta,\varepsilon)} dr \, \frac{r^2(r\cos\theta - \xi_i)}{\sqrt{r^2 + \xi_i^2 - 2r\xi_i \cos\theta}} \tag{2.2.8}$$

The overall minus sign follows from the fact that $G - \bar{G} < 0$ on the upper half-plane. We carefully evaluate this expression in appendix A.1.1. The final result is given in equation (A.1.5) and takes the form

$$J_1 = L^9 \left[\frac{64}{3\varepsilon^4} + \frac{-24 + 3m_2^2 - 8m_3}{15} + O\left(\varepsilon^2\right) \right] \tag{2.2.9}$$

Next we consider the second term

$$\begin{aligned} J_2 &= -2 \int_\Sigma d^2w \, |\partial_w h|^2 \, h \, |G|^2 \\ &= -2L^9 \int_0^\pi d\theta \, \sin\theta \int_0^{r_c(\theta,\varepsilon)} dr \, r^2 \\ &\quad \times \left\{ 2n + 2 \sum_{i<j} (-1)^{i+j} \frac{r^2 - r\cos\theta\,(\xi_i + \xi_j) + \xi_i \xi_j}{\sqrt{r^2 - 2r\xi_i\cos\theta + \xi_i^2}\sqrt{r^2 - 2r\xi_j\cos\theta + \xi_j^2}} \right\} \end{aligned} \tag{2.2.10}$$

We carefully evaluate this integral in appendix A.1.2 and the final result is (A.1.22)

$$J_2 = L^9 \left[-\frac{64}{3\varepsilon^2} - \frac{4}{3} \sum_{i<j} (-1)^{i+j} |\xi_i - \xi_j|^3 + O\left(\varepsilon^2\right) \right] \tag{2.2.11}$$

Note that the second term cannot be expressed in terms of the moments m_k.

Now we handle the integral over l. Recall that the minimal surface formula (2.2.2) describes a semicircle for which $z \in [0, R]$ and $l \in [-R, R]$. Note that $J_{1,2}$ are independent of l because the cut-off function is. The l integral diverges at both limits; rewriting via (2.2.2) as an integral over z, we regulate with a cut-off at $z = \eta$:

$$\begin{aligned} \int_{-\sqrt{R^2-\eta^2}}^{\sqrt{R^2-\eta^2}} dl \, \frac{R}{R^2 - l^2} &= 2 \int_0^{\sqrt{R^2-\eta^2}} dl \, \frac{R}{R^2 - l^2} = 2 \int_\eta^R dz \, \frac{R}{z\sqrt{R^2 - z^2}} \\ &= 2 \log \left(\frac{R + \sqrt{R^2 - \eta^2}}{\eta} \right) = 2 \log \left(\frac{2R}{\eta} \right) - \frac{\eta^2}{2R^2} + O(\eta^4) \end{aligned} \tag{2.2.12}$$

Finally we put these pieces together to compute the divergent entanglement entropy (2.2.6):

$$\begin{aligned} S_{\mathcal{A}} = \frac{L^9 \, \mathrm{Vol}(S^3)^2}{4 G_N^{(11)}} \, \Bigg[&\frac{64}{3\varepsilon^4} - \frac{64}{3\varepsilon^2} + \frac{-24 + 3m_2^2 - 8m_3}{15} \\ &- \frac{4}{3} \sum_{i<j} (-1)^{i+j} |\xi_i - \xi_j|^3 + O\left(\varepsilon^2\right) \Bigg] \log \left(\frac{2R}{\eta} \right) \end{aligned} \tag{2.2.13}$$

Employing the definitions

$$L = (\pi \, N)^{1/3} \, \ell_P, \qquad 8\pi G_N^{(11)} = 2^7 \pi^8 \ell_P^9, \qquad \mathrm{Vol}(S^3) = 2\pi^2 \tag{2.2.14}$$

this becomes

$$S_{\mathcal{A}} = \frac{4N^3}{3}\left[\frac{1}{\varepsilon^4} - \frac{1}{\varepsilon^2} + \frac{-24+3m_2^2-8m_3}{320} - \frac{1}{16}\sum_{i<j}(-1)^{i+j}|\xi_i-\xi_j|^3 + O\left(\varepsilon^2\right)\right]\log\left(\frac{2R}{\eta}\right) \tag{2.2.15}$$

Evaluating this result on the vacuum we find

$$S_{\mathcal{A}}^{(0)} = \frac{4N^3}{3}\left[\frac{1}{\varepsilon^4} - \frac{1}{\varepsilon^2} + \frac{3}{8} + O\left(\varepsilon^2\right)\right]\log\left(\frac{2R}{\eta}\right) \tag{2.2.16}$$

Subtracting this vacuum contribution from (2.2.15) we arrive at our final result for the change in entanglement entropy due to the presence of the Wilson surface:

$$\Delta S_{\mathcal{A}} = \frac{4N^3}{3}\left[\frac{16+3m_2^2-8m_3}{320} - \frac{1}{16}\sum_{i<j}(-1)^{i+j}|\xi_i-\xi_j|^3 - \frac{1}{2}\right]\log\left(\frac{2R}{\eta}\right) \tag{2.2.17}$$

Note that the power divergences with respect to the FG cut-off ε are cancelled in this subtraction and only a logarithmic divergence in η remains.

2.2.3 Physical interpretation

In this section we give a physical interpretation of our result for the entanglement entropy. First, recall that during the calculation we introduced two separate regulators. The FG cut-off ε can be viewed as a regular UV cut-off for a holographic theory with a six-dimensional $AdS_3 \times S^3$ boundary. In addition, when performing the integral over the AdS_3 coordinate l in (2.2.12) we introduced a cut-off η on the AdS_3 radial coordinate z in Poincare slicing (2.1.2). One might be tempted to view η as purely an IR cut-off that regulates the infinite volume of the boundary theory. However, it also has an interpretation as a UV cut-off on the minimal distance to the Wilson surface in the boundary theory.

This interpretation is most easily demonstrated by considering the vacuum spacetime.

The map that relates $AdS_7 \times S^4$ with $AdS_3 \times S^3$ boundary in (2.1.9) to a metric with $\mathbb{R}^6$ boundary

$$ds^2 = \frac{4L^2}{\tilde{u}^2}\left(d\tilde{u}^2 + dt^2 + dl^2 + dr^2 + r^2 ds^2_{S^3}\right) + L^2\left(dq^2 + \sin^2 q\, ds^2_{\tilde{S}^3}\right) \tag{2.2.18}$$

is given by

$$z = \tilde{u}\cosh p \qquad r = \tilde{u}\sinh p \tag{2.2.19}$$

Setting $\tilde{u} = \tilde{\varepsilon}$ imposes a (dimensionful) holographic UV cut-off on the theory living on the $\mathbb{R}^6$ boundary. Since the minimal value of the coordinate p is zero, it follows from (2.2.19) that the range of z is bounded by $z > \tilde{\varepsilon}$ and hence the AdS_3 cut-off η is related to the uniform UV cut-off $\tilde{\varepsilon}$.

At this point we do not have an analog of the map (2.2.19) for the bubbling solution that is valid for all values of the coordinates. We can construct the map for the asymptotic region defined by the FG expansion for the $AdS_3 \times S^3$ boundary theory (2.1.21), however this expansion breaks down once the FG coordinate u is not small. As discussed in [58] one can construct a map that is valid also near $z = 0$ by patching together the expansion near the AdS_3 boundary and the FG boundary. We will not pursue this construction here since we focus all our calculations on the theory living on the $AdS_3 \times S^3$ boundary. However, since the metric is asymptotically AdS, we expect that one should obtain only a small modification to the identification of the UV cut-offs that, crucially, does not affect the logarithmically divergent term in the entanglement entropy.

Physically, the interpretation of η as a UV cut-off and the form of the subtracted entanglement entropy (2.2.17) is quite natural. Note that the dominant contributions to the entanglement entropy come from UV degrees of freedom located near the entangling surface. Since the Wilson surface (at fixed time) intersects the entangling surface at two points in our geometry (see figure 2.1), the defect contribution to the entanglement entropy has essentially

the same dimensionality as the entanglement entropy of a two-dimensional CFT. This is also reflected in the AdS_3 slicing we employ and the fact that the minimal surface we find in the bulk (2.2.2) is familiar from AdS_3/CFT_2. Hence an argument along the lines of those given in [58] shows that the extra divergent contribution of the Wilson surface should be logarithmic, wherein the cut-off is associated with a minimal distance to the defect.

2.3 Holographic stress tensor

The goal of the present section is to calculate the one point function of the six-dimensional stress tensor holographically for an asymptotically $AdS_7 \times S^4$ bubbling solution. Since the bubbling solutions are eleven-dimensional one has to utilize the machinery of KK holography that was developed in [78]. Note that a similar calculation was performed in [67] for the type IIB bubbling solution dual to half-BPS Wilson loop defects and we will largely adopt their method to our case.

The KK reduction of eleven-dimensional supergravity on S^4 produces a seven-dimensional supergravity (with negative cosmological constant) with infinite towers of massive fields [79, 80]. These can be classified by their seven-dimensional spin and representation of the relevant $SO(5)$ spherical harmonics (scalar and tensorial) on S^4. One difficulty is the mixing of modes coming from the eleven-dimensional supergravity as well as the fact that seven-dimensional fields can be related by eleven-dimensional diffeomorphisms, leading to nonlinear gauge symmetries. The resulting seven-dimensional action can be diagonalized and the masses of all the fields were determined in [79–81].

Via the AdS/CFT correspondence the seven-dimensional supergravity fields are dual to operators in the six-dimensional $(2, 0)$-theory. The precise dictionary can be found for example in [82].

In [78] it was argued that in order to obtain a local seven-dimensional supergravity action without higher derivatives one needs in general to perform a KK reduction map that

is nonlinear and relates the eleven- and seven-dimensionall fields schematically as

$$\Psi_7 = \psi_{11} + \mathcal{K}\,\psi_{11}\psi_{11} + \dots \tag{2.3.1}$$

Here, $\mathcal{K}$ is a differential operator and the ellipsis denotes higher order terms with three or more eleven-dimensional fields. This nonlinear mixing in general complicates holographic calculations (see e.g. [67]). However, a simple rule was derived in [78] to determine when and which nonlinear terms appear. For a supergravity field dual to a dimension Δ operator in the CFT, the only nonlinear terms that can appear are the ones for which the sum of the dimensions of their respective dual operators is less than or equal to Δ. When this rule is applied to the stress tensor, which has $\Delta = 6$, it is clear that there can be no nonlinear mixing since the operators with lowest dimension have $\Delta = 4$.[3]

The starting point for the calculation of the holographic stress tensor is to decompose the eleven-dimensional metric into a $AdS_7 \times S^4$ part and a perturbation, denoted as $g^{(0)}$ and h respectively:

$$ds^2 = g_{MN}\,dx^M dx^N = \left(g^{(0)}_{MN} + h_{MN}\right) dx^M dx^N. \tag{2.3.2}$$

We use the FG coordinate chart (2.1.21) where we can identify $\tilde{\theta}$ as the polar angle on S^4. The Wilson surface preserves an $SO(4)$ subgroup of the R-symmetry and so does the bubbling geometry. Therefore, performing the harmonic decomposition on the eleven-dimensional fields we obtain contributions only from spherical harmonics invariant under $SO(4)$. These depend only on the polar angle $\tilde{\theta}$. The zero mode on S^4 of an eleven-dimensional field that only has nontrivial dependence on $\tilde{\theta}$ can be expressed as

$$\bar{\phi}(x) = \frac{\int_0^\pi d\tilde{\theta}\ \phi(x,\tilde{\theta})\sin^3\tilde{\theta}}{\int_0^\pi d\tilde{\theta}\sin^3\tilde{\theta}} \tag{2.3.3}$$

[3]There is a 'doubleton' field dual to an operator of dimension $\Delta = 2$, but such fields are free and decouple from the dynamics.

The reduced seven-dimensional metric, which satisfies the seven-dimensional linearized Einstein equation, is given by the following combination[4]

$$ds_7^2 = \left[\left(1 + \frac{1}{5}\bar{\pi}\right) g_{\mu\nu}^{(0)} + \bar{h}_{\mu\nu}\right] dx^\mu dx^\nu \tag{2.3.4}$$

Here, $g^{(0)}$ is the AdS_7 vacuum metric whereas $\bar{h}_{\mu\nu}$ is the zero mode of the fluctuations in the seven dimensions. The field $\bar{\pi}$ is the zero mode of the trace of the fluctuations of the metric along the S^4 directions:

$$\pi(x, \tilde{\theta}) \equiv h^{ab}\, g_{ab}^{(0)} \tag{2.3.5}$$

The factor of $\frac{1}{5}$ in (2.3.4) comes from a Weyl rescaling to bring the KK reduced metric to the Einstein frame in seven dimensions.

The calculation of the one point function of the stress tensor from the seven-dimensional metric (2.3.4) utilizes the standard method of holographic renormalization. In our case $\bar{\pi}$ vanishes, and consequently the reduced metric is already in the FG form

$$ds_7^2 = \frac{4L^2}{u^2}\left(du^2 + g_{ij}dx^i dx^j\right) \tag{2.3.6}$$

where the large r limit corresponds to $u \to 0$ and the metric g_{ij} can be expressed as a power series in u. The holographic stress tensor can then be calculated immediately using the formulae for $d = 6$ given in [30]. For the convenience of the reader and completeness we present the details of these calculations in appendix A.2. We have also checked that the counter-term approach developed in [83] gives the same result for the stress tensor. The final result for the change in the expectation value of the stress tensor in the presence of the

[4]Our index conventions are: $M, N, \ldots$ are eleven-dimensional indices, $\mu, \nu, \ldots$ are AdS_7 indices and $a, b, \ldots$ are S^4 indices.

Wilson surface on $AdS_3 \times S^3$ is

$$\Delta\langle T_{ij}\rangle\, dx^i dx^j = \frac{N^3}{160\pi^3}\left(16 + 3m_2^2 - 8m_3\right)\left(ds^2_{AdS_3} - ds^2_{S^3}\right) \tag{2.3.7}$$

Note that the dependence of N^3 is as expected from a back-reacted supergravity solution. In addition, the expression depends only on the first two nontrivial moments m_2, m_3 of the bubbling solution. The stress tensor contribution has a form that respects the $so(2,2|\mathbb{R}) \oplus so(4|\mathbb{R})$ of the Wilson surface and is traceless in line with the absence of a conformal anomaly on $AdS_3 \times S^3$. The use of this result is two-fold. First, any nontrivial holographic observable is useful to understand $(2,0)$ theory better. Second, the stress tensor expectation value is an important ingredient in the calculation of the entanglement entropy using the replica trick.

2.4 Expectation value of the Wilson surface operator

The expectation value for the Wilson surface operator can be obtained from the following formula:

$$\langle W_\Gamma\rangle = \exp\left[-(S_{11\mathrm{D}} - S^{(0)}_{11\mathrm{D}})\right] \tag{2.4.1}$$

where $S_{11\mathrm{D}}$ is the eleven-dimensional supergravity action evaluated on a general bubbling solution and $S^{(0)}_{11\mathrm{D}}$ is the action evaluated on the $AdS_7 \times S^4$ vacuum. The action is given by

$$\begin{aligned} S_{11\mathrm{D}} = \frac{1}{8\pi G_N^{(11)}}\Bigg[&\frac{1}{2}\int d^{11}x\,\sqrt{g}\left(R - \frac{1}{48}F_{MNPQ}F^{MNPQ}\right) - \frac{1}{12}\int C\wedge F\wedge F \\ &+ \int d^{10}x\,\sqrt{\gamma}\,K\Bigg] \end{aligned} \tag{2.4.2}$$

The final term is the Gibbons-Hawking boundary term, which is necessary to make the variational principle well-defined for spacetimes with boundary. The metric functions for

the bubbling solution are given in (2.1.5) and the four-form field strength is given by

$$F = (f_1)^3 g_{1m}\, \omega_{AdS_3} \wedge e^m + (f_2)^3 g_{2m}\, \omega_{S^3} \wedge e^m + (f_3)^3 g_{3m}\, \omega_{\tilde{S}^3} \wedge e^m \tag{2.4.3}$$

where e^m are the vielbeins on the Riemann surface Σ, ω_X denotes the volume form for a unit-radius space X and the expressions for g_{Im} with $I = 1, 2, 3$ can be found in appendix A.3.

2.4.1 Action as a total derivative

First we demonstrate the well-known fact that the on-shell action of eleven-dimensional supergravity is a total derivative. Using the Einstein equation, the Ricci scalar can be eliminated from the bulk term of the on-shell supergravity action (2.4.2):

$$S_{\text{11D,bulk}} = \frac{1}{16\pi G_N^{(11)}} \int \Big(-\frac{1}{3} F \wedge *F - \frac{1}{6} C \wedge F \wedge F \Big) \tag{2.4.4}$$

The equation of motion can be expressed as

$$d * F + \frac{1}{2} F \wedge F = 0 \tag{2.4.5}$$

The first term in the action can then be written as

$$\begin{aligned} F \wedge *F &= dC \wedge *F \\ &= d(C \wedge *F) + C \wedge d * F \\ &= d(C \wedge *F) - \frac{1}{2} C \wedge F \wedge F \end{aligned} \tag{2.4.6}$$

Plugging this expression into (2.4.4) the $C \wedge F \wedge F$ terms cancel and the on-shell value of the action is indeed a total derivative:

$$S_{\text{11D,bulk}} = -\frac{1}{48\pi G_N^{(11)}} \int d(C \wedge *dC) \tag{2.4.7}$$

The duals of the three contributions to the field strength are given by

$$
\begin{aligned}
*F_{(1)} &= \frac{f_2^3 f_3^3}{f_1^3}\Big(r\partial_r b_1 d\theta - \frac{1}{r}\partial_\theta b_1 dr\Big) \wedge \omega_{S^3} \wedge \omega_{\tilde{S}^3} \\
*F_{(2)} &= \frac{f_1^3 f_3^3}{f_2^3}\Big(r\partial_r b_2 d\theta - \frac{1}{r}\partial_\theta b_2 dr\Big) \wedge \omega_{AdS_3} \wedge \omega_{\tilde{S}_3} \\
*F_{(3)} &= \frac{f_1^3 f_2^3}{f_3^3}\Big(- r\partial_r b_3 d\theta + \frac{1}{r}\partial_\theta b_3 dr\Big) \wedge \omega_{AdS_3} \wedge \omega_{S^3}
\end{aligned}
\tag{2.4.8}
$$

Using the expression for the metric functions f_i from (2.1.5), the ratios appearing in (2.4.8) can be expressed as

$$
\begin{aligned}
\left(\frac{f_2 f_3}{f_1}\right)^3 &= \frac{h W_-^2}{4W_+(1-|G|^2)} \\
\left(\frac{f_1 f_3}{f_2}\right)^3 &= \frac{h W_+^2}{4W_-(1-|G|^2)} \\
\left(\frac{f_1 f_2}{f_3}\right)^3 &= \frac{16h(1-|G|^2)^2}{W_+ W_-}
\end{aligned}
\tag{2.4.9}
$$

Since the volume forms on the AdS_3 and the three-spheres are all closed, the bulk action (2.4.7) reduces to a total derivative over the two-dimensional Riemann surface Σ. In terms of the polar coordinates r, θ, which were introduced in section 2.1.1 by setting $w = re^{i\theta}$, the bulk part of the action can be written as follows:

$$
\begin{aligned}
S_{\text{11D,bulk}} &= -\frac{1}{48\pi G_N^{(11)}} \int d(C \wedge *F) \\
&= -\frac{1}{48\pi G_N^{(11)}} \int (\partial_r a_r + \partial_\theta a_\theta)\, dr \wedge d\theta \wedge \omega_{AdS_3} \wedge \omega_{S^3} \wedge \omega_{\tilde{S}^3}
\end{aligned}
\tag{2.4.10}
$$

where a_r and a_θ are given by

$$
\begin{aligned}
a_r &= -\frac{f_2^3 f_3^3}{2f_1^3} r\partial_r(b_1^2) + \frac{f_1^3 f_3^3}{2f_2^3} r\partial_r(b_2^2) + \frac{f_1^3 f_2^3}{2f_3^3} r\partial_r(b_3^2) \\
a_\theta &= -\frac{f_2^3 f_3^3}{2f_1^3} \frac{1}{r}\partial_\theta(b_1^2) + \frac{f_1^3 f_3^3}{2f_2^3} \frac{1}{r}\partial_\theta(b_2^2) + \frac{f_1^3 f_2^3}{2f_3^3} \frac{1}{r}\partial_\theta(b_3^2)
\end{aligned}
\tag{2.4.11}
$$

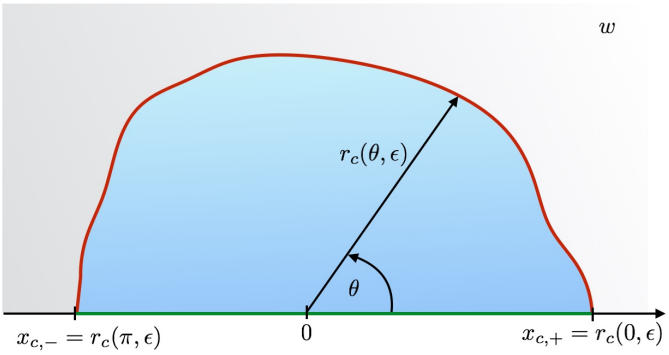

Figure 2.4: The two boundary components: the cut-off surface (red) and the boundary along $x \equiv \mathrm{Re}\, w$ (green).

We have shown that the on-shell action can be written as a boundary term: the bulk term reduces to a total derivative and the Gibbons-Hawking term is also boundary term. The boundary in the w plane has two pieces (see figure 2.4). First one has the cut-off surface parametrized by $r_c(\theta, \varepsilon)$, where ε is the FG cut-off. Second one has the real line, which is parametrized in r, θ coordinates by $r \in [0, r_c(0, \pi, \varepsilon)]$ and $\theta = 0, \pi$, respectively. In the following we will evaluate the contribution from each piece in turn.

2.4.2 Gibbons-Hawking term

The Gibbons-Hawking term in (2.4.2) is the boundary term that has to be added to the action in order to give a well-defined gravitational variational principle. A ten-dimensional surface defined by a constraint

$$F\left(x^M\right) = 0 \tag{2.4.12}$$

can be parameterized by a set of coordinates σ^α. The induced metric is defined via

$$\gamma_{\alpha\beta} = e^M_\alpha \, e^N_\beta \, g_{MN}, \quad e^M_\alpha = \frac{\partial x^M}{\partial \sigma^\alpha} \tag{2.4.13}$$

and its determinant is given by

$$\sqrt{\gamma} = \frac{1}{z^3}\, 2\rho f_1^3 f_2^3 f_3^3\, \omega_{S^3}\, \omega_{\tilde{S}^3} \tag{2.4.14}$$

The normal vector (which we assume to be always space-like) is defined via

$$\hat{n}_M = \frac{1}{\sqrt{\frac{\partial F}{\partial x^N}\frac{\partial F}{\partial x^P} g^{NP}}}\, \frac{\partial F}{\partial x^M} \tag{2.4.15}$$

The extrinsic curvature and its trace are defined via

$$K_{\alpha\beta} = (\nabla_M \hat{n}_N)\, e_\alpha^M\, e_\beta^N, \quad K = \gamma^{\alpha\beta} K_{\alpha\beta} \tag{2.4.16}$$

As discussed above the boundary has two components, which we now study in turn.

Real line contribution

The real line is defined by $F = y = 0$, where $w = x + i\, y$, and the induced metric is simply obtained by dropping the g_{yy} component of the eleven-dimensional metric. The normal vector is given by

$$\hat{n}^M = \frac{1}{2\rho}\, \delta_y^M \tag{2.4.17}$$

Using the form of the metric it is straightforward to determine the trace of the extrinsic curvature

$$K = \frac{1}{L^3}\left(\frac{3\partial_y f_1}{2\rho f_1} + \frac{3\partial_y f_2}{2\rho f_2} + \frac{3\partial_y f_3}{2\rho f_3} + \frac{\partial_y \rho}{2\rho^2}\right) \tag{2.4.18}$$

The Gibbons-Hawking term along the real line can be determined from the expansion of the metric functions in the $y \to 0$ limit given. This can be obtained from the formulae in appendix A.4. We do not present the details of this calculation but just present the final

result which is

$$\int d^{10}x\,\sqrt{\gamma}\,K = \lim_{y\to 0}\mathrm{Vol}(S^3)^2\,\mathrm{Vol}(AdS_3)\,L^9\int dx\,\left[24y^2+O(y^3)\right]=0 \tag{2.4.19}$$

which vanishes. This result was expected since at any point on the real line, one of the three-spheres shrinks to zero size and the space closes off.

Large r contribution

In this section we determine the contribution of the Gibbons-Hawking term from the large r cut-off surface defined by the equation

$$F(r,\theta) = r - r_c(\theta,\varepsilon) = 0 \tag{2.4.20}$$

for small ε, where $r_c(\theta,\varepsilon)$ is given by (2.1.26). Hence the surface extends along AdS_3 and the two three-spheres and the induced metric in these directions is identical to the metric. We choose to use θ to parametrize the cut-off surface and find the following nontrivial components of the vielbein e^M_α:

$$e^\alpha_\beta = \delta^\alpha_\beta, \quad e^r_\theta = \partial_\theta\, r_c(\theta,\varepsilon) \tag{2.4.21}$$

Using the formulae (2.4.15) and (2.4.16) we can calculate $\sqrt{\gamma}\,K$ and expand the result in a power series in ε:

$$\begin{aligned}\sqrt{\gamma}\,K = L^9\sin^3\theta\Big\{&\frac{192}{\varepsilon^6}+\frac{96m_2\cos\theta}{\varepsilon^4}\\ &+\frac{-3(16-3m_2^2-40m_3)+5\cos 2\theta(16+3m_2^2+40m_3)}{8\varepsilon^2}\\ &\frac{1}{4}\cos\theta\left[-8m_2+m_2^3-6m_2m_3+10m_4\right.\\ &\left.+\cos 2\theta(24m_2+m_2^3-10m_2m_3+70m_4)\right]\Big\}+O\left(\varepsilon^2\right)\end{aligned} \tag{2.4.22}$$

After performing the integral over θ we find that the Gibbons-Hawking term is determined completely by the contribution at large r, namely

$$S_{\rm GH} \equiv \frac{1}{8\pi G_N^{(11)}} \int d^{10}x\, \sqrt{\gamma}\, K = \frac{L^9}{8\pi G_N^{(11)}} \,\mathrm{Vol}(S^3)^2\, \mathrm{Vol}(AdS_3) \left[\frac{256}{\varepsilon^6} - \frac{16}{\varepsilon^2} + O\left(\varepsilon^2\right)\right] \quad (2.4.23)$$

2.4.3 Bulk supergravity action

The bulk part of the eleven-dimensional action integral (2.4.10) can be reduced to the following form:

$$\begin{aligned} S_{\rm 11D,bulk} &= -\frac{1}{48\pi G_N^{(11)}} \,\mathrm{Vol}(S^3)^2\, \mathrm{Vol}(AdS_3) \int d\theta \int dr\, (\partial_r a_r + \partial_\theta a_\theta) \\ &= -\frac{1}{48\pi G_N^{(11)}} \,\mathrm{Vol}(S^3)^2\, \mathrm{Vol}(AdS_3) \oint_{\partial\Sigma(\varepsilon)} d\tau\, (\hat{n}_r a_r + \hat{n}_\theta a_\theta) \end{aligned} \quad (2.4.24)$$

Here $\mathrm{Vol}(AdS_3)$ is the (regularized) volume of AdS_3 since we consider the field theory on $AdS_3 \times S^3$ and $\hat{n}_i$ is the unit outward normal. If a boundary component is parametrized by $r(\tau), \theta(\tau)$ then the unit outward normal vector is defined as

$$\hat{n}_r = \frac{d\theta}{d\tau}\, d\tau, \qquad \hat{n}_\theta = -\frac{dr}{d\tau}\, d\tau \quad (2.4.25)$$

There are three components to the boundary:

$$\begin{aligned} &\partial\Sigma_1 : \theta \in [0,\pi],\ r = r_c(\theta,\varepsilon) \\ &\partial\Sigma_2 : \theta = 0, r \in [0, r_c(0,\varepsilon)] \\ &\partial\Sigma_3 : \theta = \pi,\ r \in [0, r_c(\pi,\varepsilon)] \end{aligned} \quad (2.4.26)$$

The contribution of $\partial\Sigma_1$ corresponds to the cut-off surface, which we parametrize by $\theta \in [0,\pi]$ and $r = r_c(\theta,\varepsilon)$ as in section 2.4.2. The θ dependence of r leads to an additional contribution

to the normal vector

$$\begin{aligned} S_{(\text{cut})} &= -\frac{1}{48\pi G_N^{(11)}} \operatorname{Vol}(S^3)^2 \operatorname{Vol}(AdS_3) \oint_{\partial\Sigma_1(\varepsilon)} d\tau \left(\hat{n}_r a_r + \hat{n}_\theta a_\theta\right) \\ &= -\frac{1}{48\pi G_N^{(11)}} \operatorname{Vol}(S^3)^2 \operatorname{Vol}(AdS_3) \int_0^\pi d\theta \left(a_r - \frac{\partial r_c}{\partial\theta} a_\theta\right)\Big|_{r=r_c(\theta,\varepsilon)} \end{aligned} \tag{2.4.27}$$

The integrations over $\partial\Sigma_2$ and $\partial\Sigma_3$ combine to give the integration over the real line. Putting the two together and going back to the half-plane coordinates we find

$$\oint_{\partial\Sigma_2(\varepsilon)+\partial\Sigma_3(\varepsilon)} d\tau \left(\hat{n}_r a_r + \hat{n}_\theta a_\theta\right) = -\int_0^{r_c(\theta=0,\varepsilon)} dr\, \frac{1}{r}\, a_\theta\Big|_{\theta=0} + \int_0^{r_c(\theta=\pi,\varepsilon)} dr\, \frac{1}{r}\, a_\theta\Big|_{\theta=\pi} \tag{2.4.28}$$

Using $\frac{1}{r}\partial_\theta|_{\theta=0} = \partial_y$ and $\frac{1}{r}\partial_\theta|_{\theta=\pi} = -\partial_y$ and the expressions for a_r and a_θ given in (2.4.11), the contribution from the real line becomes

$$S_{(x)} = \frac{1}{48\pi G_N^{(11)}} \operatorname{Vol}(S^3)^2 \operatorname{Vol}(AdS_3) \int_{r_c(\theta=\pi,\varepsilon)}^{r_c(\theta=0,\varepsilon)} dx \left(-\frac{f_2^3 f_3^3}{2f_1^3}\partial_y(b_1^2) + \frac{f_1^3 f_3^3}{2f_2^3}\partial_y(b_2^2) + \frac{f_1^3 f_2^3}{2f_3^3}\partial_y(b_3^2)\right) \tag{2.4.29}$$

Large r contribution

Using the expansion of a_r and a_θ at large r one finds the integrand of (2.4.27) can be written as

$$\begin{aligned} \frac{1}{L^9}\left(a_r - \frac{\partial r_c}{\partial\theta} a_\theta\right)\Big|_{r=r_c(\theta,\varepsilon)} = {} & \frac{5\sin\theta\cos^2\theta(\cos 2\theta - 5)(16 + 3m_2^2 - 8m_3)}{4\varepsilon^2} \\ & + \frac{\sin 2\theta}{128}\Big[(2144m_2 + 445m_2^3 - 1760m_2m_3 - 860m_4 \\ & + 20\cos 2\theta\left(64m_2 + 15m_2^3 - 80m_2m_3 - 60m_4\right) \\ & + \cos 4\theta\left(-96m_2 - 25m_2^3 + 160m_2m_3 + 140m_4\right)\Big] \\ & + O\left(\varepsilon^2\right) \end{aligned} \tag{2.4.30}$$

After performing the integration over θ the finite terms above drop out and and we are left with

$$S_{(\text{cut})} = -\frac{L^9}{48\pi G_N^{(11)}} \text{Vol}(S^3)^2 \, \text{Vol}(AdS_3) \left[\frac{-64 - 12m_2^2 + 32m_3}{\varepsilon^2} + O\left(\varepsilon^2\right) \right] \tag{2.4.31}$$

Real line contribution

The expression from the real line can be obtained from expanding the integrand of (2.4.29) in the $y \to 0$ limit. The behavior of the integrand in this limit depends on the interval x is located in. We define

$$\begin{aligned} \mathcal{I}_0 &= [-\infty, \xi_1] \cup [\xi_2, \xi_3] \cup \cdots \cup [\xi_{2n}, +\infty] \\ \mathcal{I}_+ &= [\xi_1, \xi_2] \cup [\xi_3, \xi_4] \cup \cdots \cup [\xi_{2n-1}, \xi_{2n}] \end{aligned} \tag{2.4.32}$$

We present the details of the calculation in appendix A.4, with the final result given by

$$\lim_{y\to 0} \left(-\frac{f_2^3 f_3^3}{2f_1^3} \partial_y(b_1^2) + \frac{f_1^3 f_3^3}{2f_2^3} \partial_y(b_2^2) + \frac{f_1^3 f_2^3}{2f_3^3} \partial_y(b_3^2) \right) = \begin{cases} \frac{16L^9(2g_1^3+g_3)\phi_0}{(g_1^2-g_2)(g_1^2+g_2)} & x \in \mathcal{I}_0 \\ \\ \frac{32L^9(g_1^3+3g_1g_2-g_3)(\phi_0+2x)}{(g_1^2+g_2)(g_1^2+2g_2)} & x \in \mathcal{I}_+ \end{cases} \tag{2.4.33}$$

where the g_i and ϕ_0 are functions of x and can be found in (A.4.3) and (A.4.5), respectively. In this limit the integrand (2.4.33) is nonsingular for any finite x on the real line. However, the integrand grows as $x \to \pm\infty$ and we can extract the divergent behavior coming from the region near the cut-off. We determine the divergent contributions in (A.4.14) and we write the result as

$$S_{(x)} = +\frac{L^9}{48\pi G_N^{(11)}} \text{Vol}(S^3)^2 \, \text{Vol}(AdS_3) \left[-\frac{256}{\varepsilon^6} + \frac{80 - 12m_2^2 + 32m_3}{\varepsilon^2} + \mathcal{F} + O\left(\varepsilon^2\right) \right] \tag{2.4.34}$$

The finite term $\mathcal{F}$ can in principle be determined by performing the x-integral for the full integration region and subtracting the divergent contributions given above, i.e.

$$\mathcal{F} \equiv \lim_{\varepsilon\to 0}\left\{\sum_{x\in\mathcal{I}_+}\int dx\,\frac{32(g_1^3+3g_1g_2-g_3)(\phi_0+2x)}{(g_1^2+g_2)(g_1^2+2g_2)}+\sum_{x\in\mathcal{I}_0}\int dx\,\frac{16(2g_1^3+g_3)\phi_0}{(g_1^2-g_2)(g_1^2+g_2)}\right.$$
$$\left.-\left(-\frac{256}{\varepsilon^6}+\frac{80-12m_2^2+32m_3}{\varepsilon^2}\right)\right\} \tag{2.4.35}$$

The last two terms remove the divergent contributions from the integral over $\mathcal{I}_0$ that is regulated for large positive x by $x < x_{c,+}(\varepsilon)$ and for large negative x by $x > x_{c,-}(\varepsilon)$.

At this point we have not been able to find a closed expression for these integrals, but they can be evaluated numerically. If a relation to a matrix model calculation exists these integrals may be related to the resolvent. However, as no proposal for a matrix model exists at present we have not pursued the evaluation further and leave this for future work.

2.4.4 Final result

Combining all the contributions to the action, which can be found in (2.4.23), (2.4.31) and (2.4.34), we obtain for the on-shell action

$$\begin{aligned} S_{11\mathrm{D}} &= \frac{L^9}{3\pi G_N^{(11)}}\,\mathrm{Vol}(S^3)^2\,\mathrm{Vol}(AdS_3)\left[\frac{80}{\varepsilon^6}+\frac{3}{\varepsilon^2}+\frac{\mathcal{F}}{16}+O\left(\varepsilon^2\right)\right] \\ &= \frac{N^3}{12\pi}\,\mathrm{Vol}(AdS_3)\left(\frac{80}{\varepsilon^6}+\frac{3}{\varepsilon^2}+\frac{\mathcal{F}}{16}+O\left(\varepsilon^2\right)\right) \end{aligned} \tag{2.4.36}$$

The finite contribution is given by (2.4.35). This can be evaluated exactly for the vacuum and the result is

$$\mathcal{F}_{(0)} = -64 \tag{2.4.37}$$

Thus, using (2.4.1) we can express our final result for the expectation value of the Wilson surface operator as

$$\log \langle W_\Gamma \rangle = -\frac{N^3}{192\pi} \mathrm{Vol}(AdS_3) \left(\mathcal{F} + 64\right) \tag{2.4.38}$$

Note that the power divergences in ε are independent of the details of the bubbling geometry and so cancel in the subtraction. However, the result is proportional to the infinite volume of AdS_3, which is regulated by the cut-off $z = \eta$ introduced in the entanglement entropy calculation in (2.2.12).

As is the case for the stress tensor contribution, the expectation value of the Wilson surface operator constitutes a potentially useful holographic observable of the $(2,0)$ theory. This holographic result may be compared to direct calculations in this theory as well as be applied to the replica calculation of the entanglement entropy. It would be very interesting to study localization and related methods to calculate the expectation value of Wilson surface operators in the future.

2.5 Summary

In this chapter we have calculated the holographic entanglement entropy for the six-dimensional $(2,0)$ theory in the presence of a Wilson surface. In particular, we found that the change of the entanglement entropy due to the presence of the Wilson surface is given by

$$\Delta S_{\mathcal{A}} = \frac{4N^3}{3} \left[\frac{16 + 3m_2^2 - 8m_3}{320} - \frac{1}{16} \sum_{i<j} (-1)^{i+j} |\xi_i - \xi_j|^3 - \frac{1}{2} \right] \log\left(\frac{2R}{\eta}\right) \tag{2.5.1}$$

We also computed two other holographic observables. The results are the stress tensor in the presence of the Wilson surface for the $AdS_3 \times S^3$ boundary coordinates given by

$$\Delta \langle T_{ij} \rangle \, dx^i dx^j = \frac{N^3}{160\pi^3} \left(16 + 3m_2^2 - 8m_3\right) \left(ds^2_{AdS_3} - ds^2_{S^3}\right) \tag{2.5.2}$$

and the expectation value of the Wilson surface operator, found by evaluating the regularized on-shell supergravity action:

$$\log \langle W_\Gamma \rangle = -\frac{N^3}{192\pi} \mathrm{Vol}(AdS_3) \left(\mathcal{F} + 64\right) \tag{2.5.3}$$

The $m_{2,3}$ are quantities that depend on the parameters ξ_i of a general bubbling solution. We notice that the final term in the result for the entanglement entropy (2.2.17) cannot in general be expressed in terms of the moments m_k . The cut-off η is the distance from the Wilson surface, as discussed in more detail in section 2.2.3. Also, $\mathcal{F}$ is a finite one-dimensional integral that is defined in section 2.4.3. While it is possible to evaluate this finite part for $n = 1$ and $n = 2$ in closed form, we have been unable to evaluate it in general. Some numerical experiments however indicate that this integral does not have a simple expression in terms of the moments m_k or the final term in the entanglement entropy (2.2.17).

It would be interesting to see whether the calculation of the entanglement entropy in the presence of a Wilson loop in $SU(N)$ $\mathcal{N} = 4$ SYM due to Lewkowycz and Maldacena [62] generalizes to the Wilson surface in the $(2, 0)$ theory. Recall that their calculation used the replica trick and involved the expectation value of the Wilson loop and the stress tensor in the presence of the Wilson loop on the space $S^1 \times H^3$. A generalization would most likely start from the expectation value the Wilson surface and the stress tensor in the presence of the Wilson surface on $S^1 \times H^5$. Since our holographic calculation gives these two quantities for the $AdS_3 \times S^3$ boundary, if it is possible to map the results to $S^1 \times H^5$ then it should be possible to compare the Lewkowycz and Maldacena calculation to the holographic entanglement entropy calculation we have performed. One complication is that unlike a one-dimensional Wilson loop, the two-dimensional Wilson surface has a conformal anomaly [84–86] and it is not clear how to determine its contribution in our case. A simpler case in which to consider the anomaly might be the case of an abelian Wilson surface, as studied in [86].

Chapter 3

Surface Defects Entanglement Entropy

In this chapter we focus on another kind of surface defects, which is the disorder-type. As described in 1.2.2, these cannot be written as operator insertions written in terms of the fundamental fields of the theory. Instead, they are characterized by the singular behavior of the fundamental fields close to the defect. One example is the 't Hooft loop in gauge theories, which is mapped to the ordered-type Wilson loop under S-duality [87].

The case of interest here is the disorder-type surface defects in four-dimensional $\mathcal{N} = 4$ $U(N)$ SYM theory constructed in [41, 88]. Their dual description as bubbling geometries of type IIB supergravity was identified in [42] using the solutions constructed in [43, 89]. For notational ease we will drop the qualifier 'disorder-type' and simply call these 'surface defects'.

The goal is to calculate the holographic entanglement entropy in the presence of the surface defects for $\mathcal{N} = 4$ SYM and compare them to the result obtained by mapping the entanglement entropy to a thermal entropy as in [90].The geometric setup of the surface defect is best visualized in $\mathbb{R}^4$. At fixed time the entangling region $\mathcal{A}$ is a three-dimensional ball with a spherical boundary. The surface defect Σ extends in one spatial direction (and

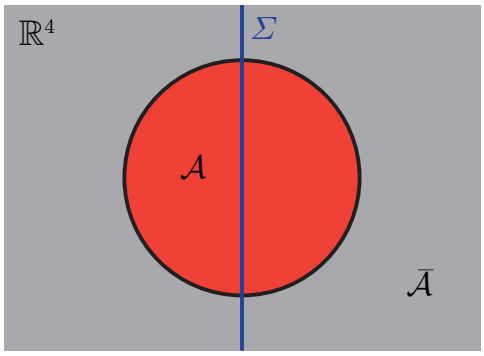

Figure 3.1: Geometry of the entangling region and surface defect in $\mathbb{R}^4$. The entangling region $\mathcal{A}$ is a three-dimensional ball with a two-sphere boundary. The surface defect extends along a spatial line and bisects the two-sphere.

time). We depict the setup in figure 3.1, with one spatial and the time direction suppressed. Notice that the entanglement setup is similar to the one used for the Wilson surface in figure 2.1. We also use different geometries, namely $AdS_3 \times S^1$ and $S^1 \times H^3$, which are related to $\mathbb{R}^4$ by a coordinate change and Weyl rescaling.

The rest of the chapter is outlined as follows: in section 3.1 we review the field theory description of half-BPS surface defects in $\mathcal{N} = 4$ SYM theory. In section 3.2 we review the bubbling supergravity solutions dual to these defects. In section 3.3 we calculate the entanglement entropy for a spherical entangling region that intersects the surface defect. In section 3.4 we calculate the expectation value of the surface defect by evaluating the on-shell supergravity action on the bubbling solution and review the result for the one-point function of the stress energy tensor in the presence of a surface defect. In section 3.5 the expectation values are used to calculate the entanglement entropy following the method of Lewkowycz and Maldacena [90] which we then compare with our holographic result. [1]

3.1 Review of surface defects in $\mathcal{N} = 4$ SYM

In this section we review the construction of half-BPS surface defects in $\mathcal{N} = 4$ SYM theories first obtained in [41] and studied in detail holographically in [1, 42].

[1] Notation: To avoid conflict in notation, in this chapter we denote the Ryu-Takayanagi minimal surface as $\mathcal{M}$.

The defects are supported on a two-dimensional surface Σ in $\mathbb{R}^4$. They are disorder-type operators so, unlike Wilson line operators, cannot be written as an integral of the fundamental gauge fields over Σ. Instead, they are characterized by singularities of the gauge fields and/or scalar fields at the surface Σ as well as holonomies along cycles in the space normal to the surface. Furthermore, we are interested in half-BPS defects that preserve half the superconformal symmetry $PSU(1,1|2) \times PSU(1,1|2)$ inside $PSU(2,2|4)$. For such superconformal defects it is possible to perform a Weyl transformation from $\mathbb{R}^4$ to $AdS_3 \times S^1$, in which the surface Σ is mapped to the boundary of AdS_3. This has two advantages: first, the singularities of the fields along Σ are mapped to boundary behavior in AdS_3 and second, the $AdS_3 \times S^1$ geometry appears naturally in the dual bubbling supergravity solutions that we will review in section 3.2.

The half-BPS surface defect is characterized by the following data. The non-trivial conditions on the gauge field and scalars break the $U(N)$ gauge group to the Levi subgroup $L = \prod_{i=1}^{M} U(N_i)$ with M factors. Near the boundary of AdS_3 the gauge field has a non-vanishing component along the $U(1)$ coordinate, which we denote by ψ:

$$A_\psi = \text{diag}\left\{\alpha_1 \mathbb{1}_{N_1}, \alpha_2 \mathbb{1}_{N_2}, \ldots, \alpha_M \mathbb{1}_{N_M}\right\} \quad \text{with} \quad \sum_{i=1}^{M} N_i = N \tag{3.1.1}$$

There are M theta angles for the M unbroken $U(1)$ factors (see [1, 42] for details), which can be parametrized by the matrix

$$\eta = \text{diag}\left\{\eta_1 \mathbb{1}_{N_1}, \eta_2 \mathbb{1}_{N_2}, \ldots, \eta_M \mathbb{1}_{N_M}\right\} \tag{3.1.2}$$

A complex scalar, which we can choose as $\Phi = \phi_5 + i\phi_6$, has non-trivial behavior along the S^1:

$$\Phi = \frac{e^{-i\psi}}{\sqrt{2}} \text{ diag}\left\{(\beta_1 + i\gamma_1)\, \mathbb{1}_{N_1}, (\beta_2 + i\gamma_2)\, \mathbb{1}_{N_2}, \ldots, (\beta_M + i\gamma_M)\, \mathbb{1}_{N_M}\right\} \tag{3.1.3}$$

To summarize, the surface defect is characterized by the set of M integers N_i and a set of

$4M$ real parameters $(\alpha_i, \eta_i, \beta_i, \gamma_i)$ with $i = 1, 2, \ldots, M$.

We also cite the results for the expectation value of the surface defect and the one-point function of the stress tensor calculated in [1] in order to compare them with the results of our holographic calculations. In the semiclassical approximation the expectation value of the surface operator is determined by evaluating the classical $N = 4$ SYM action on the field background. It was shown in [1] that this gives zero and hence

$$\langle \mathcal{O}_\Sigma \rangle = e^{-S_{YM}}|_{\text{surface}} = 1 \tag{3.1.4}$$

In addition, several one-point functions of local operators and Wilson line operators in the presence of the surface defect were calculated in [1]. The only one relevant here is the one-point function of the stress tensor, which takes the following form due to $AdS_3 \times S^1$ symmetry and the fact that the stress tensor is traceless:

$$\langle T_{\mu\nu} \rangle_\Sigma \, dx^\mu \, dx^\nu = h_\Sigma \left(ds^2_{AdS_3} - 3 \, d\psi^2 \right) \tag{3.1.5}$$

The semiclassical value for the scaling weight h_Σ is found by evaluating the stress tensor of $\mathcal{N} = 4$ SYM on the field background:

$$h_\Sigma = -\frac{2}{3 g^2_{YM}} \sum_{i=1}^{M} N_i (\beta_i^2 + \gamma_i^2) \tag{3.1.6}$$

3.2 Review of bubbling supergravity solutions

In [1, 42] it was proposed that the solution found in [43, 89] is the holographic dual of the surface defect operator. The solution is constructed as a $AdS_3 \times S^3 \times U(1)$ fibration over a three-dimensional space with boundary parametrized by the coordinates y, x_1, x_2, where the

boundary is located at $y = 0$. The metric takes the form

$$ds^2 = y\sqrt{\frac{2f+1}{2f-1}}\, ds^2_{AdS_3} + y\sqrt{\frac{2f-1}{2f+1}}\, ds^2_{S^3} + \frac{2y}{\sqrt{4f^2-1}}\,(d\chi + V)^2 + \frac{\sqrt{4f^2-1}}{2y}\, ds^2_X \quad (3.2.1)$$

where the AdS_3 metric is in Poincaré coordinates and the metric on the base is simply the flat Euclidean metric:

$$ds^2_{AdS_3} = \frac{dt^2 + dl^2 + dz^2}{z^2}, \quad ds^2_X = (dy^2 + dx_1^2 + dx_2^2), \quad (3.2.2)$$

The function $f(y, x_1, x_2)$ satisfies a linear partial differential equation with M sources located in the bulk of the base space X at $y = y_i, x = \vec{x}_i$ with $i = 1, 2, \ldots, M$:

$$\partial_1^2 f + \partial_2^2 f + y\partial_y\left(\frac{\partial_y f}{y}\right) = \sum_{i=1}^{M} 2\pi y_i\, \delta(y - y_i)\, \delta^2(\vec{x} - \vec{x}_i) \quad (3.2.3)$$

V is a one-form on X that can be obtained from f by solving

$$dV = \frac{1}{y} \star_3 df \quad (3.2.4)$$

Note that (3.2.4) only fixes V up to an exact form and the freedom to redefine $V \to V + d\omega$ will be important to obtain a manifestly asymptotically AdS metric as detailed in appendix B.1.1. The only other non-trivial field is the self-dual five-form field strength, which takes the form

$$\begin{aligned} F_5 = &-\frac{1}{4}\Big(d\Big[y^2\frac{2f+1}{2f-1}(d\chi + V)\Big] - y^3 \star_3 d\Big[\frac{f+1/2}{y^2}\Big]\Big) \wedge \omega_{AdS_3} \\ &-\frac{1}{4}\Big(d\Big[y^2\frac{2f-1}{2f+1}(d\chi + V)\Big] - y^3 \star_3 d\Big[\frac{f-1/2}{y^2}\Big]\Big) \wedge \omega_{S_3} \end{aligned} \quad (3.2.5)$$

where $\star_3$ denotes the Hodge dual[2] in the-three dimensional base space X with metric given by (3.2.2).

This solution was first constructed in [89] as a double analytic continuation of the LLM

[2]The sign of the Hodge dual is fixed by $\star_3 dy = dx_1 \wedge dx_2$ and cyclic permutations of dy, dx_1 and dx_2.

solution [43]. Indeed (3.2.1) becomes the LLM metric by continuing the $U(1)$ fiber coordinate to a time like coordinate and continuing AdS_3 to S^3. Note however that the boundary condition on the function f is different: the AdS_3 volume can never shrink to zero size in a smooth solution so we must have $f \to \frac{1}{2}$ as y approaches the boundary of X. Hence for the bubbling surface solution the coloring of the boundary determined by the regions where $\lim_{y\to 0} f = \pm\frac{1}{2}$ in the LLM solution gets replaced by the bulk sources in (3.2.3).

The supergravity solutions depend on $3M$ parameters, which are the M sources on the right hand side of (3.2.3), located in X at $y_i, \vec{x}_i$ with $i = 1, 2, \ldots, M$. There is an overall translation symmetry along $\vec{x}$; this allows us to choose 'center-of-mass' coordinates, which sets

$$\vec{x}^{(0)} \equiv \sum_{i=1}^{M} y_i^2 \vec{x}_i = 0 \tag{3.2.6}$$

This choice will make the expressions considerably more compact. The general solution of (3.2.3) for the function f is then given by

$$f = \frac{1}{2} + \sum_{i=1}^{M} f_i \tag{3.2.7}$$

with

$$f_i = -\frac{1}{2} + \frac{(\vec{x} - \vec{x}_i)^2 + y^2 + y_i^2}{2\sqrt{[(\vec{x} - \vec{x}_i)^2 + y^2 + y_i^2]^2 - 4y^2 y_i^2}} \tag{3.2.8}$$

For such an f the solution of the differential equation (3.2.4) for the one-form V is given by

$$V_I \, dx^I = -\sum_{i=1}^{M} \sum_{I,J} \epsilon_{IJ} \frac{(x_J - x_{iJ})[(\vec{x} - \vec{x}_i)^2 + y^2 - y_i^2]}{2(\vec{x} - \vec{x}_i)^2 \sqrt{[(\vec{x} - \vec{x}_i)^2 + y^2 + y_i^2]^2 - 4y^2 y_i^2}} \, dx^I \tag{3.2.9}$$

where the indices I, J run over x_1, x_2.

In [1, 42] the parameters of the supergravity solution were identified with the parameters

of the gauge theory surface defect as follows:

$$\frac{1}{2\pi l_s^2}\left(x_{i1}+ix_{i2}\right)=\beta_i+i\gamma_i,\quad \frac{y_i^2}{L^4}=\frac{N_i}{N} \tag{3.2.10}$$

where L denotes the radius of AdS_5. The parameters α_i and η_i are identified with periods of the NSNS and RR two-form potentials on non-trivial two-cycles in the solutions. On the supergravity side these periods carry only topological information since the three-form field strengths of the two-form potentials vanish. As the calculations performed in section 3.3 and 3.4 depend only on the metric and the five-form, we conclude that all our calculations will be independent of the periods and hence the parameters α_i and η_i.

3.2.1 The vacuum solution

In order to develop intuition for the geometry it is useful to consider the $AdS_5\times S^5$ vacuum solution, which can be obtained by considering only one source, i.e. setting $M=1$. Translation invariance allows one to set $\vec{x}_1=0$ and from (3.2.10) we can fix $y_1=L$ since $N_1=N$. To exhibit the $AdS_5\times S^5$ metric explicitly it is convenient to introduce new coordinates:

$$\begin{aligned}
\chi&=\frac{1}{2}\left(\psi-\phi\right)\\
y&=L^2\sqrt{\rho^2+1}\,\cos\theta\\
x_1&=x_1^{(0)}+L^2\rho\sin\theta\cos\left(\psi+\phi\right)\\
x_2&=x_2^{(0)}+L^2\rho\sin\theta\sin\left(\psi+\phi\right)
\end{aligned} \tag{3.2.11}$$

where the range of the angular variables is given by $\theta\in[0,\pi/2]$, $\psi\in[0,2\pi]$, $\phi\in[0,2\pi]$. It is straightforward to verify that for this choice the function f (3.2.7) and the one-form V (3.2.9) for the vacuum solution take the following form

$$f=\frac{1}{2}\,\frac{\rho^2+\cos^2\theta+1}{\rho^2+\sin^2\theta}\quad\text{and}\quad V=\frac{1}{2}\,\frac{\rho^2-\sin^2\theta}{\rho^2+\sin^2\theta}\,d(\psi+\phi) \tag{3.2.12}$$

where the gauge transformation can be set to zero, i.e. $\omega = 0$. Using the expressions given in (3.2.1) the metric can be calculated and gives

$$ds^2 = L^2 \left[\left(\rho^2 + 1\right) ds^2_{AdS_3} + \frac{d\rho^2}{\rho^2 + 1} + \rho^2 \, d\psi^2 + d\theta^2 + \sin^2\theta \, d\phi^2 + \cos^2\theta \, ds^2_{S^3} \right] \tag{3.2.13}$$

which is indeed $AdS_5 \times S^5$. Note that the metric is written in a form for which the conformal boundary is $AdS_3 \times S^1$. In the following we will set the AdS radius $L = 1$ and restore it by dimensional analysis when needed.

3.2.2 Asymptotics and regularization of the bubbling solution

The integrals appearing later in the holographic entanglement entropy and the expectation value calculations are divergent. Therefore, we need to regulate them introducing a cut-off. In this section we map the general metric to a Fefferman-Graham (FG) form (3.2.19), we find the FG coordinate map (B.1.6) and derive the cut-off surface (3.2.20) in terms of the FG UV cut-off.

The fact that a general solution must be asymptotically $AdS_5 \times S^5$ implies the following restriction on y_i:

$$\sum_{i=1}^{M} y_i^2 = 1 \tag{3.2.14}$$

It is straightforward to see this considering the map to field theory parameters (3.2.10) and $\sum_{i=1}^{M} N_i = N$.

We will work in the coordinate system introduced in (3.2.11) and expand the general solution at large ρ. As mentioned above, the one-form V is defined up to an exact form. Thus, we use a gauge transformation to remove the V_ρ component of this vector. This brings the metric into a manifestly asymptotic form and makes it as compact as possible which is

convenient for our calculations. Fixing the gauge, ω becomes:

$$\omega = -\frac{M-1}{2}\,\alpha + \sin\theta \sum_{n=1}^{\infty} \frac{V_1^{(n+1)}(\theta,\alpha)\cos\alpha + V_2^{(n+1)}(\theta,\alpha)\sin\alpha}{n\rho^n} \tag{3.2.15}$$

where the $V_I^{(n+1)}$ are the coefficients in a large ρ expansion of the functions given in (3.2.9). The detailed procedure and the explicit form of ω are given in the appendix B.1.1.

The next step is to write the metric in terms of the $\{\rho, \psi, \theta, \phi\}$ coordinates. We write it as a deviation of the vacuum (3.2.13):

$$\begin{aligned} ds^2 = {} & \frac{1}{(\rho^2+1)}\,(1+F_\rho)\,d\rho^2 + \left(\rho^2+1\right)(1+F_1)\; ds^2_{AdS_3} + \rho^2\,(1+F_2)\,d\psi^2 \\ & + \cos^2\theta\,(1+F_3)\; ds^2_{S^3} + (1+F_4)\,d\theta^2 + \sin^2\theta\,(1+F_5)\,d\phi^2 \\ & + F_6\,d\theta\,d\psi + F_7\,d\psi\,d\phi + F_8\,d\theta\,d\phi \end{aligned} \tag{3.2.16}$$

with the F_a being functions of $\{\rho, \theta, \alpha \equiv \psi + \phi\}$ expanded at large ρ. Specifically, $F_\rho, F_m \sim O\left(\rho^{-2}\right)$ for $m \in \{1, 2, \ldots, 7\}$ and $F_8 \sim O\left(\rho^{-4}\right)$. Only certain coefficients in the F_ρ expansion emerge in our calculations and their expressions are given in the appendix B.1.2. These coefficients are expressed in terms of dimensionless moments. We will mainly express quantities in terms of these moments and therefore it is convenient to define them in advance:

$$m_{abc} \equiv \sum_{i=1}^{M} y_i^a x_{i1}^b x_{i2}^c \tag{3.2.17}$$

Note that for the $AdS_5 \times S^5$ vacuum only the following moments are non-zero:

$$m_{k00}^{(0)} = 1 \quad \text{for} \quad k = 2, 4, 6, \ldots \tag{3.2.18}$$

A general bubbling solution, preserving the $AdS_3 \times S^3 \times S^1$ isometry, can then be written

in the following Fefferman-Graham form:

$$ds^2 = \frac{1}{u^2}\left(du^2 + \alpha_1\, ds^2_{AdS_3} + \alpha_2\, d\tilde{\psi}^2\right) + \alpha_3\, ds^2_{S^3} + \alpha_4\, d\tilde{\theta}^2 + \alpha_5\, d\tilde{\phi}^2 + \alpha_6\, d\tilde{\theta}\, d\tilde{\psi} + \alpha_7\, d\tilde{\psi}\, d\tilde{\phi} + \alpha_8\, d\tilde{\theta}\, d\tilde{\phi} \tag{3.2.19}$$

The condition that the metric must asymptote to $AdS_5 \times S^5$ with $AdS_3 \times S^1$ boundary implies that the new coordinates $u, \tilde{\psi}, \tilde{\theta}, \tilde{\phi}$ and the α_m (expressed as functions of ρ, ψ, θ, ϕ) fall off as

$$u = \frac{1}{\rho}\left(1 + \ldots\right), \quad \tilde{\psi} = \psi + \ldots, \quad \tilde{\theta} = \theta + \ldots, \quad \tilde{\phi} = \phi + \ldots$$

$$\alpha_1 = 1 + \ldots, \quad \alpha_2 = 1 + \ldots, \quad \alpha_3 = \cos^2\theta\left(1 + \ldots\right), \quad \alpha_4 = 1 + \ldots$$

$$\alpha_5 = \sin^2\theta\left(1 + \ldots\right), \quad \alpha_6 = \ldots, \quad \alpha_7 = \ldots, \quad \alpha_8 = \ldots$$

The ellipses denote powers of ρ^{-1} whose coefficients are determined by equating (3.2.16) and (3.2.19). The explicit coordinate map is given in (B.1.6).

The integrals in the entanglement entropy and expectation value calculations diverge at large ρ. It is useful to express the coordinate map as a cut-off relation $\rho = \rho_c(\varepsilon, \psi, \theta, \phi)$. This is found by solving the first equation in (B.1.6) for ρ at the small u limit and identifying u with the FG cut-off, $u = \varepsilon$. The outcome is:

$$\rho_c(\varepsilon, \psi, \theta, \phi) = \frac{1}{\varepsilon} + \frac{F_\rho^{(2)} - 1}{4}\,\varepsilon + \frac{F_\rho^{(3)}}{6}\,\varepsilon^2 + \frac{16\left[F_\rho^{(4)} - F_\rho^{(2)}\left(F_\rho^{(2)} - 1\right)\right] - \left(\partial_\theta F_\rho^{(2)}\right)^2 - \left(\partial_\phi F_\rho^{(2)}\right)^2 \csc^2\theta}{128}\,\varepsilon^3 + O\left(\varepsilon^4\right) \tag{3.2.20}$$

Once we substitute for the coefficients of F_ρ we find that this function can be written as $\rho_c(\varepsilon, \theta, \alpha)$ with $\alpha = \psi + \phi$.

3.3 Holographic entanglement entropy

In the following section we apply the Ryu-Takayanagi prescription (1.3.11) to our solutions. First, we derive the minimal surface $\mathcal{M}$ for a general bubbling solution and show that its restriction to the boundary, which is a theory on $AdS_3 \times S^1$, maps to a two-sphere in the Weyl-related $\mathbb{R}^4$. We then evaluate its regulated area.

3.3.1 Minimal surface geometry

A bubbling geometry is a $AdS_3 \times S^3 \times U(1)$ fibration over X. We consider a surface $\mathcal{M}$ at constant t that fills the S^3 and has profile $z = z(l, \chi, y, x_1, x_2)$, where z is the AdS_3 radial coordinate defined in section 3.2. The induced metric on $\mathcal{M}$ is

$$\begin{aligned} h_{\alpha\beta}\, dx^\alpha\, dx^\beta = {} & y\sqrt{\frac{2f+1}{2f-1}}\,\frac{1}{z^2}\left[dl^2 + \left(\frac{\partial z}{\partial l}\, dl + \frac{\partial z}{\partial \chi}\, d\chi + \frac{\partial z}{\partial y}\, dy + \frac{\partial z}{\partial x_1}\, dx_1 + \frac{\partial z}{\partial x_2}\, dx_2\right)^2\right] \\ & + y\sqrt{\frac{2f-1}{2f+1}}\, ds^2_{S^3} + \frac{2y}{\sqrt{4f^2-1}}\left[d\chi^2 + 2V_I\, dx^I\, d\chi + \left(V_I\, dx^I\right)^2\right] \\ & + \frac{\sqrt{4f^2-1}}{2y}\left(dy^2 + dx_1^2 + dx_2^2\right) \end{aligned} \tag{3.3.1}$$

where α, β run over all coordinates except t and z. The area functional becomes

$$\begin{aligned} A(\mathcal{M}) = \mathrm{Vol}\left(S^3\right) \int dl\, d\chi\, dy\, dx_1\, dx_2\, \frac{\left(f-\frac{1}{2}\right) y}{z} \Bigg\{ 1 + \left(\frac{\partial z}{\partial l}\right)^2 + \frac{y^2}{\left(f-\frac{1}{2}\right) z^2}\Bigg[\left(\frac{\partial z}{\partial y}\right)^2 \\ + \left(\frac{\partial z}{\partial x_1} - V_1\,\frac{\partial z}{\partial \chi}\right)^2 + \left(\frac{\partial z}{\partial x_2} - V_2\,\frac{\partial z}{\partial \chi}\right)^2 + \frac{\left(f+\frac{1}{2}\right)\left(f-\frac{1}{2}\right)}{y^2}\left(\frac{\partial z}{\partial \chi}\right)^2\Bigg]\Bigg\}^{\frac{1}{2}} \end{aligned} \tag{3.3.2}$$

The equation of motion that follows from this functional is very complicated, but can be solved by

$$z(l, \chi, y, x_1, x_2)^2 + l^2 = R^2 \tag{3.3.3}$$

This semicircle is a co-dimension two minimal surface in AdS_3. Following [57, 58] one can show that within this ansatz this is in fact the surface of minimal area.

The surface (3.3.3) is independent of the AdS_5 radial coordinate. Thus, the boundary $\partial\mathcal{A}$ of the entangling region on $AdS_3 \times S^1$ satisfies the same formula. To understand this better, let us consider two coordinate charts on $\mathbb{R}^4$:

$$ds^2_{\mathbb{R}^4} = z^2 \left(\frac{dz^2 + dt^2 + dl^2}{z^2} + d\psi^2 \right) = dt^2 + dx^2 + x^2 \left(d\vartheta^2 + \sin^2\vartheta \, d\psi^2 \right) \tag{3.3.4}$$

The map between these two charts is given by

$$z = x \, \sin\vartheta, \qquad l = x \, \cos\vartheta \tag{3.3.5}$$

Thus, our entangling surface $\partial\mathcal{A}$ on the space $AdS_3 \times S^1$ can be written as a two-sphere of radius R on $\mathbb{R}^4$ (given by $x = R$) upon Weyl rescaling.

3.3.2 Evaluating the area integral

The minimal area can be written as follows:

$$A_{\text{min}} = \text{Vol}\left(S^3\right) \text{Vol}\left(S^1\right) \int dl \, \frac{R}{R^2 - l^2} \, I \tag{3.3.6}$$

where we have defined

$$I \equiv \int_X dy \, dx_1 \, dx_2 \left(f - \tfrac{1}{2} \right) y \tag{3.3.7}$$

with the function f given in (3.2.7). The area integral, and hence the entanglement entropy, diverges. This is expected due to the infinite number of degrees of freedom localized near the entangling surface and is present even in the vacuum. However, the intersection between the entangling surface and the surface operator leads to an additional divergence. Our goal is to extract the change in entanglement entropy in the presence of the surface operator,

which requires a careful treatment of these divergences.

We introduce two independent cut-offs, which we now argue is consistent with our field theory living on $AdS_3 \times S^1$. Firstly, the integral over X diverges due to the infinite volume of AdS_5. We regulate this with our Fefferman-Graham cut-off ε, which is a UV cut-off on $AdS_3 \times S^1$. Secondly, after using (3.3.3) to rewrite the l integral as an integral over z, we find a divergence at $z = 0$. This is the location of the surface operator and is at infinite proper distance from other points in the AdS_3. We therefore interpret this as an IR cut-off and regulate at $z = \eta$.

It is instructive to focus first on the case with no surface operator present in order to exhibit the divergence structure of these integrals most clearly. We begin by changing coordinates via (3.2.11). Defining $\alpha \equiv \psi + \phi$ and using the vacuum formula (3.2.12) for f we find

$$I^{(0)} = \int_0^{2\pi} d\alpha \int_0^{\pi/2} d\theta \, \cos^3\theta \, \sin\theta \int_0^{\rho_c^{(0)}} d\rho \, \rho \tag{3.3.8}$$

We denote by $\rho_c^{(0)}$ the Fefferman-Graham cut-off function (3.2.20) evaluated on the vacuum moments (3.2.18). In this special case it truncates to just two terms and is in fact independent of the angular coordinates: $\rho_c^{(0)} = 1/\varepsilon - \varepsilon/4$. Reinstating the overall factor of L^8, the full result for the integral over X is then

$$I^{(0)} = L^8 \left(\frac{\pi}{4\varepsilon^2} - \frac{\pi}{8} + \frac{\pi\varepsilon^2}{64} \right) \tag{3.3.9}$$

Next we handle the integral over l. Recall that the minimal surface formula (3.3.3) describes a semicircle for which $z \in [0, R]$ and $l \in [-R, R]$. The l integral diverges at both limits; rewriting via (3.3.3) as an integral over z, we regulate with a cut-off at $z = \eta$:

$$\begin{aligned} \int_{-\sqrt{R^2-\eta^2}}^{\sqrt{R^2-\eta^2}} dl \, \frac{R}{R^2 - l^2} &= 2 \int_0^{\sqrt{R^2-\eta^2}} dl \, \frac{R}{R^2 - l^2} = 2 \int_\eta^R dz \, \frac{R}{z\sqrt{R^2 - z^2}} \\ &= 2 \log \left(\frac{R + \sqrt{R^2 - \eta^2}}{\eta} \right) = 2 \log \left(\frac{2R}{\eta} \right) - \frac{\eta^2}{2R^2} + O\left(\eta^4\right) \end{aligned} \tag{3.3.10}$$

To compute the entanglement entropy (1.3.11) we need the following relations between gravity and gauge theory quantities

$$4G_N^{(10)} = (2\pi)^7(4\pi)^{-1}g_s^2\alpha'^4, \quad L^4 = 4\pi g_s N\alpha'^2 \tag{3.3.11}$$

as well as the volume $\mathrm{Vol}\,(S^3) = 2\pi^2$. Our final result for the divergent terms of the entanglement entropy in the absence of the surface operator is

$$S_{\mathcal{A}}^{(0)} = N^2\left[\frac{1}{\varepsilon^2} - \frac{1}{2} + O\left(\varepsilon^2\right)\right]\log\left(\frac{2R}{\eta}\right) \tag{3.3.12}$$

This result looks very different to that for a spherical entangling surface on $\mathbb{R}^4$ with a single Poincaré-invariant UV cut-off (see [14], for example). The reason is that the AdS_5 boundary in the slicing (3.2.13) can be reached in two ways: $z \to 0$ at fixed ρ (the location of the surface defect) or $\rho \to \infty$ at fixed z (some point away from the defect). We therefore need two cut-offs in this chart.[3] For a field theory on $AdS_3 \times S^1$, the cut-off η can be viewed as an IR cut-off that regulates the infinite volume of AdS_3. As we will discuss in some detail in section 3.5, from the point of view, of the surface defect η should be viewed as a UV cut-off.

Now let us evaluate the area integral in the presence of a surface operator. Our result (3.3.10) for the integral over l is unchanged. Whilst it is possible to evaluate the integral for I given in (3.3.7) for a general bubbling geometry after changing coordinates via (3.2.11), the result is extremely lengthy and cumbersome to deal with. We found the following approach to be much simpler.

For a general bubbling geometry, the integral (3.3.7) is actually a sum of integrals:

$$I = \sum_{i=1}^{M} I_i \quad \text{with} \quad I_i \equiv \int_X dy\, dx_1\, dx_2\, y f_i \tag{3.3.13}$$

[3]This situation is also familiar from the $S^1 \times H^{d-1}$ slicing of AdS_{d+1} — see figure 1 of [91], for example.

where the f_i are given in (3.2.8). We can perform a change of variables for each value of i separately

$$x_1 = y_i\,\bar{x}_1 + x_{i1}, \quad x_2 = y_i\,\bar{x}_2 + x_{i2}, \quad y = y_i\,\bar{y} \tag{3.3.14}$$

after which the I_i integral becomes

$$I_i = y_i^4 \int_{\bar{X}} d\bar{y}\, d\bar{x}_1\, d\bar{x}_2\, \bar{y}\, f_i \quad \text{with} \quad f_i = -\frac{1}{2} + \frac{\bar{y}^2 + \bar{x}_1^2 + \bar{x}_2^2 + 1}{2\sqrt{\left(\bar{y}^2 + \bar{x}_1^2 + \bar{x}_2^2 + 1\right)^2 - 4\bar{y}^2}} \tag{3.3.15}$$

Now f_i takes the same form as for the vacuum configuration. With a further change of variables the integral can be brought into the same form as (3.3.8):

$$I_i = y_i^4 \int d\bar{\alpha}\, d\bar{\theta}\, d\bar{\rho}\, \bar{\rho}\, \cos^3\bar{\theta}\, \sin\bar{\theta} \tag{3.3.16}$$

$$\bar{y} = \sqrt{\bar{\rho}^2 + 1}\, \cos\bar{\theta}, \quad \bar{x}_1 = \bar{\rho}\, \sin\bar{\theta}\, \cos\bar{\alpha}, \quad \bar{x}_2 = \bar{\rho}\, \sin\bar{\theta}\, \sin\bar{\alpha} \tag{3.3.17}$$

All that remains is to impose the correct cut-off in the new variables $\bar{\rho}_c(\varepsilon, \bar{\theta}, \bar{\alpha})$ and then sum up the results for each I_i.

As a side remark, it is interesting that we can express the general integral in the same form as the vacuum. This is because the function f for the general solution is constructed by superimposing terms that each have the same form as the vacuum solution. This simple behavior is special to this system and we do not expect such a simplification to be possible generically.

In order to find $\bar{\rho}_c(\varepsilon, \bar{\theta}, \bar{\alpha})$, our strategy is first to express the unbarred variables $\{\rho, \theta, \alpha\}$ in terms of the barred variables $\{\bar{\rho}, \bar{\theta}, \bar{\alpha}\}$ then to write the FG coordinate u as an asymptotic series in large $\bar{\rho}$. Solving this relation asymptotically for $\bar{\rho}$ and setting $u = \varepsilon$ we obtain the

following cut-off function:

$$\begin{aligned}\bar{\rho}_c(\varepsilon,\bar{\theta},\bar{\alpha}) = \frac{1}{y_i\,\varepsilon} - \frac{r_i\cos(\bar{\alpha}+\beta_i)\sin\bar{\theta}}{y_i} + \frac{1}{8y_i}\big[-1-4r_i^2-2y_i^2-2(y_i^2-1)\cos 2\bar{\theta} \\ -2m_{220}-2m_{202}+m_{400}+\sin^2\bar{\theta}\left(3+2r_i^2+2r_i^2\cos(2\bar{\alpha}+2\beta_i)\right. \\ \left.+6m_{220}+6m_{202}-3m_{400}+12m_{211}\sin 2\bar{\alpha}+6\left(m_{220}-m_{202}\right)\cos 2\bar{\alpha}\right)\big]\,\varepsilon \\ +O\left(\varepsilon^2\right) \end{aligned} \tag{3.3.18}$$

where we have defined $x_{i1} = r_i\cos\beta_i$ and $x_{i2} = r_i\sin\beta_i$. The details on the derivation of the cut-off function $\bar{\rho}_c(\varepsilon,\bar{\theta},\bar{\alpha})$ are presented in appendix B.2. Since the coordinate change (3.3.14) is simply a rescaling followed by a translation, we deduce the following ranges for the integration variables in the I_i integral (3.3.16):

$$0 \le \bar{\rho} < \bar{\rho}_c(\varepsilon,\bar{\theta},\bar{\alpha}), \quad \bar{\theta}\in[0,\pi/2], \quad \bar{\alpha}\in[0,2\pi] \tag{3.3.19}$$

We are now ready to evaluate I_i. We perform the $\bar{\rho}$ integral first due to its variable limit. It turns out that the moments drop out in the integration over the angular coordinates. However, they do appear in the final result for I once we sum over i:

$$I = \sum_{i=1}^{M} I_i = \frac{\pi L^8}{4\varepsilon^2} + \frac{\pi L^8}{24}\left[1-4\left(m_{220}+m_{202}+m_{400}\right)\right] + O(\varepsilon) \tag{3.3.20}$$

where we restored the overall factor of L^8. As a leading order check we do indeed recover the vacuum result (3.3.9) when evaluated on the vacuum moments (3.2.18). The holographic entanglement entropy in the presence of a surface operator (1.3.11) is evaluated using the minimal area via (3.3.6) in terms of the two regulated integrals (3.3.10) and (3.3.20). At the end, gravity expressions are translated to gauge theory ones using (3.3.11). Putting all this

together, the result is

$$S_{\mathcal{A}} = N^2 \left[\frac{1}{\varepsilon^2} + \frac{1 - 4\left(m_{220} + m_{202} + m_{400}\right)}{6} + O\left(\varepsilon\right) \right] \log\left(\frac{2R}{\eta}\right) \tag{3.3.21}$$

Subtracting the vacuum contribution from (3.3.21) and taking $\varepsilon \to 0$ we arrive at our final result for the change in entanglement entropy due to the presence of a surface operator:

$$\Delta S_{\mathcal{A}} = \frac{2N^2}{3}\left(1 - m_{220} - m_{202} - m_{400}\right) \log\left(\frac{2R}{\eta}\right) \tag{3.3.22}$$

3.3.3 A 2D CFT interpretation

Let us make a few comments on the form of the result (3.3.22) for the change in the entanglement entropy. Note immediately that it diverges as $\eta \to 0$. This additional divergence was anticipated due to the intersection between the entangling surface and the surface defect. The intersection occurs at two points separated by an interval, so it seems natural for the divergence to be logarithmic: our result takes the same form as the entanglement entropy across an interval in the vacuum of a generic two dimensional CFT [47, 92].

Note that the field theory description of the surface operators in section 3.1 did not require any additional 2D degrees of freedom localized at the surface defect. However, in the original paper [41] an alternative construction of the surface defects by coupling a nonlinear sigma model on Σ to the SYM fields was described. Such a sigma model could describe the 2D CFT we are looking for in the infrared. This construction is based on an intersecting D3-D3' brane system that was first discussed in [93]. Alternatively the defect can be realized by a probe D3-brane in $AdS_5 \times S^5$ with an $AdS_3 \times S^1$ worldvolume. Following Karch and Randall [37] and letting holography 'act twice' makes it likely that a 2D CFT is described by the modes on the probe brane.

Consequently it seems possible that the coefficient of the logarithmic divergence in the subtracted entanglement entropy to be equal to (one third of) the central charge of this

CFT [92]. We now provide evidence realizing this expectation. Recall that our metric (3.2.1) takes the form

$$ds^2 = L^2 \left(e^{2W} \, ds^2_{AdS_3} + ds^2_Z \right) \tag{3.3.23}$$

We define an effective central charge via the Brown-Henneaux fomula [8]:

$$c_{\text{eff}} = \frac{3L}{2G_N^{(3)}} \tag{3.3.24}$$

where $G_N^{(3)}$ is the three-dimensional Newton's constant of the theory obtained by reducing on the remaining directions in Z. To compute $G_N^{(3)}$ we must take into account the non-trivial warp factor in front of $ds^2_{AdS_3}$:

$$\frac{1}{16\pi G_N^{(3)}} = \frac{1}{16\pi G_N^{(10)}} \, \Delta \left(\int_Z d^7x \, \sqrt{g_Z} \, e^W \right) \tag{3.3.25}$$

where in order to isolate the contribution from the surface operator we should subtract off the vacuum answer. Substituting the metric (3.2.1) and reinstating the correct powers of L, our result for the effective central charge via (3.3.24) is given by

$$c_{\text{eff}} = \frac{3}{2G_N^{(10)}} \, \text{Vol}\left(S^3\right) \, \text{Vol}\left(S^1\right) \, \Delta I \tag{3.3.26}$$

where I is the integral (3.3.7) appearing in the entanglement entropy. From the minimal area prescription (1.3.11) and integral (3.3.6) we deduce that

$$\Delta S_{\mathcal{A}} = \frac{c_{\text{eff}}}{3} \, \log\left(\frac{2R}{\eta}\right) \tag{3.3.27}$$

which is indeed the entanglement entropy across an interval of length $2R$. Note that from the point of view of the two dimensional CFT the cut-off η is a UV cut-off.

Using (3.3.26) the central charge c_{eff} can be expressed in terms of the moments

$$c_{\text{eff}} = 2N^2\big(1 - m_{400} - m_{220} - m_{202}\big) \tag{3.3.28}$$

which shows that it scales like N^2. This is to be contrasted with the sigma model or probe brane construction mentioned above where one would expect that central charge to scale like N^0 or N^1, respectively. This result makes sense since the holographic supergravity solution is described by a fully back-reacted geometry in which the number of probe branes scales like N, leading to a number of localized degrees of freedom of order N^2. It is also instructive to use the map (3.2.10) to express c_{eff} in terms of field theory quantities:

$$c_{\text{eff}} = 2\left(N^2 - \sum_{i=1}^{M} N_i^2\right) - \frac{8\pi^2}{g_{YM}^2}\sum_{i=1}^{M} N_i\left(\beta_i^2 + \gamma_i^2\right) \tag{3.3.29}$$

It is intriguing that the first term agrees with the central charge for the sigma model for an $\mathcal{N} = (4,4)$ two dimensional quiver gauge theory which is related to a pure monodromy defect (where the β_i and γ_i vanish), discussed in [94]. It would be very interesting to explore whether the discussion of [94] can be generalized for nonvanishing β_i and γ_i.[4]

3.4 Holographic expectation values

This section is devoted to holographic expectation values of different observables. Specifically, we calculate the expectation value of the surface defect $\mathcal{O}_\Sigma$ at strong coupling and large N. Our result (3.4.18) is new and is expressed in terms of the moments we introduced in (3.2.17). We also quote the result of [1] for the holographic one-point function of the stress tensor in the presence of $\mathcal{O}_\Sigma$ (3.4.21, 3.4.22). In section 3.5 we will make use of these two expectation values in an attempt to relate them to the entanglement entropy computed in section 3.3.

[4]We are grateful to Bruno Le Floch for pointing out reference [94] and useful discussions on the possible relation to our results.

3.4.1 $\langle \mathcal{O}_\Sigma \rangle$ calculation

A holographic calculation for the expectation value of the surface operator relies on evaluating the on-shell ten-dimensional type IIB supergravity action on the bubbling supergravity solution presented in section 3.2. The obstacle here is well-known: it is difficult to reconcile Poincaré invariance of the action with the self-duality condition of the five-form F_5. Different approaches to this problem have been introduced in the literature: Covariant Lagrangians were constructed with the introduction of an infinite number of auxiliary fields [95–101], a single auxiliary field in a non-polynomial way [102–105] and most recently a construction with a free auxiliary four-form field [106]. Formalisms with non-manifest Lorentz symmetry were also considered [107–109]. The solutions presented in section 3.2 follow from the standard IIB action where the the self-duality constraint (3.4.2) has to be imposed by hand and not derived from varying the action.

In the holographic approach, the expectation value of the surface operator is given by the on-shell action $S_{\rm IIB}$:

$$\langle \mathcal{O}_\Sigma \rangle = \exp\left[-\left(S_{\rm IIB} - S^{(0)}_{\rm IIB} \right) \right] \tag{3.4.1}$$

where we subtract off the vacuum contribution $I_{(0)}$. The total action is a sum of a bulk term and the Gibbons-Hawking term:

$$S_{\rm IIB} = S_{\rm IIB,bulk} + S_{\rm GH} \tag{3.4.2}$$

$$\begin{aligned} S_{\rm IIB,bulk} = \frac{1}{2\kappa^2}\Bigg[& \int d^{10}x\sqrt{-g}\left(R - \frac{1}{2}\frac{\partial_M \tau\, \partial^M \bar{\tau}}{(\mathrm{Im}\,\tau)^2} \right) \\ & - \int \left(\frac{1}{2} M_{ab} H_3^a \wedge \star H_3^b + 4F_5 \wedge \star F_5 + \epsilon_{ab} C_4 \wedge H_3^a \wedge H_3^b \right) \Bigg] \end{aligned} \tag{3.4.3}$$

$$S_{\rm GH} = \frac{1}{\kappa^2}\int d^9x\,\sqrt{-\gamma}\,K \tag{3.4.4}$$

In our case the complex scalar τ field is constant and the three-forms H_3^a vanish. The trace

of the equation of motion for the metric implies $R = 0$ and thus the bulk term reduces to

$$S_{\text{IIB, bulk}} = -\frac{2}{\kappa^2}\int F_5 \wedge \star F_5 \tag{3.4.5}$$

To evaluate the bulk term we have to deal with the self-duality of F_5 which when imposed makes (3.4.5) vanish. In the following we employ a pragmatic method proposed in [110,111]. The prescription suggests to replace F_5 by its electric part only and double the relevant term in the action. The electric part of F_5 is the component with a time-like leg. As argued in [110,111] this approach is consistent with Kaluza-Klein reduction and T-duality. It would be interesting to use some of the alternative approaches to deal with the self-dual five-form. This would however imply redoing the derivation of the BPS supergravity solutions in the respective formalism, which is a somewhat daunting task.

Thus, instead of (3.4.5) we need to evaluate

$$S_{\text{IIB,bulk}} = -\frac{4}{\kappa^2}\int F_5^{\text{el.}} \wedge \star F_5^{\text{el.}} \tag{3.4.6}$$

As the electric part $F_5^{\text{el.}}$ is not self-dual , the integrand of (3.4.6) does not vanish in general. In particular, since the time coordinate lies in the AdS_3, the electric part of F_5 in (3.2.5) consists of the terms that have legs on AdS_3. It follows from the self-duality of F_5 that the Hodge dual of $F_5^{\text{el.}}$ is the magnetic piece of F_5, which has legs in S^3. Consequently we get

$$F_5^{\text{el.}} = -\frac{1}{4}\Big(d\Big[y^2\frac{2f+1}{2f-1}(d\chi+V)\Big] - y^3 \star_3 d\Big[\frac{f+1/2}{y^2}\Big]\Big)\wedge\omega_{AdS_3} \tag{3.4.7}$$

$$\star F_5^{\text{el.}} = -\frac{1}{4}\Big(d\Big[y^2\frac{2f-1}{2f+1}(d\chi+V)\Big] - y^3 \star_3 d\Big[\frac{f-1/2}{y^2}\Big]\Big)\wedge\omega_{S_3} \tag{3.4.8}$$

Using the equation (3.2.4) for the one-form V we can write the integrand in (3.4.6) as

$$F_5^{\text{el.}} \wedge \star F_5^{\text{el.}} = -\frac{yf}{2(1-4f^2)^2}\Big[1 - 8f^2 + 16f^4 + \frac{2y}{f}(1-4f^2)\partial_y f \tag{3.4.9}$$

$$+ 4y^2\left((\partial_1 f)^2 + (\partial_2 f)^2 + (\partial_y f)^2\right)\Big]\omega_{AdS_3} \wedge \omega_{S_3} \wedge d\chi \wedge dx_1 \wedge dx_2 \wedge dy \tag{3.4.10}$$

which can be rewritten in the following way:

$$F_5^{\text{el.}} \wedge \star F_5^{\text{el.}} = \left(-\frac{1}{2}yf + \partial_I u_I + \frac{y^3}{4(1-4f^2)}\left[\partial_1^2 f + \partial_2^2 f + y\partial_y\left(\frac{\partial_y f}{y}\right)\right]\right)$$

$$\times\, \omega_{AdS_3} \wedge \omega_{S_3} \wedge d\chi \wedge dx_1 \wedge dx_2 \wedge dy \tag{3.4.11}$$

where I labels coordinates which run over the base space X, $I = \{x_1, x_2, y\}$ and

$$u_I \equiv -\frac{y^3}{4(1-4f^2)}\,\partial_I f \tag{3.4.12}$$

Using the equation (3.2.3) for f, we can eliminate the final term in (3.4.11) since its denominator diverges. This is because f diverges at the location of the sources $y_i, \vec{x}_i$. Thus, the expression for the integrand is given by

$$F_5^{\text{el.}} \wedge \star F_5^{\text{el.}} = \left(-\frac{1}{2}yf + \partial_I u_I(x_1, x_2, y)\right)\omega_{AdS_3} \wedge \omega_{S_3} \wedge d\chi \wedge dx_1 \wedge dx_2 \wedge dy \tag{3.4.13}$$

The first term appearing in (3.4.13) includes the holographic entanglement entropy integral (3.3.7). The last term is a total derivative that can be integrated by applying Stoke's theorem. For the convenience of the reader and completeness we present the evaluation of the integrals for the bulk term in the appendix B.5.1. The result found in (B.5.18) is as follows:[5]

$$S_{\text{IIB,bulk}} = \frac{\pi}{2\kappa^2}\,\text{Vol}\,(AdS_3)\,\text{Vol}\left(S^3\right)\text{Vol}\left(S^1\right)\left[\frac{1}{\varepsilon^4} + \frac{1}{\varepsilon^2} + \frac{3}{8} - m_{400} - \mathcal{F}\right] \tag{3.4.14}$$

[5] $\mathcal{F}$ is identical to the expression $128\Delta\Phi_{2,k}\Delta\Phi_{2,-k}$ with $k = -2, 0, 2$ appearing in [1]. $\Delta\Phi_{2,k}$ are the asymptotic coefficients in a spherical harmonic expansion. Details on this expansion and the relation of $\Delta\Phi_{2,k}$ to our moments can be found in appendix B.4.

where ε is the FG cut-off appearing in (3.2.20). The final term in the finite piece takes the following form in terms of the moments:

$$\begin{aligned}\mathcal{F} \equiv \frac{3}{32}\big[1 + 4m_{220} + 4m_{202} - 2m_{400} + 10\left(m_{220}^2 + m_{202}^2\right) \\ +24m_{211}^2 - 4\left(m_{220} + m_{202}\right)m_{400} + m_{400}^2 - 4m_{220}m_{202}\big]\end{aligned} \tag{3.4.15}$$

The computation of the Gibbons-Hawking term is performed in the appendix B.5.2. The outcome (B.5.24) is given by

$$S_{\rm GH} = \frac{\pi}{2\kappa^2}\,\mathrm{Vol}\left(AdS_3\right)\mathrm{Vol}\left(S^3\right)\mathrm{Vol}\left(S^1\right)\left(\frac{4}{\varepsilon^4} + \frac{1}{\varepsilon^2}\right) \tag{3.4.16}$$

We note that the Gibbons-Hawking term does not depend on the moments and is hence independent of the details of the bubbling solution. It is notable that in the analogous calculation of the expectation value for the Wilson surface operator in six-dimensional $(2,0)$ theories [2] the Gibbons-Hawking term is also independent of the moments.

3.4.2 Result and comments

Now we are ready to put all the pieces together to build the total on-shell action (3.4.2). Our result is

$$S_{\rm IIB} = \frac{\pi}{2\kappa^2}\,\mathrm{Vol}\left(AdS_3\right)\mathrm{Vol}\left(S^3\right)\mathrm{Vol}\left(S^1\right)\left[\frac{5}{\varepsilon^4} + \frac{2}{\varepsilon^2} + \frac{3}{8} - m_{400} - \mathcal{F}\right] \tag{3.4.17}$$

Subtracting the vacuum contribution (which has $m_{400} = 1$), reinstating the overall factor of L^8 and converting to field theory quantities using (3.3.11) along with $\kappa^2 = 8\pi G_N^{(10)}$, we arrive at our final result for the expectation value:

$$\log\langle\mathcal{O}_\Sigma\rangle = \frac{N^2}{(2\pi)^2}\left(m_{400} - 1 + \mathcal{F}\right)\mathrm{Vol}\left(AdS_3\right)\mathrm{Vol}\left(S^1\right) \tag{3.4.18}$$

We should compare our holographic result for the expectation value with the semi-classical field theory calculation given in [42]. There, the SYM action was evaluated on $AdS_3 \times S^1$ with the surface defect boundary conditions (3.1.1) and (3.1.3) imposed and it was found that $\log \langle \mathcal{O}_\Sigma \rangle = 0$. A field theory interpretation of the holographic result (3.4.18) in the weak coupling limit is not direct. This is since our result is evaluated using holography and it is valid at strong coupling and large N. Even though the surface operator preserves supersymmetry it is not clear that the holographic results can be trusted at weak coupling. For completeness, however, we make use of the identifications (3.2.10) and (3.3.11) to express the moments appearing in (3.4.18) in terms of field theory quantities:

$$m_{400} = \sum_{i=1}^{M} \frac{N_i^2}{N^2} \tag{3.4.19}$$

and

$$\begin{aligned} \frac{\mathcal{F}}{6144} = & \left[\frac{1}{2} - \frac{1}{2N^2} \sum_{i=1}^{M} N_i^2 + \frac{4\pi^2}{g_{YM}^2 N^2} \sum_{i=1}^{M} N_i \left(\beta_i^2 + \gamma_i^2 \right) \right]^2 \\ & + \frac{24\pi^4}{g_{YM}^4 N^4} \sum_{i=1}^{M} N_i \left(\beta_i + i\gamma_i \right)^2 \sum_{j=1}^{M} N_j \left(\beta_j - i\gamma_j \right)^2 \end{aligned} \tag{3.4.20}$$

The interpretation of $\mathcal{F}$ in the field theory is not clear at this point. One would expect that this term should be a higher order correction to the semi-classical calculation of [42] and it would be interesting to calculate quantum corrections to surface defect operators systematically.

3.4.3 $\langle T_{\mu\nu} \rangle_\Sigma$

Here we present the stress-energy tensor $\langle T_{\mu\nu} \rangle_\Sigma$ result, evaluated in [1], which we use in the next section. Conformal symmetry constrains the stress-energy tensor form in the presence

of the surface defect $\mathcal{O}_\Sigma$ to (3.1.5):

$$\langle T_{\mu\nu}\rangle_\Sigma \, dx^\mu dx^\nu = h_\Sigma \left(ds^2_{AdS_3} - 3\, d\psi^2 \right) \tag{3.4.21}$$

$\langle T_{\mu\nu}\rangle_\Sigma$ is preserved and traceless, in line with the fact that Weyl anomaly vanishes for $AdS_3 \times S^1$.

The exact value of h_Σ is calculated in [1] following the holographic renormalization method performed in [112]. We give the dictionary of the result of [1] in terms of the moments (3.2.17) in appendix B.4. The final result for h_Σ then takes the following form

$$h_\Sigma = \frac{N^2}{2\pi^2}\left[\frac{1}{16} - \frac{1}{3}\left(m_{220} + m_{202} + \frac{1 - m_{400}}{2}\right)\right] \tag{3.4.22}$$

3.5 Comparing entanglement entropies

Our main result in this chapter is the subtracted entanglement entropy (3.3.22) calculated in section 3.3. The geometric setup is easier to visualize in $\mathbb{R}^4$ where the spherical entangling surface is a sphere. The setup on $\mathbb{R}^4$ is related to $AdS_3 \times S^1$ by a diffeomorphism and a Weyl rescaling. We review the various coordinate systems and the geometry of the entangling surface and surface defect in appendix B.3.

In fact, spherical entangling surfaces are special, since the corresponding modular Hamiltonian is (an integral of) a local operator. In [50], the authors used this fact to write the entanglement entropy across a spherical entangling surface of radius R on $\mathbb{R}^{1,d-1}$ as a thermal entropy on the hyperbolic spacetime $\mathbb{R} \times H^{d-1}$. The latter is conformally related to the causal development of the entangling region on the original Minkowski spacetime.

In [62] this mapping of entanglement entropy to thermal entropy was applied to the calculation of entanglement entropy in the presence of Wilson loops in $\mathcal{N} = 4$ SYM theory and ABJM theories. In particular, it was shown that the additional entanglement entropy due to the presence of the Wilson loop can be calculated from the expectation value of the

Wilson loop and the one-point function of the stress tensor. The formula for the additional entanglement entropy due to the presence of a Wilson loop is given by[6]

$$\Delta S = \log\langle W\rangle - \int\limits_{S^1\times H^{d-1}} d^d x\,\sqrt{g}\,\Delta\langle T_{\tau\tau}\rangle_W \tag{3.5.1}$$

where $\Delta\langle T_{\tau\tau}\rangle_W$ denotes the subtracted (by the one-point function without the Wilson loop inserted) time component of the stress tensor. The two expectation values in (3.5.1) are calculated on the hyperbolic space $S^1 \times H^{d-1}$, where the coordinate of the thermal circle S^1 is denoted by $\tau \sim \tau + \beta$ with periodicity $\beta = 2\pi R$.

The formula (3.5.1) is valid for arbitary representations of the Wilson surface. If the representation becomes very large, i.e. the associated Young tableaux have N^2 boxes, the backreaction on the dual supergravity solution cannot be neglected. This case was examined in [65] by two of the present authors. There, the holographic entanglement entropy was calculated using the bubbling supergravity solutions dual to half-BPS Wilson loops [59]. The expectation values reduce by localization to matrix model integrals [63]. Once matrix model and supergravity solution data are appropriately identified, following [66, 67], it was found that the holographic entanglement entropy exactly agrees with (3.5.1).

We are also studying a setup with a spherical entangling surface in a CFT, so it is interesting to see whether the same formula (3.5.1) can be applied to our system. (Of course, the map to a thermal entropy [50] should still hold because the isometry in τ is unbroken.) Here, the Wilson loop operator is replaced by a surface defect. To evaluate (3.5.1) we have to calculate the values of $\langle\mathcal{O}_\Sigma\rangle$ and the stress tensor on $S^1 \times H^3$. In section 3.4 we determined them on $AdS_3 \times S^1$, so the first step is map these quantities to the hyperboloid.

Our setup admits a simple description in $\mathbb{R}^4$. The three spaces are conformally related as follows:

$$ds^2_{AdS_3\times S^1} = z^{-2}\,ds^2_{\mathbb{R}^4} = \Omega^2\,ds^2_{S^1\times H^3} \tag{3.5.2}$$

[6]Note that we use the opposite sign convention for the stress tensor from the one used in [62]. Specifically, our convention makes use of the definition $T_{\mu\nu} = \frac{2}{\sqrt{g}}\frac{\delta S}{\delta g^{\mu\nu}}$.

where the expressions for the 4D metrics (in the coordinate charts of interest) and the conformal factor Ω are given in (B.3.1) and (B.3.3):

$$ds^2_{S^1\times H^3} = d\tau^2 + R^2\left(d\rho^2 + \sinh^2\rho\left(d\vartheta^2 + \sin^2\vartheta\, d\psi^2\right)\right) \quad \text{and} \quad \Omega^2 = \frac{1}{R^2\sinh^2\rho\sin^2\vartheta} \tag{3.5.3}$$

For convenience of the reader, further details on the coordinate maps and the description of our setup in these charts is given in appendix B.3.

It was shown in [84] that even-dimensional surface observables suffer from a conformal anomaly. In particular, the infinitesimal change in the expectation value of $\mathcal{O}_\Sigma$ is proportional to a linear combination of integrals of the intrinsic and extrinsic curvatures of the surface, whose precise expression is given in equation (2.9) of [1]. The coefficients in this combination depend on the surface operator and the theory and are generically non-zero. However, the curvature integrals all vanish in our setup of a planar surface at $\partial AdS_3 \subset AdS_3 \times S^1$, so we conclude that $\langle\mathcal{O}_\Sigma\rangle$ is invariant under this conformal transformation. (Of course, the 4D trace anomaly also vanishes on this space, as noted in section 3.4.3.)

The one-point function of the stress tensor (3.4.21) transforms in the usual way under a conformal transformation in four dimensions; for example

$$\begin{aligned}\langle\tilde{T}_{\tau\tau}\rangle_\Sigma &= \Omega^{-2}\left[\left(\frac{\partial t}{\partial\tau}\right)^2\langle T_{tt}\rangle_\Sigma + \left(\frac{\partial l}{\partial\tau}\right)^2\langle T_{ll}\rangle_\Sigma + \left(\frac{\partial z}{\partial\tau}\right)^2\langle T_{zz}\rangle_\Sigma\right] \\ &= \frac{h_\Sigma}{R^4\,\sinh^4\rho\,\sin^4\vartheta}\end{aligned} \tag{3.5.4}$$

where we used the coordinate map from $AdS_3 \times S^1$ to the hyperboloid in (B.3.4). The full result is traceless as expected since the trace anomaly vanishes on $S^1 \times H^3$:

$$\langle\tilde{T}_{\mu\nu}\rangle_\Sigma\, d\tilde{x}^\mu\, d\tilde{x}^\nu = \frac{h_\Sigma}{R^4\,\sinh^4\rho\,\sin^4\vartheta}\left[d\tau^2 + R^2\left(d\rho^2 + \sinh^2\rho\left(d\vartheta^2 - 3\sin^2\vartheta\, d\psi^2\right)\right)\right] \tag{3.5.5}$$

Note that in even dimensions there is also an inhomogeneous term that generalizes the Schwarzian derivative for the two-dimensional stress tensor. As pointed out in [50, 113] this

term does not depend on the state of the theory. Hence it will drop out of the vacuum subtracted stress tensor component $\Delta\langle\tilde{T}_{\tau\tau}\rangle_\Sigma$ in (3.5.1).

For reasons that will become clear later we write the volume factors in the expression of the expectation value, (3.4.18), in integral form and change variables. The new variables are the coordinates on the hyperboloid, $\{\tau, \rho, \vartheta, \psi\}$, which have one-to-one map with $AdS_3 \times S^1$ coordinates, $\{t, l, z, \psi\}$. The volume is written as

$$\begin{aligned} \mathrm{Vol}\left(AdS_3 \times S^1\right) &= \int\limits_{AdS_3\times S^1} d^4x\sqrt{g} = \int\limits_{S^1\times H^3} d^4\tilde{x}\,\Omega^{-2}\,\sqrt{\tilde{g}} \\ &= \frac{\beta\,\mathrm{Vol}\,(S^1)}{R}\int\frac{d\vartheta}{\sin^3\vartheta}\int\frac{d\rho}{\sinh^2\rho} \end{aligned} \tag{3.5.6}$$

where the integration over ψ and the thermal cycle have been performed. We omit the limits of the integrals over ϑ and ρ to treat them later. Substituting this relation into (3.4.18) we write the expectation value as

$$\log\langle\mathcal{O}_\Sigma\rangle = N^2\left(m_{400} - 1 + \mathcal{F}\right)\int\frac{d\vartheta}{\sin^3\vartheta}\int\frac{d\rho}{\sinh^2\rho} \tag{3.5.7}$$

The third ingredient in (3.5.1) is (dropping tildes)

$$\int\limits_{S^1\times H^3} d^4x\,\sqrt{g}\,\Delta\langle T_{\tau\tau}\rangle_\Sigma = (2\pi)^2\,\Delta h_\Sigma\int\frac{d\vartheta}{\sin^3\vartheta}\int\frac{d\rho}{\sinh^2\rho} \tag{3.5.8}$$

where Δh_Σ is the vacuum subtracted value of (3.4.22).

We notice that both ingredients (3.5.7, 3.5.8) contain the same integrals. The integrals diverge since the domain of integration is $\vartheta \in [0, \pi]$ and $\rho \in [0, \infty)$. To compute them we introduce two independent cut-offs as follows:

$$\int_{\eta/R}^{\pi-\eta/R}\frac{d\vartheta}{\sin^3\vartheta}\int_a^\infty\frac{d\rho}{\sinh^2\rho} = \left[\frac{R^2}{\eta^2} + \log\left(\frac{2R}{\eta}\right) - \frac{1}{6} + O\left(\eta^2\right)\right]\left(\frac{1}{a} - 1 + O(a)\right) \tag{3.5.9}$$

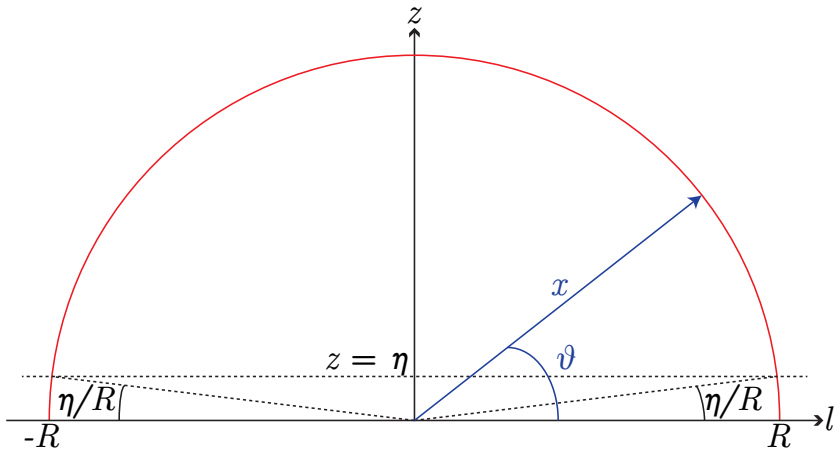

Figure 3.2: Mapping the $z = \eta$ cut-off to polar coordinates. The red semicircle is the entangling surface while the location of $\mathcal{O}_\Sigma$ is at $z = 0$. A uniform cut-off $z = \eta$ close to the location of $\mathcal{O}_\Sigma$ is introduced. It is denoted with a dashed horizontal line. This limits integration over ϑ between η/R and $\pi - \eta/R$.

The cut-off η is identified with the homonymous cut-off introduced in the holographic entanglement entropy calculation. The divergence comes from degrees of freedom close to the entangling surface $x = R$. Therefore, for small $z = \eta$ the first map in (B.3.4) sets the cut-off values of ϑ to η/R and $\pi - \eta/R$ (see figure 3.2). Since we are interested in the universal term of (3.5.9) where a is absent, no identification for this cut-off is needed.

We are now ready to combine all the ingredients in (3.5.1) (with the Wilson loop replaced by the surface defect). The right hand side is

$$\log \langle \mathcal{O}_\Sigma \rangle - \int\limits_{S^1 \times H^3} d^d x \, \sqrt{g} \, \Delta \langle T_{\tau\tau} \rangle_\Sigma = \frac{2N^2}{3} \left(1 - m_{220} - m_{202} - m_{400} - \frac{3}{2} \mathcal{F} \right) \log \left(\frac{2R}{\eta} \right)$$
$$= \Delta S_{\mathcal{A}} - N^2 \, \mathcal{F} \log \left(\frac{2R}{\eta} \right) \tag{3.5.10}$$

We immediately notice that there is a discrepancy compared to (3.5.1). The mismatch amounts to the second term in (3.5.10), which is proportional to $\mathcal{F}$. The minimal relation (3.5.1), derived in [62] for Wilson loops, does not work here.

The two new elements in our setup compared to [62] were the conformal anomaly for even-dimensional surface observables and the intersection between the entangling surface

and the defect. So one possibility is that either element should contribute an extra term to the thermal entropy in addition to those we considered. The same two elements are present in our previous calculations (in chapter 2) for a Wilson surface in the six-dimensional $(2,0)$ theory. Whilst we do not have a general closed-form expression for the expectation value of the Wilson surface, a case-by-case check yields a similar mismatch. It would be very interesting to pin this down in future work with a direct field theory replica trick calculation.

In order to compute the required thermal entropy, one must compute the free energy in the presence of the defect, which involves taking a derivative with respect to the inverse temperature β. This can be written as a derivative of the field theory Lagrangian with respect to the metric, as utilized in [62]. It could be that we have missed a contribution to the stress tensor localized at the defect. Whilst the origin of such a term is unclear, it would contribute to the entanglement entropy, so its existence (or lack thereof) should be clear from a replica trick calculation.

3.6 Summary

Let us summarize the results found in this chapter. We studied two-dimensional planar surface defects in $\mathcal{N}=4$ SYM theory via their dual supergravity bubbling description. First we computed the entanglement entropy across a ball-shaped region bisected by a surface defect. The additional entropy due to the presence of the defect is given by

$$\Delta S_{\mathcal{A}} = \frac{2N^2}{3}\big(1 - m_{400} - m_{220} - m_{202}\big)\,\log\left(\frac{2R}{\eta}\right) \tag{3.6.1}$$

In addition we calculated two other holographic observables: the one-point function of the stress tensor

$$\langle T_{\mu\nu}\rangle_{\Sigma}\, dx^{\mu}dx^{\nu} = \frac{N^2}{2\pi^2}\left[\frac{1}{16} - \frac{1}{3}\left(m_{220} + m_{202} + \frac{1-m_{400}}{2}\right)\right]\left(ds^2_{AdS_3} - 3\,d\psi^2\right) \tag{3.6.2}$$

and the expectation value of the surface defect

$$\log \langle \mathcal{O}_\Sigma \rangle = \frac{N^2}{(2\pi)^2} \left(m_{400} - 1 + \mathcal{F} \right) \mathrm{Vol}\left(AdS_3 \right) \mathrm{Vol}\left(S^1 \right) \tag{3.6.3}$$

where $\mathcal{F}$ is given in (3.4.20) in terms of CFT parameters. The m_{ijk} are quantities that depend on the parameters the locations of the charges (in the base space X) of a general bubbling solution. The cut-off η is the distance from the surface defect, similarly to the case of the Wilson surface.

Chapter 4

Entanglement Entropy and Free Energy in 5d SCFTs

The holographic entanglement entropy can be generalized for the case of CFTs with additional structure, other than the case of conformal defects. A particularly interesting case is five-dimensional SCFTs. Their existence is predicted in the classification of [114], which states that there is a unique superconformal algebra with 16 supercharges in five dimensions, given by the superalgebra $F(4)$ [115]. There is no known standard Lagrangian description for the 5d SCFTs obtained as UV fixed points of the gauge theories. However, the theories can be engineered using brane constructions in type IIA and IIB string theory [116–118]. Therefore the AdS/CFT correspondence is the perfect tool for extracting valuable quantitative information about them.

In this chapter, we study large classes of holographic duals for 5d SCFTs which have been constructed in type IIB supergravity recently [119–121]. Their geometry takes the form of $\mathrm{AdS}_6\times\mathrm{S}^2$ warped over a two-dimensional Riemann surface Σ.[1] The solutions are singular at isolated points and avoid a recent no-go theorem [127]. The appearing singularities have a clear interpretation as remnants of the external 5-branes appearing in the brane-web

[1] For earlier work on AdS_6 type IIB solutions see [122–126].

constructions.

The rest of the chapter is structured as follows: in sec. 4.1 we briefly review the structure of the type IIB supergravity solutions [119–121] and introduce the quantities that will be relevant for our computations. In sec. 4.2 we derive a general expression for the on-shell action of the solutions and discuss as special cases the 3- and 4-pole solutions that were spelled out in detail in [121]. This provides a holographic calculation of the free energy on S^5 for the dual SCFTs. In sec. 4.3 we similarly discuss the computation of codimension-2 minimal surfaces anchored on the boundary of AdS_6 at a constant time, which compute the entanglement entropy for the dual SCFTs. After deriving a general expression we discuss the same special cases as previously for the free energy, and show that the finite part for a spherical entangling region agrees with the free energy on S^5.

4.1 Review of type IIB supergravity solutions

The type IIB supergravity solutions we consider have been derived and discussed in detail in [119–121], and we will only give a brief review introducing the quantities that will be relevant for the computation of free energy and entanglement entropy.

The relevant bosonic fields of type IIB supergravity are the metric, the complex axion-dilaton scalar B and the complex 2-form $C_{(2)}$ [128, 129]. The real 4-form $C_{(4)}$ and the fermionic fields vanish. The geometry of the solutions is $AdS_6 \times S^2$ warped over a Riemann surface Σ, which for the solutions considered here will be the upper half plane. With a complex coordinate w on Σ, the metric and the 2-form field are parametrized by scalar functions f_2^2, f_6^2, ρ^2 and $\mathcal{C}$ on Σ,

$$ds^2 = f_6^2\, ds^2_{\mathrm{AdS}_6} + f_2^2\, ds^2_{\mathrm{S}^2} + 4\rho^2 dw d\bar{w} \ , \qquad C_{(2)} = \mathcal{C}\, \mathrm{vol}_{S^2} \ . \tag{4.1.1}$$

The solutions are expressed in terms of two holomorphic functions $\mathcal{A}_\pm$ on Σ, which are given

by

$$\mathcal{A}_\pm(w) = \mathcal{A}^0_\pm + \sum_{\ell=1}^{L} Z^\ell_\pm \ln(w - p_\ell) \ . \tag{4.1.2}$$

The p_ℓ are restricted to be on the real line and are poles with residues $Z^\ell_\pm$ in $\partial_w \mathcal{A}_\pm$. The residues are related by complex conjugation $Z^\ell_\pm = -\overline{Z^\ell_\mp}$. The explicit form of the solutions is conveniently expressed in terms of the composite quantities

$$\kappa^2 = -|\partial_w \mathcal{A}_+|^2 + |\partial_w \mathcal{A}_-|^2 \ , \qquad \partial_w \mathcal{B} = \mathcal{A}_+ \partial_w \mathcal{A}_- - \mathcal{A}_- \partial_w \mathcal{A}_+ \ , \tag{4.1.3}$$

$$\mathcal{G} = |\mathcal{A}_+|^2 - |\mathcal{A}_-|^2 + \mathcal{B} + \bar{\mathcal{B}} \ , \qquad R + \frac{1}{R} = 2 + 6\,\frac{\kappa^2\,\mathcal{G}}{|\partial_w \mathcal{G}|^2} \ . \tag{4.1.4}$$

Regularity of the solutions requires that κ^2 and $\mathcal{G}$ are both positive in the interior of Σ and vanish on the boundary. These regularity conditions are satisfied if the residues are given by

$$Z^\ell_+ = \sigma \prod_{n=1}^{L-2} (p_\ell - s_n) \prod_{k \neq \ell}^{L} \frac{1}{p_\ell - p_k} \ . \tag{4.1.5}$$

and the s_n are restricted to be in the upper half plane. Moreover, the p_ℓ and s_n have to be chosen such that they satisfy

$$\mathcal{A}^0 Z^k_- + \bar{\mathcal{A}}^0 Z^k_+ + \sum_{\ell \neq k} Z^{[\ell k]} \ln|p_\ell - p_k| = 0 \ , \tag{4.1.6}$$

where $Z^{[\ell k]} \equiv Z^\ell_+ Z^k_- - Z^k_+ Z^\ell_-$ and $2\mathcal{A}^0 \equiv \mathcal{A}^0_+ - \bar{\mathcal{A}}^0_-$. The explicit form of the functions parametrizing the metric is then given by

$$f_6^2 = \sqrt{6\mathcal{G}} \left(\frac{1+R}{1-R}\right)^{1/2} \ , \quad f_2^2 = \frac{1}{9}\sqrt{6\mathcal{G}} \left(\frac{1-R}{1+R}\right)^{3/2} \ , \quad \rho^2 = \frac{\kappa^2}{\sqrt{6\mathcal{G}}} \left(\frac{1+R}{1-R}\right)^{1/2} \ , \tag{4.1.7}$$

where we used the expressions of [121] with $c_6^2 = 1$, which was shown there to be required

for regularity. The function $\mathcal{C}$ parametrizing the 2-form field is given by

$$\mathcal{C} = \frac{4i}{9}\left(\frac{\partial_{\bar{w}}\bar{\mathcal{A}}_-\,\partial_w\mathcal{G}}{\kappa^2} - 2R\,\frac{\partial_w\mathcal{G}\,\partial_{\bar{w}}\bar{\mathcal{A}}_- + \partial_{\bar{w}}\mathcal{G}\,\partial_w\mathcal{A}_+}{(R+1)^2\,\kappa^2} - \bar{\mathcal{A}}_- - 2\mathcal{A}_+\right) \tag{4.1.8}$$

and the axion-dilaton scalar B is given by

$$B = \frac{\partial_w\mathcal{A}_+\,\partial_{\bar{w}}\mathcal{G} - R\,\partial_{\bar{w}}\bar{\mathcal{A}}_-\partial_w\mathcal{G}}{R\,\partial_{\bar{w}}\bar{\mathcal{A}}_+\partial_w\mathcal{G} - \partial_w\mathcal{A}_-\partial_{\bar{w}}\mathcal{G}}\ . \tag{4.1.9}$$

4.2 On-shell action and free energy on S^5

We will now evaluate the on-shell action for the solutions reviewed in the previous section explicitly. Formulating an action for type IIB supergravity is subtle due to the self-duality constraint on the 4-form potential, but since $C_{(4)} = 0$ in our solutions this is not an issue. Moreover, the on-shell action can be expressed as a boundary term [66]. We relegate the details of translating the result of [66] to our convention to appendix C.1, and start from the result (C.1.7)

$$\begin{aligned} S^{\rm E}_{\rm IIB} &= \frac{1}{64\pi G_{\rm N}}\int_{\mathcal{M}} d\left[\frac{1}{2}f^2(1+|B|^2)\,\bar{C}_2\wedge\star dC_2 - f^2\bar{B}C_2\wedge\star dC_2 + \text{c.c.}\right] \\ &= \frac{1}{64\pi G_{\rm N}}\int_{\partial\mathcal{M}} f^2\left[\frac{1}{2}(1+|B|^2)\bar{C}_2 - \bar{B}C_2\right]\wedge\star dC_2 + \text{c.c.} \end{aligned} \tag{4.2.1}$$

where $f^{-2} = 1-|B|^2$. We now use that $C_2 = \mathcal{C}\text{vol}_{\rm S^2}$, where $\text{vol}_{\rm S^2}$ is the volume form on the S^2 of unit radius. This yields

$$\star dC_2 = f_6^6 f_2^{-2}\text{vol}_{\rm AdS_6}\wedge\star_\Sigma d\mathcal{C}\ , \tag{4.2.2}$$

where $\text{vol}_{\text{AdS}_6}$ is the volume form on AdS_6 of unit curvature radius and $\star_\Sigma$ is the Hodge dual on Σ with metric $g_\Sigma = 4\rho^2|dw|^2$. We then find

$$S^{\text{E}}_{\text{IIB}} = \frac{1}{64\pi G_{\text{N}}}\int_{\partial M} f^2 f_6^6 f_2^{-2}\left[\frac{1}{2}(1+|B|^2)\bar{\mathcal{C}} - \bar{B}\mathcal{C}\right]\text{vol}_{\text{S}^2}\wedge\text{vol}_{\text{AdS}_6}\wedge\star_\Sigma d\mathcal{C} + \text{c.c.} \tag{4.2.3}$$

The AdS_6 volume can be regularized and renormalized in the usual way for an AdS_6 with unit radius of curvature and we will just use $\text{Vol}_{\text{AdS}_6,\text{ren}}$ to denote the renormalized volume. As we discuss in appendix C.2, there are no finite contributions to the on-shell action from the boundary introduced when regularizing the AdS_6 volume. The explicit expression for the renormalized volume of global AdS_6 with a renormalization scheme preserving the S^5 isometries of the sphere slices is also derived in appendix C.2 and given by

$$\text{Vol}_{\text{AdS}_6,\text{ren}} = -\frac{8}{15}\text{Vol}_{\text{S}^5}\ . \tag{4.2.4}$$

Note that we denote by e.g. Vol_{S^5} the actual volume, i.e. $\text{Vol}_{\text{S}^5} = \int_{\text{S}^5}\text{vol}_{\text{S}^5}$. The only (remaining) boundary then is the boundary of Σ. We note that $\partial\Sigma$ is not an actual boundary of the ten-dimensional geometry, so in particular there are no extra boundary terms to be added, but for the evaluation of the on-shell action as a total derivative we have to take it into account. We thus find

$$S^{\text{E}}_{\text{IIB}} = \frac{1}{64\pi G_{\text{N}}}\text{Vol}_{\text{AdS}_6,\text{ren}}\text{Vol}_{\text{S}^2}\int_{\partial\Sigma} f^2 f_6^6 f_2^{-2}\left[\frac{1}{2}(1+|B|^2)\bar{\mathcal{C}} - \bar{B}\mathcal{C}\right]\star_\Sigma\, d\mathcal{C} + \text{c.c.} \tag{4.2.5}$$

The task at hand is to evaluate the various ingredients in this expression more explicitly. To evaluate the metric factors more explicitly we use the expressions in (4.1.7), which yields

$$f_6^6 f_2^{-2} = 54\,\mathcal{G}\left(\frac{1+R}{1-R}\right)^3\ . \tag{4.2.6}$$

The pullback of $\star_\Sigma d\mathcal{C}$ to $\partial\Sigma$ does not involve ρ^2, and to evaluate it explicitly we note that $\partial\Sigma = \mathbb{R}$. It will be convenient for the explicit expansions to introduce real coordinates, $w = x + iy$, which yields

$$\star_\Sigma d\mathcal{C} = -(\partial_y \mathcal{C}) dx \ . \tag{4.2.7}$$

Using eq. (4.2.6) and (4.2.7), the regularized on-shell action (4.2.5) becomes

$$S^{\mathrm{E}}_{\mathrm{IIB}} = -\frac{1}{64\pi G_{\mathrm{N}}} 54 \mathrm{Vol}_{\mathrm{AdS}_6,\mathrm{ren}} \mathrm{Vol}_{\mathrm{S}^2} \int_{\mathbb{R}} dx\, f^2 \mathcal{G} \left(\frac{1+R}{1-R}\right)^3 (\partial_y \mathcal{C}) \left(\frac{1}{2}(1+|B|^2)\bar{\mathcal{C}} - \bar{B}\mathcal{C}\right) + \text{c.c.}\,, \tag{4.2.8}$$

where the integrand is evaluated at $y = 0$. Close to the boundary we have $\kappa^2, \mathcal{G} \to 0$ and

$$R = 1 - \sqrt{\frac{6\kappa^2 \mathcal{G}}{|\partial_w \mathcal{G}|^2}} + \dots \ . \tag{4.2.9}$$

As discussed in sec. 5.5 of [119], $\mathcal{G}/(1-R)$ remains finite at the boundary and the same applies for f^2. We can thus simplify the on-shell action to

$$S^{\mathrm{E}}_{\mathrm{IIB}} = \frac{1}{8\pi G_{\mathrm{N}}} \mathrm{Vol}_{\mathrm{AdS}_6,\mathrm{ren}} \mathrm{Vol}_{\mathrm{S}^2} I_0 \ , \tag{4.2.10a}$$

$$I_0 = 54 \int_{\mathbb{R}} dx\, \frac{\mathcal{G}}{1-R} \times \frac{\partial_y \mathcal{C}}{(1-R)^2} \times \left(\bar{B} f^2 \mathcal{C} - \frac{2f^2 - 1}{2}\bar{\mathcal{C}}\right) + \text{c.c.}\ , \tag{4.2.10b}$$

where each factor in the integrand is finite separately on the real line.

4.2.1 Explicit expansions

To further evaluate the on-shell action in (4.2.10), we explicitly expand the composite quantities κ^2, $\mathcal{G}$ as well as the actual supergravity fields around the real line, and it turns out that the subleading orders in the expansion play a crucial role. For the explicit expansions

it is convenient to introduce

$$f_\pm = \mathcal{A}^0_\pm + \sum_{\ell=1}^{L} Z^\ell_\pm \ln|x-p_\ell| \ , \qquad D_\pm = i\pi \sum_{\ell=1}^{L} Z^\ell_\pm \Theta(p_\ell - x) \ , \tag{4.2.11}$$

such that the holomorphic functions $\mathcal{A}_\pm$ and their differentials can be written as

$$\mathcal{A}_\pm = D_\pm + \sum_{n=0}^{\infty} \frac{1}{n!}(iy)^n f^{(n)}_\pm \ , \qquad \partial_w \mathcal{A}_\pm = \sum_{n=0}^{\infty} \frac{1}{n!}(iy)^n f^{(n+1)}_\pm \ , \tag{4.2.12}$$

where $f^{(n)}_\pm = (\partial_x)^n f_\pm$. The composite quantity κ^2 can be evaluated straightforwardly. For $\mathcal{G}$ we use $\partial_y \mathcal{G} = i(\partial_w \mathcal{G} - \partial_{\bar{w}} \mathcal{G})$ along with the fact that $\mathcal{G} = 0$ on the boundary. This allows us to simply integrate the explicit expression for $\partial_y \mathcal{G}$, which can be obtained straightforwardly from (4.1.3), to obtain an explicit expression for the expansion of $\mathcal{G}$ in y. We then find

$$\kappa^2 = y\kappa_0^2 + \frac{1}{6}y^3\kappa_3^2 + \mathcal{O}(y^5) \ , \tag{4.2.13}$$

$$\mathcal{G} = y\mathcal{G}_0 + \frac{1}{6}y^3\mathcal{G}_3 + \mathcal{O}(y^5) \ , \tag{4.2.14}$$

where

$$\kappa_0^2 = 2i(f'_- f''_+ - f''_- f'_+) \ , \qquad \kappa_3^2 = -(\kappa_0^2)'' + 8i\left(f'''_+ f''_- - f'''_- f''_+\right) \ , \tag{4.2.15}$$

$$\mathcal{G}_0 = 4i\left(f_+ f'_- - f_- f'_+\right) \ , \qquad \mathcal{G}_3 = -(\mathcal{G}_0)'' - 4\kappa_0^2 \ . \tag{4.2.16}$$

The expansion coefficients are real by construction and, by the regularity conditions, $\kappa_0^2 > 0$ and $\mathcal{G}_0 > 0$. Since $\mathcal{G}$ is constant along each piece of the boundary without poles, we also have $|\partial_w \mathcal{G}|^2 = \frac{1}{4}|\partial_y \mathcal{G}|^2 = \frac{1}{4}\mathcal{G}_0^2$ (noting that $\partial_w = \frac{1}{2}(\partial_x - i\partial_y)$). Using these expansions to find $\mathcal{C}$ yields

$$\mathcal{C} = -\frac{4}{3}iD_+ + \frac{4}{9}y^3\left[\frac{f'_+\mathcal{G}_3}{\mathcal{G}_0} + f'''_+ + \frac{6\kappa_0^2}{\mathcal{G}_0^2}\left(3f'_+\mathcal{G}_0 - f_+(\mathcal{G}_0)'\right)\right] \ . \tag{4.2.17}$$

This shows that the factors in (4.2.10) are indeed all finite as $y \to 0$. The last ingredient we need is the limit of B at the real axis, for which we find

$$B = \frac{2f_+\kappa_0 - if'_+\sqrt{6\mathcal{G}_0}}{if'_-\sqrt{6\mathcal{G}_0} - 2f_-\kappa_0} \,, \tag{4.2.18}$$

and we note that this is not a pure phase. Finally, for f^2 this yields

$$f^2 = \frac{1}{2} - \frac{4f_+f_-\kappa_0^2 + 6f'_+f'_-\mathcal{G}_0}{\sqrt{6\mathcal{G}_0^3\kappa_0^2}} \,. \tag{4.2.19}$$

With the explicit expansions in hand, we now return to evaluating the integral I_0 in (4.2.10). For the factors in the integrand we find

$$\frac{\mathcal{G}}{1-R} \times \frac{\partial_y \mathcal{C}}{(1-R)^2} = \sqrt{\frac{\mathcal{G}_0^3}{24\kappa_0^2}} \times \frac{1}{18\kappa_0^2}\left[f'_+\mathcal{G}_3 + \mathcal{G}_0 f'''_+ + 6\kappa_0^2\left(3f'_+ - f_+(\ln\mathcal{G}_0)'\right)\right] \,, \tag{4.2.20}$$

$$\bar{B}f^2\mathcal{C} - \frac{2f^2-1}{2}\bar{\mathcal{C}} = -\frac{4}{3}\frac{i}{\sqrt{6\mathcal{G}_0^3\kappa_0^2}}\left[6\mathcal{G}_0 f'_-\left(D_+f'_- - D_-f'_+\right) + 4\kappa_0^2 f_-\left(D_+f_- - D_-f_+\right)\right] \,, \tag{4.2.21}$$

where we used $\bar{B}f^2 = (6\mathcal{G}_0(f'_-)^2 + 4\kappa_0^2 f_-^2)/\sqrt{6\mathcal{G}_0^3\kappa_0^2}$ for the last expression. The full integral then becomes

$$I_0 = -\frac{i}{3}\int_{\mathbb{R}} dx \frac{1}{\kappa_0^4}\left[f'_+\mathcal{G}_3 + \mathcal{G}_0 f'''_+ + 6\kappa_0^2\left(3f'_+ - f_+(\ln\mathcal{G}_0)'\right)\right] \times \\ \left[6\mathcal{G}_0 f'_-\left(D_+f'_- - D_-f'_+\right) + 4\kappa_0^2 f_-\left(D_+f_- - D_-f_+\right)\right] + \text{c.c.} \tag{4.2.22}$$

Adding the complex conjugate explicitly yields

$$I_0 = \int_{\mathbb{R}} dx\, \mathcal{G}_0\left[\frac{16}{3}(D_+f_- - D_-f_+) - \frac{\mathcal{G}_0(\kappa_0^2)' - 3(\mathcal{G}_0)'\kappa_0^2}{\kappa_0^4}(D_+f'_- - D_-f'_+)\right] \,. \tag{4.2.23}$$

Via (4.2.10), this translates to an explicit expression for the on-shell action.

4.2.2 Integrability of the poles

We will now show that the integrand in (4.2.23) is well-behaved at the poles, $x = p_\ell$, such that the integral can be evaluated straightforwardly. To this end, we first evaluate $\mathcal{G}_0$ and κ_0^2 more explicitly. For $\mathcal{G}_0$ we find, by straightforward evaluation,

$$\mathcal{G}_0 = 4i \sum_{k=1}^{L} \frac{\mathcal{A}_+^0 Z_-^k - \mathcal{A}_-^0 Z_+^k}{x - p_k} + 4i \sum_{\ell \neq k} Z^{[\ell k]} \frac{\ln|x - p_\ell|}{x - p_k} \ . \tag{4.2.24}$$

The integration constants $\mathcal{A}_\pm^0$ are constrained by the regularity conditions (4.1.6), which, with $\mathcal{A}_+^0 = -\bar{\mathcal{A}}_-^0$, read

$$\mathcal{A}_+^0 Z_-^k - \mathcal{A}_-^0 Z_+^k + \sum_{\ell \neq k} Z^{[\ell k]} \ln|p_\ell - p_k| = 0 \ . \tag{4.2.25}$$

We therefore find that for generic solutions satisfying the regularity conditions

$$\mathcal{G}_0 = 4i \sum_{k=1}^{L} \sum_{\ell \neq k} \frac{Z^{[\ell k]}}{x - p_k} \ln\left|\frac{x - p_\ell}{p_\ell - p_k}\right| \ . \tag{4.2.26}$$

The evaluation of κ_0^2 is straightforward and yields

$$\kappa_0^2 = 2i \sum_{k=1}^{L} \sum_{\ell \neq k} \frac{Z^{[\ell k]}}{(x - p_\ell)(x - p_k)^2} \ . \tag{4.2.27}$$

Moreover, due to the antisymmetry of $Z^{[\ell k]}$ the derivatives of $\mathcal{G}_0$ and κ_0^2 take a simple form and are given by

$$(\mathcal{G}_0)' = -4i \sum_{k=1}^{L} \sum_{\ell \neq k} \frac{Z^{[\ell k]}}{(x - p_k)^2} \ln\left|\frac{x - p_\ell}{p_\ell - p_k}\right| \ , \qquad (\kappa_0^2)' = -4i \sum_{k=1}^{L} \sum_{\ell \neq k} \frac{Z^{[\ell k]}}{(x - p_\ell)(x - p_k)^3} \ . \tag{4.2.28}$$

With these expressions in hand, we can now analyze the behavior of the integrand in

(4.2.23). We set $x = p_m + \epsilon$, where ϵ is real and $|\epsilon|$ small compared to 1 and to all $|p_k - p_\ell|$, and find

$$\mathcal{G}_0 = 4i\eta_m \ln|\epsilon| + \mathcal{O}(1) \ , \qquad \kappa_0^2 = -2i\frac{\eta_m}{\epsilon^2} + \mathcal{O}(\epsilon^{-1}) \ , \qquad \eta_m = \sum_{k\neq m} \frac{Z^{[mk]}}{p_m - p_k} \ , \tag{4.2.29}$$

$$(\mathcal{G}_0)' = \mathcal{O}(\epsilon^{-1}) \ , \qquad (\kappa_0^2)' = 4i\frac{\eta_m}{\epsilon^3} + \mathcal{O}(\epsilon^{-1}) \ . \tag{4.2.30}$$

Note that the behavior of $\mathcal{G}_0$ and $(\mathcal{G}_0)'$ would be different if the parameters were not constrained by the regularity conditions in (4.1.6). The near-pole expansions consequently would be qualitatively different. For regular solutions, however, it is now straightforward to verify, with the explicit expansions of the composite quantities around the pole, that the integrand in (4.2.23) is $\mathcal{O}\big((\ln|\epsilon|)^2\big)$ and thus integrable across the pole.

4.2.3 The on-shell action

The integral I_0 in (4.2.23) can be further simplified as follows. We isolate the second term in the square brackets and rewrite the sum in the numerator as a total derivative,

$$I_0 = I_1 + \frac{16}{3}\int_{\mathbb{R}} dx\, \mathcal{G}_0(D_+f_- - D_-f_+) \ , \qquad I_1 = \int_{\mathbb{R}} dx \left(\frac{\mathcal{G}_0^3}{\kappa_0^2}\right)' \frac{D_+f_-' - D_-f_+'}{\mathcal{G}_0} \ . \tag{4.2.31}$$

Using integration by parts we can further evaluate I_1. This yields

$$I_1 = \frac{\mathcal{G}_0^2}{\kappa_0^2}(D_+f_-' - D_-f_+')\Big|_{x=-\infty}^{x=\infty} - \int_{\mathbb{R}} dx\, \frac{\mathcal{G}_0^3}{\kappa_0^2}\left(\frac{D_+f_-' - D_-f_+'}{\mathcal{G}_0}\right)' \ . \tag{4.2.32}$$

The first term vanishes, since $D_\pm = 0$ if either $x > p_\ell$ or $x < p_\ell$ for all ℓ, thanks to $\sum_\ell Z_\pm^\ell = 0$. The $D_\pm$ given in (4.2.11) depend on x only through Θ-functions, and we have to take into

account their non-trivial distributional derivatives. The second term then evaluates to

$$I_1 = -\int_{\mathbb{R}} dx \left[\frac{\mathcal{G}_0^2}{\kappa_0^2}(D_+ f_-'' - D_- f_+'') + \frac{\mathcal{G}_0^2}{\kappa_0^2}(D_+' f_-' - D_-' f_+') - \frac{\mathcal{G}_0' \mathcal{G}_0}{\kappa_0^2}(D_+ f_-' - D_- f_+') \right] . \tag{4.2.33}$$

Since $D_\pm' = -i\pi \sum_{\ell=1}^{L} Z_\pm^\ell \delta(p_\ell - x)$ and, by the analysis of the previous subsection, $\mathcal{G}_0^2 f_\pm'/\kappa_0^2 = \mathcal{O}(\epsilon(\ln|\epsilon|)^2)$ close to the poles, the second term vanishes. The first and last term can be combined thanks to the following identity, which follows from the expressions for κ_0^2 and $\mathcal{G}_0$ in terms of $f_\pm$,

$$2 f_\pm \kappa_0^2 = \mathcal{G}_0 f_\pm'' - \mathcal{G}_0' f_\pm' . \tag{4.2.34}$$

The result is

$$I_1 = -2 \int_{\mathbb{R}} dx\, \mathcal{G}_0 (D_+ f_- - D_- f_+) . \tag{4.2.35}$$

This reproduces exactly the structure of the remaining term in I_0 in (4.2.31) and we simply find

$$I_0 = \frac{10}{3} \int_{\mathbb{R}} dx\, \mathcal{G}_0 (D_+ f_- - D_- f_+) . \tag{4.2.36}$$

Evaluating $D_+ f_- - D_- f_+$ more explicitly, using the regularity condition (4.2.25), yields

$$D_+ f_- - D_- f_+ = i\pi \sum_{k=1}^{L} \sum_{\ell \neq k} \Theta(p_\ell - x) Z^{[\ell k]} \ln \left| \frac{x - p_k}{p_\ell - p_k} \right| . \tag{4.2.37}$$

Together with (4.2.26) this shows that I_0 explicitly depends on the residues only through the combinations $Z^{[\ell k]}$. With (4.2.10), we finally find the on-shell action as

$$S_{\rm IIB}^{\rm E} = -\frac{5}{3G_{\rm N}}{\rm Vol}_{{\rm AdS}_6,{\rm ren}}{\rm Vol}_{{\rm S}^2}\sum_{\substack{\ell,k,m,n=1\\ \ell\neq k,m\neq n}}^{L} Z^{[\ell k]}Z^{[mn]}\int_{-\infty}^{p_\ell} dx\,\ln\left|\frac{x-p_k}{p_\ell-p_k}\right|\,\ln\left|\frac{x-p_m}{p_m-p_n}\right|\frac{1}{x-p_n}\ . \tag{4.2.38}$$

We note that the lower bound in the integral can be moved from $-\infty$ to $\min_\ell(p_\ell)$ due to $\sum_\ell Z_+^\ell = 0$. The integral can be solved explicitly and involves polylogarithms. While the result for generic configurations does not seem particularly illuminating, this allows us to get analytic results for particular solutions, as we will discuss in sec. 4.2.5. Note also that the $Z^{[\ell k]}$ are imaginary, so the expression (4.2.38) is manifestly real.

4.2.4 Scaling of the free energy

As shown in [121], the residues $Z_\pm^\ell$ of the differentials $\partial_w\mathcal{A}_\pm$ at the poles p_ℓ correspond to the charges of external 5-branes in brane-web constructions for 5d SCFTs. The details of the SCFT depend on the precise charge assignments, and the same applies for the free energy and, correspondingly, the gravitational on-shell action. Before coming to those details, we can address a more general question: how does the free energy scale under overall rescalings of the 5-brane charges?

To address this question we can assume to start with a generic solution to the regularity conditions in (4.1.6). Namely,

$$\mathcal{A}^0 Z_-^k + \bar{\mathcal{A}}^0 Z_+^k + \sum_{\ell\neq k} Z^{[\ell k]}\ln|p_\ell - p_k| = 0\ . \tag{4.2.39}$$

We note that the equation is invariant under the following scaling

$$Z_+^\ell \to \gamma Z_+^\ell\ , \qquad Z_-^\ell \to \bar\gamma Z_-^\ell\ , \qquad \mathcal{A}^0 \to \gamma\mathcal{A}^0\ , \qquad p_\ell \to p_\ell\ , \tag{4.2.40}$$

where we have allowed for $\gamma \in \mathbb{C}$. For the residues this simply amounts to a change of the overall complex normalization parametrized by σ in (4.1.2). So starting with a solution $(Z^\ell_\pm, \mathcal{A}^0, p_\ell)$ to the regularity conditions, a rescaling of this form produces another solution, and this precisely allows us to isolate the overall scale of the charges Z^ℓ_+. From (4.2.38) we immediately see that the on-shell action scales as

$$S^{\rm E}_{\rm IIB} \to |\gamma|^4 S^{\rm E}_{\rm IIB} \ . \tag{4.2.41}$$

For a real overall scaling by N, we thus obtain a free energy scaling as N^4. This is different from the N^2 scaling one would expect for the 't Hooft limit of a four dimensional Yang-Mills theory, and as exhibited by $\mathcal{N}=4$ SYM and its $\mathrm{AdS}_5\times\mathrm{S}^5$ dual. But this is certainly not surprising, given the more exotic nature of the field theories described by 5-brane web constructions. It is also different from the $N^{5/2}$ scaling exhibited by the UV fixed points of 5d USp(N) gauge theories and their gravity duals [130]. As a curious aside, however, we note that the free energy for the orbifold quivers obtained from the USp(N) theories, which scales as $N^{5/2}k^{3/2}$, shows the same scaling if one naïvely sets $k = N$. As discussed in [121], there actually are classes of brane intersections described by the solutions discussed here which would naturally correspond to long quiver gauge theories with gauge groups of large rank, and we will discuss these examples in more detail in the next section.

4.2.5 Solutions with 3, 4 and 5 poles

We now evaluate the general expression for the free energy in (4.2.38) for classes of solutions with 3 up to 5 poles. It will be convenient to separate off the general overall factors as in (4.2.10a), and focus on the solution-specific part I_0.

3-pole solutions

We start with the 3-pole case. As discussed in sec. 4.1 of [121], the $\mathrm{SL}(2,\mathbb{R})$ automorphisms of the upper half plane can be used to fix the position of all poles, which we once again choose as

$$p_1 = 1 \ , \qquad p_2 = 0 \ , \qquad p_3 = -1 \ . \tag{4.2.42}$$

The regularity conditions are solved by $\mathcal{A}^0 = \omega_0\lambda_0 s \ln 2$. The free parameters of the solutions are given by the residues, corresponding to the charges of the external 5-branes, subject to charge conservation. The integral I_0 in (4.2.36) for a generic choice of residues evaluates to

$$I_0 = -80\pi\zeta(3)(Z^{[12]})^2 \ . \tag{4.2.43}$$

The on-shell action therefore is a simple function that is quartic in the residues, and manifestly invariant under the $\mathrm{SU}(1,1)$ duality symmetry of type IIB supergravity since the $Z^{[\ell k]}$ are.[2] Note also that $Z^{[\ell k]}$ is imaginary, and I_0 positive. For the particular case of the "N-junction" [131], discussed in sec. 4.3 of [121] and realized by the charge assignment $Z^1_+ = N$, $Z^2_+ = iN$, we have $Z^{[12]} = 2iN^2$ and thus find the free energy quartic in N.

4-pole solutions

For solutions with four poles we can once again fix the position of three poles by $\mathrm{SL}(2,\mathbb{R})$, but the position of one pole remains a genuine parameter. It is fixed by the regularity conditions in (4.1.6) and thus becomes an in general non-trivial function of the residues. We therefore expect in general more interesting dependence on the charges compared to the 3-pole case.

[2] The transformations spelled out in sec. 5.1 of [119] can be realized by transforming the residues as $Z^\ell_+ \to uZ^\ell_+ - vZ^\ell_-$ and $Z^\ell_- \to \bar{u}Z^\ell_- - \bar{v}Z^\ell_+$.

However, for the special class of 4-pole solutions discussed in sec. 4.2 of [121], where

$$Z_+^3 = -Z_+^1 \ , \qquad\qquad Z_+^4 = -Z_+^2 \ , \tag{4.2.44}$$

the position of the fourth pole is independent of the residues. In that case the regularity conditions are solved by

$$p_1 = 1 \ , \qquad p_2 = \frac{2}{3} \ , \qquad p_3 = \frac{1}{2} \ , \qquad p_4 = 0 \ , \tag{4.2.45}$$

along with $\mathcal{A}^0 = Z_+^2 \ln 3 - Z_+^1 \ln 2$. The position of all poles is therefore fixed regardless of the choice of charges, and we may again expect the on-shell action to be a simple quartic function of the residues. Indeed, the result for the integral is

$$I_0 = -280\pi\zeta(3)(Z^{[12]})^2 \ , \tag{4.2.46}$$

and of the same general form as the 3-pole result. We also note the factor $\zeta(3)$ appearing again. For the solutions discussed in sec. 4.2 of [121], with $-Z_+^1 = Z_+^3 = (1+i)N$ and $Z_+^2 = -Z_+^4 = (1-i)M$, we have $Z^{[12]} = 4iMN$. In particular, for $M = N$ the free energy again scales like N^4, a feature which we will come back to in the discussion.

We will now discuss a different configuration with 4 poles, for which the position of the fourth pole actually depends on the choice of charges. To this end, it is convenient to move the position of one pole off to infinity, which we will discuss here for a generic L-pole solution. To move the L-th pole p_L to infinity, we perform the following replacements and limit

$$p_L \to -\infty \ , \qquad\qquad \mathcal{A}_\pm^0 \to \tilde{\mathcal{A}}_\pm^0 = \mathcal{A}_\pm^0 - Z_\pm^L \ln|p_L| \ . \tag{4.2.47}$$

Note that the conjugation relation between the original integration constants, $\bar{\mathcal{A}}_\pm^0 = -\mathcal{A}_\pm^0$, holds in the same form for $\tilde{\mathcal{A}}_\pm^0$. In terms of the redefined integration constants, the expres-

sions for the holomorphic functions then become

$$\mathcal{A}_\pm = \tilde{\mathcal{A}}^0_\pm + \sum_{\ell=1}^{L-1} Z^\ell_\pm \ln(w - p_\ell) \ . \tag{4.2.48}$$

Note that this expression explicitly involves only $L-1$ poles and $L-1$ residues. These residues, however, are not constrained to sum to zero and the number of independent parameters is therefore unchanged. The conditions for $\mathcal{G} = 0$ on the boundary become

$$\tilde{\mathcal{A}}^0_+ Z^k_- - \tilde{\mathcal{A}}^0_- Z^k_+ + \sum_{\substack{\ell=1 \\ \ell\neq k}}^{L-1} Z^{[\ell k]} \ln|p_\ell - p_k| = 0 \ , \qquad k = 1, .., L-1 \ . \tag{4.2.49}$$

These are only $L-1$ conditions, as compared to L conditions previously. However, the sum does not manifestly vanish and the number of independent conditions therefore is also not modified. The class of 4-pole solutions with (4.2.44) can now be realized as

$$p_1 = 1 \ , \qquad p_2 = 0 \ , \qquad p_3 = -1 \ , \qquad \tilde{\mathcal{A}}^0_\pm = 0 \ , \tag{4.2.50}$$

and computing the on-shell action reproduces (4.2.46).

The class of 4-pole solutions we wish to discuss next is parametrized by an overall scale n of the residues and an angle θ, and obtained by fixing

$$Z^1_+ = n \ , \qquad Z^2_+ = in \qquad Z^3_+ = ne^{i\theta} \ , \qquad Z^4_+ = -(1 + i + e^{i\theta})n \ . \tag{4.2.51}$$

The position of three of the poles can once again be fixed arbitrarily, and we choose

$$p_1 = 1 \ , \qquad p_2 = 0 \ , \qquad p_4 \to -\infty \ . \tag{4.2.52}$$

This leaves the position of the third pole, p_3, along with the (complex) constant $\mathcal{A}^0$ to be determined from the conditions in (4.1.6). The resulting equation determining p_3 after

solving for $\mathcal{A}^0$ is

$$Z^{[1,3]}Z^{[2,4]}\ln(1-p_3)^2 = Z^{[1,4]}Z^{[2,3]}\ln p_3^2\ . \tag{4.2.53}$$

Note that n drops out of this equation and p_3 therefore depends on θ only. We take the position of the pole as parameter and solve for θ, which can be done in closed form and yields four branches of solutions. The criterion for the choice of branch is that θ should be real and the zeros s_n in the upper half plane. The explicit expressions are bulky and not very illuminating, and we show a plot of θ as function of p_3 in fig. 4.1(a) instead.

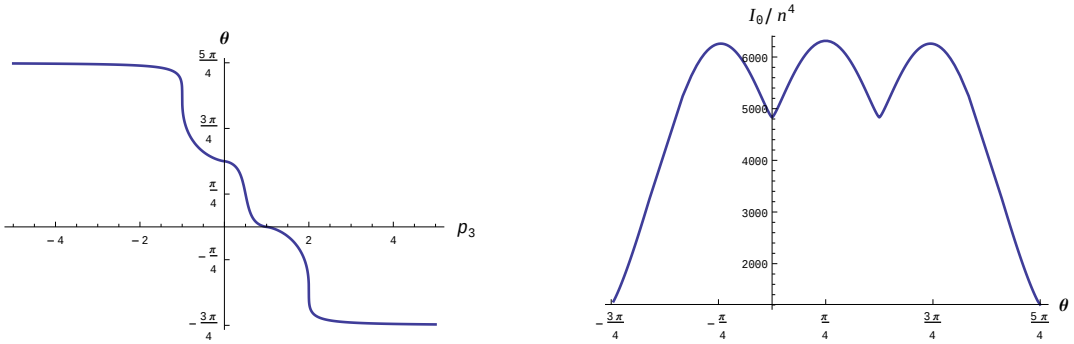

(a) (b)

Since p_3 is independent of n, the on-shell action depends on n only through an overall factor n^4, as expected from the scaling analysis in sec. 4.2.4. The dependence on θ, however, is non-trivial and we show the result in fig. 4.1(b). We note the presence of three minima, which all correspond to the 4-pole solution degenerating to a 3-pole solution: for $\theta \to 0$ we have $Z_+^3 \to Z_+^1$ and $p_3 \to p_1$, for $\theta \to \pi/2$ we have $Z_+^3 \to Z_+^2$ and $p_3 \to p_2$, and for $\theta \to 5\pi/4$ we have $Z_+^3 \to (1+\sqrt{2})Z_+^4$ and $p_3 \to p_4$. That means in all these cases two poles coalesce and their residues add. The free energy coincides with that of the resulting 3-pole configuration. The 3-pole configurations resulting from $\theta \to 0$ and $\theta \to \pi/2$ have two charges with the same moduli and the same relative phase up to a sign. Since the formula in (4.2.43) is insensitive to these differences, this explains the coincident free energies. It is intriguing to observe that the value of the free energy assumes a local minimum for all the cases where the solution

reduces to a 3-pole configuration. The sphere free energy in odd dimension can be used as a measure for the number of degrees of freedom, and one may speculate that splitting one pole into two, or equivalently one external 5-brane into two, will generically increase that number. While certainly true for this specific example, it is an interesting open question whether this behavior holds more generally.

5-pole solutions

As a final example we will consider a class of solutions with five poles. In general we now have two positions of the poles depending on the choice of residues, but we will focus on a class of solutions which are parametrized by only two real numbers, with residues given by

$$Z_+^1 = -Z_+^3 = M \ , \qquad Z_+^2 = 2iN \ , \qquad -Z_+^4 = iZ_+^5 = (1+i)N \ . \tag{4.2.54}$$

The corresponding 5-brane intersection is shown in fig. 4.1(c).

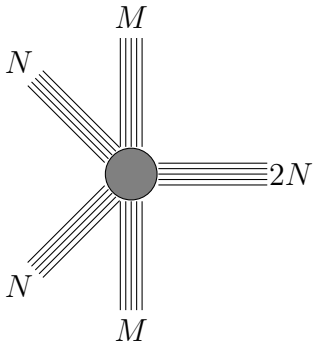

(c)

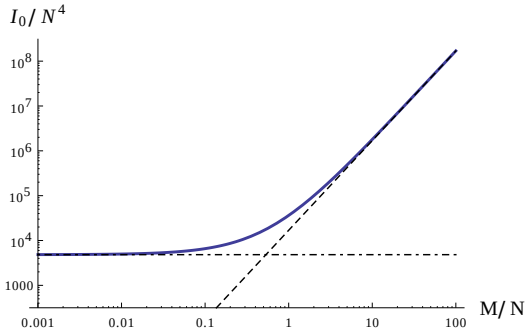

(d)

Figure 4.1: The left hand side shows a 5-brane intersection corresponding to the charges in (4.2.54). On the right hand side is a log-log plot of I_0 for the 5-pole solution with residues given in (4.2.54). Via (4.2.10) this corresponds to the on-shell action, as function of M/N. The constant dot-dashed line shows $80\pi\zeta(3)\cdot 16N^4$, which, via (4.2.43), is the value of I_0 for the 3-pole solution resulting from (4.2.54) for $M=0$. The dashed line shows $280\pi\zeta(3)\cdot 16M^2N^2$, which, via (4.2.46), is I_0 for a 4-pole solution with $-Z_+^1 = Z_+^3 = 2iN$ and $Z_+^2 = -Z_+^4 = M$.

As before three poles can be fixed by $\mathrm{SL}(2,\mathbb{R})$ and we resort to the choice in (4.2.42).

The regularity conditions in (4.1.6) are solved by

$$p_5 = -p_4 \ , \qquad\qquad A^0 = iN \log|p_4^2 - 1| \ , \tag{4.2.55}$$

where p_4 is determined by the equation

$$(M-N)\log(p_4-1)^2 - (M+N)\log(p_4+1)^2 + N\log 16 = 0 \ . \tag{4.2.56}$$

The choice of residues can be realized via (4.1.5), by fixing $\sigma = -2iNp_4^2/(s_1 s_2 s_3)$ and the zeros s_1, s_2, s_3 as the three solutions to the cubic equation

$$isM(s^2 - p_4^2) + p_4 N(s^2-1)(p_4 - is) = 0 \ . \tag{4.2.57}$$

To solve (4.2.56) it is once again convenient to fix p_4 and determine the resulting ratio M/N. We choose $p_4 \leq -\sqrt{5}$, which produces zeros in the upper half plane and positive M/N. The on-shell action divided by N^4, as function of the ratio M/N, is shown in fig. 4.1(d). We clearly see that the dependence on M/N is not simply quadratic, which we would have expected if the position of the poles had not depended on M/N. Instead, I_0/N^4 interpolates between approaching a constant for small M/N and quadratic dependence for large M/N.

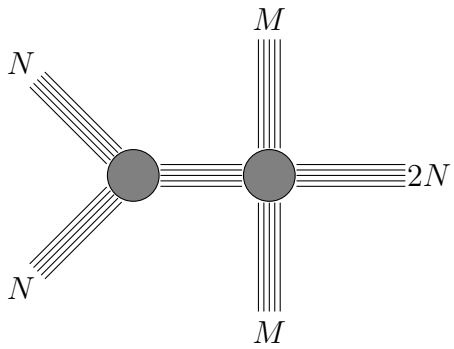

Figure 4.2: Global deformation (in the classification of [116, 117]) of the brane intersection shown in fig. 4.1(c), corresponding to a relevant deformation of the dual SCFT.

The asymptotic behavior for $M/N \to 0$ and $M/N \to \infty$ can be understood in more detail

as follows. For $M \to 0$, we expect the solution to reduce to a 3-pole configuration, since two of the residues in (4.2.54) vanish. Indeed, in that limit two of the zeros s_n approach the real line and annihilate the poles p_1, p_3. With one zero remaining in the interior of the upper half plane and three poles on the real line, we indeed find a regular 3-pole configuration. Correspondingly, the on-shell action as shown in fig. 4.1(d) for $M/N = 0$ agrees with (4.2.43) evaluated with the remaining residues. For large M/N, the behavior is not quite as immediately clear from the form of the residues. But we can gain some intuition from looking at deformations of the web. The solutions we are considering here describe the conformal phase of the dual SCFTs, where in the brane construction all external branes intersect at one point. Deformations of the web where the external branes are moved correspond to relevant deformations of the dual SCFT [116, 117], and a particular example is shown in fig. 4.2. We may view it as gluing an intersection of M NS5-branes and $2N$ D5-branes with an SL(2,$\mathbb{R}$) rotated version of the "N-junction". For large M, it suggests that the structure of the web is dominated by the intersection of M NS5-branes and $2N$ D5-branes. The number of degrees of freedom provided by the "extra vertex" compared to the 4-brane intersection of NS5 and D5-branes does not appear to scale with M, and we therefore expect the free energy of the 5-pole solution at large M/N to approach the free energy of a 4-pole solution with charges corresponding to M NS5 and $2N$ D5-branes. As shown in fig. 4.1(d), this is indeed the case.

4.3 Entanglement entropy

In this section we use the Ryu-Takayanagi prescription [14] to compute holographic entanglement entropies for the 5d SCFTs dual to the supergravity solutions. The main parts of the derivation will hold for a generic choice of the region for which we compute the entanglement entropy, as we will explain shortly, but our main interest is in regions of spherical shape.

The entanglement entropy is given by the area of a codimension-2 surface, anchored at a fixed time on the boundary of AdS_6 such that it coincides with the entangling surface. For a generic choice of entangling surface, we thus have to compute the area of an eight-

dimensional surface γ_8 wrapping S^2 and Σ, and which is of codimension-2 in AdS_6. The resulting expression for the entanglement entropy reads

$$S_{\rm EE} = \frac{\text{Area}(\gamma_8)}{4G_{\rm N}} = \frac{1}{4G_{\rm N}} \int_{\gamma_8} \text{vol}_{\gamma_8} \ . \tag{4.3.1}$$

The volume form reduces to

$$\text{vol}_{\gamma_8} = f_6^4 f_2^2 \, \text{vol}_{\gamma_4} \wedge \text{vol}_{S^2} \wedge \text{vol}_{\Sigma} \ , \tag{4.3.2}$$

where γ_4 is the codimension-2 minimal surface in a unit radius AdS_6 which is anchored at the conformal boundary and ends there on the entangling surface. The computation of $S_{\rm EE}$ as a result simplifies to

$$S_{\rm EE} = \frac{1}{4G_{\rm N}} \, \text{Vol}_{S^2} \cdot \mathcal{I} \cdot \text{Area}(\gamma_4) \ , \tag{4.3.3}$$

where $\text{Area}(\gamma_4)$ is the area of the four-dimensional minimal surface in AdS_6 and with $g_\Sigma = 4\rho^2 |dw|^2$ we have

$$\mathcal{I} = 4 \int_\Sigma d^2w f_6^4 f_2^2 \rho^2 \ . \tag{4.3.4}$$

The factor 4 is a result of the ansatz (4.1.1) and we have $d^2w = dxdy$. With the expressions for the metric functions in (4.1.7), we can further evaluate the integrand to find

$$\mathcal{I} = \frac{8}{3} \int_\Sigma d^2w \ \kappa^2 \mathcal{G} \ . \tag{4.3.5}$$

We note in particular that, due to the factorization in (4.3.3), once $\mathcal{I}$ is known the computation of entanglement entropies reduces to the analogous computation in AdS_6.

4.3.1 Integrability near the poles

We now show that even though the supergravity solution is singular at the poles $x = p_\ell$ on the boundary of Σ, the entanglement entropy is finite and does not receive contributions from the poles. To this end we use equation (4.3.5) together with the explicit expressions for κ and $\mathcal{G}$ close to a pole derived in [121]. Namely, for $w = p_m + re^{i\theta}$ we have

$$\mathcal{G} = 2\kappa_m^2 r|\ln r|\sin\theta + \mathcal{O}(r^2\ln r)\ , \qquad \partial_w\mathcal{G} = i\kappa_m^2\ln r + \mathcal{O}(r\ln r)\ , \tag{4.3.6a}$$

and

$$\kappa^2 = \kappa_m^2\frac{\sin\theta}{r} + \mathcal{O}(r^0)\ , \tag{4.3.6b}$$

where

$$\kappa_m^2 = 2i\sum_{\ell\neq m}\frac{Z^{[\ell m]}}{p_m - p_\ell}\ . \tag{4.3.7}$$

This implies that the integrand of $\mathcal{I}$ close to the pole behaves as $\mathcal{O}(r|\ln r|)$, which is integrable. Moreover, we see that, like in the direct computation of the free energy in sec. 4.2, we can introduce a cut-off around the poles and evaluate the integrals, and removing the cut-off does not yield localized contributions from the poles.

4.3.2 Explicit evaluation

We now turn to a more explicit evaluation of the integral $\mathcal{I}$ given in (4.3.5). We can use the fact that

$$\kappa^2 = -\partial_w\partial_{\bar{w}}\mathcal{G}\ , \tag{4.3.8}$$

to integrate by parts. Namely, using $\kappa^2\mathcal{G} = -\partial_w(\mathcal{G}\partial_{\bar{w}}\mathcal{G}) + (\partial_{\bar{w}}\mathcal{G})\partial_w\mathcal{G}$. From the near-pole expansions in eq. (4.3.6), we see that $\mathcal{G}\partial_{\bar{w}}\mathcal{G}$ goes to zero not only at generic points of the boundary, but also at the poles. The boundary contribution therefore vanishes and we find

$$\mathcal{I} = \frac{8}{3}\int_\Sigma d^2w(\partial_{\bar{w}}\mathcal{G})\partial_w\mathcal{G} \ . \tag{4.3.9}$$

The generic form of $\partial_w\mathcal{G}$ can be obtained straightforwardly from (4.1.3) and yields

$$\partial_w\mathcal{G} = (\bar{\mathcal{A}}_+ - \mathcal{A}_-)\partial_w\mathcal{A}_+ + (\mathcal{A}_+ - \bar{\mathcal{A}}_-)\partial_w\mathcal{A}_- \ . \tag{4.3.10}$$

Evaluating this explicitly using the regularity conditions (4.1.6) yields

$$\partial_w\mathcal{G} = \sum_{\substack{\ell,k=1\\ \ell\neq k}}^{L} Z^{[\ell k]} \ln\left|\frac{w-p_\ell}{p_k-p_\ell}\right|^2 \frac{1}{w-p_k} \ . \tag{4.3.11}$$

This relation allows us to write $\mathcal{I}$ explicitly as

$$\mathcal{I} = -\frac{8}{3}\sum_{\substack{\ell,k,m,n=1\\ \ell\neq k,m\neq n}}^{L} Z^{[\ell k]}Z^{[mn]}\int_\Sigma d^2w \ln\left|\frac{w-p_\ell}{p_k-p_\ell}\right|^2 \ln\left|\frac{w-p_m}{p_m-p_n}\right|^2 \frac{1}{\bar{w}-p_n}\frac{1}{w-p_k} \ . \tag{4.3.12}$$

This expression becomes manifestly real upon symmetrizing the integrand under the exchange of the index pairs (ℓ,k) and (m,n), which are independently summed over. In addition, using charge conservation, one can show that the combination $dw\partial_w\mathcal{G}$ is invariant under SL(2,$\mathbb{R}$) transformations

$$w \to \frac{aw+b}{cw+d} \ , \qquad\qquad p_k \to \frac{ap_k+b}{cp_k+d} \ , \tag{4.3.13}$$

with $ad-bc=1$. The expression for $\mathcal{I}$ in (4.3.9) is therefore SL(2,$\mathbb{R}$) invariant, as expected, and we can again fix the location of three poles at arbitrary positions.

4.3.3 Spherical regions

For the specific case of a spherical entangling surface of radius r_0 at a fixed $t = t_0$, we just have to evaluate the area of the corresponding minimal surface in an AdS_6 of unit radius. we choose coordinates in AdS_6 such that

$$ds^2_{AdS_6} = \frac{dz^2 - dt^2 + dr^2 + r^2 d\Omega^2_{S^3}}{z^2} \ . \tag{4.3.14}$$

The minimal surface can be parametrized by $r = r(z)$ and its area is given by

$$\text{Area}(\gamma_4) = \text{Vol}_{S^3} \int dz \frac{r(z)^3 \sqrt{1 + r'(z)^2}}{z^4} \ . \tag{4.3.15}$$

Extremizing this functional yields the usual solution

$$r(z) = \sqrt{r_0^2 - z^2} \ . \tag{4.3.16}$$

The z integral is divergent at $z = 0$, and the choice of cut-off follows the same logic as outlined for the free energy in appendix C.2. With a bulk IR/field theory UV cutoff at $z = \epsilon$, the integral becomes

$$\int_\epsilon^{r_0} dz \frac{r(z)^3}{z^4} \sqrt{1 + r'(z)^2} = \frac{r_0^3}{3\epsilon^3} - \frac{r_0}{\epsilon} + \frac{2}{3} + \mathcal{O}(\epsilon) \ . \tag{4.3.17}$$

Although holographic renormalization for submanifolds is well understood [84], the divergences in the entanglement entropy are usually kept, as a reflection of the short-distance behavior of QFTs. The universal part in odd dimensions, however, is the finite contribution and for the surfaces considered here given by

$$\text{Area}_{\text{ren}}(\gamma_4) = \frac{2}{3} \text{Vol}_{S^3} \ . \tag{4.3.18}$$

In summary, the entanglement entropy for a spherical region is given by the expression in (4.3.3), with the universal part of the area of the minimal surface in (4.3.18) and $\mathcal{I}$ given in (4.3.12). We note that this expression manifestly exhibits the same scaling with the residues Z_+^ℓ, corresponding to the charges of the external 5-branes, as the expression for the on-shell action in (4.2.38).

4.3.4 Matching to free energy

In this section we show that for all the examples discussed in sec. 4.2.5 the finite part of the holographic entanglement entropy for a spherical region is equal to minus the finite part of the free energy on S^5. To accomplish this we will reduce part of the two-dimensional integral over Σ appearing in equation (4.3.5) to a one-dimensional integral over the real line which has the same form as the one-dimensional integral appearing in the on-shell action (4.2.38), and show that the remaining part vanishes.

Using $\kappa^2 = -\partial_w \partial_{\bar{w}} \mathcal{G}$ and the definition of $\mathcal{G}$ in (4.1.4), the integral $\mathcal{I}$ given in (4.3.5) can be rewritten as

$$\mathcal{I} = -\frac{8}{3} \int_\Sigma d^2w \, \partial_w \partial_{\bar{w}} \mathcal{G} \left(|\mathcal{A}_+|^2 - |\mathcal{A}_-|^2 + \mathcal{B} + \bar{\mathcal{B}} \right) \ . \tag{4.3.19}$$

We split $\mathcal{I}$ into two terms:

$$\mathcal{I} = \mathcal{I}_1 + \mathcal{I}_2 \ , \tag{4.3.20a}$$

$$\mathcal{I}_1 = -\frac{4}{3} \int_\Sigma d^2w \, \partial_w \partial_{\bar{w}} \mathcal{G} \left(\mathcal{B} + \bar{\mathcal{B}} \right) \ , \tag{4.3.20b}$$

$$\mathcal{I}_2 = -\frac{8}{3} \int_\Sigma d^2w \, \partial_w \partial_{\bar{w}} \mathcal{G} \left(|\mathcal{A}_+|^2 - |\mathcal{A}_-|^2 + \frac{1}{2} \left(\mathcal{B} + \bar{\mathcal{B}} \right) \right) \ . \tag{4.3.20c}$$

First we evaluate $\mathcal{I}_1$ and will argue below that the second integral $\mathcal{I}_2$ vanishes. Since $\mathcal{B}$ is

holomorphic, we can write the integrand of $\mathcal{I}_1$ as a sum of total derivatives

$$\partial_w \partial_{\bar{w}} \mathcal{G}\left(\mathcal{B}+\bar{\mathcal{B}}\right) = \partial_{\bar{w}}\left(\partial_w \mathcal{G}(\mathcal{B}+\bar{\mathcal{B}})\right) - \partial_w\left(\mathcal{G}\partial_{\bar{w}}\bar{\mathcal{B}}\right) \ . \tag{4.3.21}$$

The boundary term resulting from the second term vanishes since $\mathcal{G}=0$ on $\partial\Sigma$. Switching to real coordinates we therefore find

$$\mathcal{I}_1 = \frac{2i}{3}\int_{-\infty}^{\infty} dx\, \partial_w \mathcal{G}\left(\mathcal{B}+\bar{\mathcal{B}}\right)\Big|_{y=0} \ . \tag{4.3.22}$$

To evaluate the integrand we use that $\mathcal{G}=0$ on the real line and hence $\mathcal{B}+\bar{\mathcal{B}} = -|\mathcal{A}_+|^2 + |\mathcal{A}_-|^2$. This yields

$$\partial_w \mathcal{G}\Big|_{y=0} = 2\sum_{\substack{m,n=1\\ m\neq n}}^{L} \frac{Z^{[mn]}}{x-p_n}\ln\left|\frac{x-p_m}{p_m-p_n}\right| \ , \tag{4.3.23}$$

$$\mathcal{B}+\bar{\mathcal{B}}\Big|_{y=0} = 2\pi i\sum_{\substack{\ell,k=1\\ k\neq \ell}}^{L} Z^{[\ell k]}\ln\left|\frac{x-p_k}{p_k-p_\ell}\right|\Theta\left(p_\ell - x\right) \ . \tag{4.3.24}$$

Thus we get

$$\mathcal{I}_1 = -\frac{8\pi}{3}\sum_{\substack{\ell,k,m,n=1\\ \ell\neq k, m\neq n}}^{L}\int_{-\infty}^{\infty} dx \frac{Z^{[\ell k]}Z^{[mn]}}{x-p_n}\ln\left|\frac{x-p_m}{p_m-p_n}\right|\ln\left|\frac{x-p_k}{p_k-p_\ell}\right|\Theta\left(p_\ell-x\right) \ . \tag{4.3.25}$$

Plugging this result into (4.3.3) gives the following contribution to the entanglement entropy

$$S_{\text{EE1}} = -\frac{4\pi}{9G_N}\text{Vol}_{\text{S}^2}\text{Vol}_{\text{S}^3}\sum_{\substack{\ell,k,m,n=1\\ \ell\neq k, m\neq n}}^{L} Z^{[\ell k]}Z^{[mn]}\int_{-\infty}^{p_\ell} dx \ln\left|\frac{x-p_m}{p_m-p_n}\right|\ln\left|\frac{x-p_k}{p_k-p_\ell}\right|\frac{1}{x-p_n} \ . \tag{4.3.26}$$

We can compare this result with the value of the finite part of the on-shell action derived in

section 4.2.3:

$$(S^{\rm E}_{\rm IIB})^{\rm finite} = \frac{8}{9G_{\rm N}}{\rm Vol}_{\rm S^5}{\rm Vol}_{\rm S^2}\sum_{\substack{\ell,k,m,n=1\\ \ell\neq k, m\neq n}}^{L} Z^{[\ell k]}Z^{[mn]}\int_{-\infty}^{p_\ell} dx\, \ln\left|\frac{x-p_k}{p_\ell-p_k}\right|\,\ln\left|\frac{x-p_m}{p_m-p_n}\right|\,\frac{1}{x-p_n}\ . \tag{4.3.27}$$

Inserting the expressions for the volumes of the 2-, 3- and 5-sphere given by

$${\rm Vol}_{\rm S^2} = 4\pi\ , \qquad {\rm Vol}_{\rm S^3} = 2\pi^2\ , \qquad {\rm Vol}_{\rm S^5} = \pi^3\ , \tag{4.3.28}$$

confirms the equality of the finite parts of the entanglement entropy and the on-shell action

$$(S_{\rm EE1})^{\rm finite} = -(S^{\rm E}_{\rm IIB})^{\rm finite}\ . \tag{4.3.29}$$

What remains to be shown is that the integral $\mathcal{I}_2$ vanishes and hence $S_{\rm EE1}$ given in (4.3.26) is the complete expression for the finite part of the entanglement entropy. The integral $\mathcal{I}_2$ given in (4.3.20c) can be rearranged as follows

$$\mathcal{I}_2 = -\frac{4}{3}\int_\Sigma d^2w\ (\mathcal{G}+|\mathcal{A}_+|^2-|\mathcal{A}_-|^2)\partial_w\partial_{\bar w}\mathcal{G} \tag{4.3.30}$$

$$= -\frac{4}{3}\int_\Sigma d^2w\left(-\partial_w\mathcal{G}\partial_{\bar w}\mathcal{G}+\partial_w\partial_{\bar w}\mathcal{G}(|\mathcal{A}_+|^2-|\mathcal{A}_-|^2)\right)\ . \tag{4.3.31}$$

Using the explicit expressions of $\mathcal{A}_+$ and $\mathcal{A}_-$ we get:

$$\mathcal{I}_2 = -\frac{4}{3}\sum_{\substack{\ell,k,m,n=1\\ \ell\neq k, m\neq n}}^{L} Z^{[mn]}Z^{[\ell k]}\int_\Sigma d^2w\,\frac{1}{\bar w-p_m}\Bigg(\ln\left|\frac{w-p_\ell}{p_k-p_\ell}\right|^2\ln\left|\frac{w-p_n}{p_m-p_n}\right|^2\frac{1}{w-p_k}$$
$$+\ln\frac{w-p_\ell}{|p_k-p_\ell|}\ln\frac{\bar w-p_k}{|p_k-p_\ell|}\frac{1}{w-p_n}\Bigg)\ . \tag{4.3.32}$$

For the three-pole solutions we have shown analytically that this term vanishes, and for the four and five pole solutions discussed in sec. 4.2.5 we have verified this numerically. For all

these cases we therefore find that the finite parts of the entanglement entropy and the on-shell action are related as expected on general grounds [50]. Although we do not currently have an analytic proof, this certainly suggests that the relation between free energy and entanglement entropy holds for all the solutions reviewed in sec. 4.1.

4.4 Summary

In this chapter we have studied the free energy and entanglement entropy of the field theories described by the supergravity solutions constructed in [120, 121]. The free energy is proportional to the on-shell action given by

$$S_{\text{IIB}}^{\text{E}} = -\frac{5}{3G_{\text{N}}}\text{Vol}_{\text{AdS}_6,\text{ren}}\text{Vol}_{\text{S}^2}\sum_{\substack{\ell,k,m,n=1\\ \ell\neq k,m\neq n}}^{L} Z^{[\ell k]}Z^{[mn]}\int_{-\infty}^{p_\ell} dx\, \ln\left|\frac{x-p_k}{p_\ell-p_k}\right|\ln\left|\frac{x-p_m}{p_m-p_n}\right|\frac{1}{x-p_n} \tag{4.4.1}$$

The entanglement entropy is given by

$$S_{\text{EE}} = -\frac{4}{9G_{\text{N}}}\,\text{Vol}_{\text{S}^2}\,\text{Vol}_{\text{S}^3}\sum_{\substack{\ell,k,m,n=1\\ \ell\neq k,m\neq n}}^{L} Z^{[\ell k]}Z^{[mn]}\int_{\Sigma} d^2w \ln\left|\frac{w-p_\ell}{p_k-p_\ell}\right|^2\ln\left|\frac{w-p_m}{p_m-p_n}\right|^2\frac{1}{\bar{w}-p_n}\frac{1}{w-p_k} \tag{4.4.2}$$

The finite parts were verified to match, for the case of three-, four-, and five-pole solutions following CHM in [50] as expected. The same matching is expected to hold for all the supergravity solutions, although this would correspond to non-trivial integral identities between the integrals appearing in the results. Additionally, these results support the interpretation of the solutions as holographic duals to the five-dimensional superconformal field theories engineered in type IIB string theory via 5-brane webs, and give first quantitative indications on the nature of the dual field theories.

Chapter 5

Conclusion

This dissertation is based on [2–4] in which we study superconformal field theories in excited states. We employ the AdS/CFT correspondence to compute observables using the corresponding holographic duals, which are given as bubbling solutions in 10- and 11-dimensional supergravity.

In [2] and [3] we obtain the holographic entanglement entropy of a spherical entangling surface corresponding to the 6-dimensional (2,0) theory in the presence of Wilson surfaces and the 4-dimensional $\mathcal{N} = 4$ $SU(N)$ SYM theory in the presence of surface defects. Additionally, we compute two other holographic observables in each case: the stress tensor and the expectation value of the surface operator. Our results are summarized in sections 2.5 and 3.6. In [4] we holographically compute the free energy and the entanglement entropy across a ball-shaped region for 5-dimensional SCFTs. We also verify that the finite parts of the two results match, as expected. A summary of these results is presented in 4.4.

Our calculations provide results that could be compared to field theory or localization calculations. In particular, in the Wilson surface case the possibility of a matrix model is encouraged by the existence of such a model after compactifying the theory on a circle, to get 5-dimensional SYM theory in the presence of a Wilson loop. In the 5-dimensional SCFTs the overall factor $\zeta(3)$ appearing in our results may originate from the eigenvalue distribution

of a matrix model (e.g. the matrix model action derived in [132] involves explicit factors of $\zeta(3)$).

One avenue to be explored is the probe brane approximation, in which most of the systems we investigate have a clear construction [1, 74]. This will be a check of validity of our results in the limit where backreaction is neglected or treated perturbatively. At the same time, probe brane results may reveal extra components entering the results, e.g. additional surface conformal anomaly contributions localized on the defects. This would be really interesting since, based on our calculations, traditional holography in the full-backreacted limit does not seem to be able to probe such components.

Appendix A

Wilson surface calculations

A.1 Contributions to the entanglement entropy

In this appendix we carefully discuss the contribution to the area integrals that are needed in section 2.2.2.

A.1.1 J_1

First we consider J_1, given in (2.2.8). The radial integral can be performed directly, but it is useful to rewrite it in terms of Legendre polynomials using (2.1.15). We divide the integration range into two regions: $0 \leq r \leq |\xi_i|$ and $|\xi_i| \leq r \leq r_c(\theta, \varepsilon)$. For each region we choose the Legendre representation that converges, yielding

$$J_1 = -4L^9 \sum_{i=1}^{2n} (-1)^i \int_0^\pi d\theta \, \sin\theta \left\{ \int_{|\xi_i|}^{r_c(\theta,\varepsilon)} dr \, \frac{r^2(r\cos\theta - \xi_i)}{r} \sum_{\ell=0}^{\infty} P_\ell(\cos\theta) \left(\frac{\xi_i}{r}\right)^\ell \right.$$
$$\left. + \int_0^{|\xi_i|} dr \, \frac{r^2(r\cos\theta - \xi_i)}{|\xi_i|} \sum_{\ell=0}^{\infty} P_\ell(\cos\theta) \left(\frac{r}{\xi_i}\right)^\ell \right\} \tag{A.1.1}$$

Performing the two radial integrals directly we find

$$J_1 = -4L^9 \sum_{i=1}^{2n} (-1)^i \int_0^\pi d\theta \, \sin\theta \left\{ \left[\cos\theta \, P_0 \, \frac{r^3}{3} + (\cos\theta \, P_1 - P_0) \, \xi_i \, \frac{r^2}{2} + (\cos\theta \, P_2 - P_1) \, \xi_i^2 \, r \right.\right.$$
$$\left. + (\cos\theta \, P_3 - P_2) \, \xi_i^3 \, \log r - \sum_{\ell=1}^{\infty} \frac{(\cos\theta P_{\ell+3} - P_{\ell+2})}{\ell} \, \frac{\xi_i^{\ell+3}}{r^\ell} \right]_{|\xi_i|}^{r_c(\theta,\varepsilon)}$$
$$\left. + \frac{1}{|\xi_i|} \left[-P_0 \, \xi_i \, \frac{r^3}{3} + \sum_{\ell=4}^{\infty} \frac{(\cos\theta P_{\ell-4} - P_{\ell-3})}{\ell} \, \frac{r^\ell}{\xi_i^{\ell-4}} \right]_0^{|\xi_i|} \right\} \tag{A.1.2}$$

Orthogonality of the Legendre polynomials can be expressed via

$$\int_0^\pi d\theta \, \sin\theta P_\ell \, (\cos\theta) P_k \, (\cos\theta) = \frac{2}{2\ell + 1} \, \delta_{\ell k} \tag{A.1.3}$$

We use this to simplify the above expression dramatically:

$$J_1 = -4L^9 \sum_{i=1}^{2n} (-1)^i \left\{ \int_0^\pi d\theta \, \sin\theta \left[\cos\theta \, P_0 \, \frac{r_c^3}{3} + (\cos\theta \, P_1 - P_0) \, \xi_i \, \frac{r_c^2}{2} + (\cos\theta \, P_2 - P_1) \, \xi_i^2 \, r_c \right.\right.$$
$$\left. \left. + (\cos\theta \, P_3 - P_2) \, \xi_i^3 \, \log r_c - \sum_{\ell=1}^{\infty} \frac{(\cos\theta P_{\ell+3} - P_{\ell+2})}{\ell} \, \frac{\xi_i^{\ell+3}}{r_c^\ell} \right] + \frac{2}{15} \, \xi_i^3 \right\} \tag{A.1.4}$$

Note that the final term is a sum of contributions at $r = |\xi_i|$. Substituting for the cut-off function $r_c(\theta, \varepsilon)$ given in (2.1.26), we then expand in ε up to and including $O\left(\varepsilon^0\right)$ and perform the remaining integrals over θ. We find the final result

$$J_1 = L^9 \left[\frac{64}{3\varepsilon^4} + \frac{-24 + 3m_2^2 - 8m_3}{15} + O\left(\varepsilon^2\right) \right] \tag{A.1.5}$$

A.1.2 J_2

Next we calculate J_2, which we reproduce from (2.2.10):

$$J_2 = -2L^9 \int_0^\pi d\theta \, \sin\theta \int_0^{r_c(\theta,\varepsilon)} dr \, r^2 \\ \times \left\{ 2n + 2\sum_{i<j} (-1)^{i+j} \frac{r^2 - r\cos\theta\,(\xi_i + \xi_j) + \xi_i\xi_j}{\sqrt{r^2 - 2r\xi_i\cos\theta + \xi_i^2}\sqrt{r^2 - 2r\xi_j\cos\theta + \xi_j^2}} \right\} \tag{A.1.6}$$

We can split the integral into two terms coming from the sum in the last line of (A.1.6). The first term is simply

$$J_{2,a} \equiv -\frac{4}{3} nL^9 \int_0^\pi d\theta \, \sin\theta \, r_c\,(\theta,\varepsilon)^3 \\ = L^9 \left[-\frac{64n}{3\varepsilon^6} + \frac{n(40 + 3m_2^2 - 8m_3)}{18\varepsilon^2} + O\left(\varepsilon^2\right) \right] \tag{A.1.7}$$

The evaluation of the second term, denoted $J_{2,b} \equiv J_2 - J_{2,a}$, is more involved than that of J_1. Our strategy is to divide up the radial integration range and replace the square root factors with the appropriate convergent series of Legendre polynomials in each interval. The fraction in the summand is symmetric under $(i \leftrightarrow j)$ so we can choose $|\xi_i| < |\xi_j|$ without loss of generality and write:

$$J_{2,b} = -4L^9 \sum_{i<j} (-1)^{i+j} \int_0^\pi d\theta \, \sin\theta \\ \times \left\{ \int_{|\xi_j|}^{r_c(\theta,\varepsilon)} dr \, \frac{r^2(r^2 - r\cos\theta\,(\xi_i + \xi_j) + \xi_i\xi_j)}{r^2} \sum_{\ell=0}^\infty P_\ell\left(\frac{\xi_i}{r}\right)^\ell \sum_{k=0}^\infty P_k\left(\frac{\xi_j}{r}\right)^k \right. \\ + \int_{|\xi_i|}^{|\xi_j|} dr \, \frac{r^2(r^2 - r\cos\theta\,(\xi_i + \xi_j) + \xi_i\xi_j)}{r|\xi_j|} \sum_{\ell=0}^\infty P_\ell\left(\frac{\xi_i}{r}\right)^\ell \sum_{k=0}^\infty P_k\left(\frac{r}{\xi_j}\right)^k \\ \left. + \int_0^{|\xi_i|} dr \, \frac{r^2(r^2 - r\cos\theta\,(\xi_i + \xi_j) + \xi_i\xi_j)}{|\xi_i||\xi_j|} \sum_{\ell=0}^\infty P_\ell\left(\frac{r}{\xi_i}\right)^\ell \sum_{k=0}^\infty P_k\left(\frac{r}{\xi_j}\right)^k \right\} \\ \equiv K_1 + K_2 + K_3 \tag{A.1.8}$$

where the Legendre polynomials are all functions of $\cos\theta$, as before. First let us consider K_1:

$$K_1 \equiv -4L^9 \sum_{i<j} (-1)^{i+j} \int_0^\pi d\theta \, \sin\theta \\ \times \sum_{\ell,k=0}^{\infty} P_\ell P_k \, \xi_i^\ell \xi_j^k \int_{|\xi_j|}^{r_c(\theta,\varepsilon)} dr \, \left(r^2 - r\cos\theta\,(\xi_i+\xi_j) + \xi_i\xi_j\right) r^{-\ell-k} \tag{A.1.9}$$

We must perform the radial integral first because its upper limit depends on θ. This results in several sums over powers of r and a logarithm:

$$K_1 = -4L^9 \sum_{i<j} (-1)^{i+j} \int_0^\pi d\theta \, \sin\theta \left\{ \sum_{\substack{\ell,k=0 \\ \ell+k\neq 3}}^{\infty} \frac{P_\ell P_k \, \xi_i^\ell \xi_j^k \, r^{3-\ell-k}}{3-\ell-k} \right. \\ - \cos\theta(\xi_i+\xi_j) \sum_{\substack{\ell,k=0 \\ \ell+k\neq 2}}^{\infty} \frac{P_\ell P_k \, \xi_i^\ell \xi_j^k \, r^{2-\ell-k}}{2-\ell-k} + \xi_i\xi_j \sum_{\substack{\ell,k=0 \\ \ell+k\neq 1}}^{\infty} \frac{P_\ell P_k \, \xi_i^\ell \xi_j^k \, r^{1-\ell-k}}{1-\ell-k} \\ \left. + \left(\sum_{\substack{\ell,k=0 \\ \ell+k=3}}^{3} P_\ell P_k \, \xi_i^\ell \xi_j^k - \cos\theta(\xi_i+\xi_j) \sum_{\substack{\ell,k=0 \\ \ell+k=2}}^{2} P_\ell P_k \, \xi_i^\ell \xi_j^k + \xi_i\xi_j \sum_{\substack{\ell,k=0 \\ \ell+k=1}}^{1} P_\ell P_k \, \xi_i^\ell \xi_j^k \right) \log r \right\}_{|\xi_j|}^{r_c(\theta,\varepsilon)} \tag{A.1.10}$$

We only require the entanglement entropy up to and including $O(\varepsilon^0)$. Recall that the cut-off function $r_c(\theta,\varepsilon)$ given (2.1.26) leads with $O(\varepsilon^{-2})$, and therefore only the logarithm and non-negative powers of r contribute to the upper limit. Specifically, we can terminate the infinite sums in the first and second lines at $3, 2$ and 1, respectively. Integrating over θ we find

$$K_1^{\text{upper}} = L^9 \left[\frac{64n}{3\varepsilon^6} - \frac{n(40+3m_2^2-8m_3)}{18\varepsilon^2} - \frac{64}{3\varepsilon^2} + O\left(\varepsilon^2\right) \right] \tag{A.1.11}$$

where we have made use of the following results:

$$\sum_{i<j}(-1)^{i+j} = -n, \qquad \sum_{i<j}(-1)^{i+j}(\xi_i - \xi_j)^2 = -4 \tag{A.1.12}$$

Next let us consider the lower limit and perform the integral over θ. The terms with no explicit $\cos\theta$ factor vanish unless $\ell = k$ by orthogonality (A.1.3). To deal with the terms that do have an explicit $\cos\theta$ factor, let us define

$$\begin{aligned} X_{\ell k} &\equiv \int_0^\pi d\theta\, \sin\theta\cos\theta P_\ell(\cos\theta) P_k(\cos\theta) = 2\begin{pmatrix} 1 & \ell & k \\ 0 & 0 & 0 \end{pmatrix}^2 \\ &= \frac{2(\ell-k)^2(1+\ell+k)}{(\ell+k)(2+\ell+k)(1+\ell-k)!(1-\ell+k)!} \end{aligned} \tag{A.1.13}$$

These terms are only non-zero when $X_{\ell k}$ is too, which occurs when $|\ell - k| = 1$. These two observations imply that the coefficient of the logarithm vanishes and that the conditions on the sums in the first two lines of (A.1.10) have no effect for the lower limit. All that remains is

$$\begin{aligned} K_1^{\text{lower}} = +4L^9 \sum_{i<j}(-1)^{i+j} \sum_{\ell,k=0}^{\infty} \xi_i^\ell \xi_j^k \Bigg[&\frac{2}{2\ell+1}\,\delta_{\ell k}\left(\frac{|\xi_j|^{3-\ell-k}}{3-\ell-k} + \frac{|\xi_j|^{1-\ell-k}}{1-\ell-k}\,\xi_i\xi_j\right) \\ &- \frac{|\xi_j|^{2-\ell-k}}{2-\ell-k}\,(\xi_i+\xi_j)\,X_{\ell k}\Bigg] \end{aligned} \tag{A.1.14}$$

Performing the sum over k and using the definition (A.1.13) we find

$$\begin{aligned} K_1^{\text{lower}} = +4L^9 \sum_{i<j}(-1)^{i+j} \sum_{\ell=0}^{\infty} \frac{2}{2\ell+1}\,\xi_i^\ell \xi_j^\ell \Bigg[&\frac{|\xi_j|^{3-2\ell}}{3-2\ell} + \frac{|\xi_j|^{1-2\ell}}{1-2\ell}\,\xi_i\xi_j \\ &- \frac{(\ell+1)\,|\xi_j|^{1-2\ell}}{(2\ell+3)(1-2\ell)}\,(\xi_i+\xi_j)^2\Bigg] \end{aligned} \tag{A.1.15}$$

The limits on the radial integrals in $K_{2,3}$ are independent of θ so we are free to reverse the

order of integration. Let us begin with K_2:

$$\begin{aligned} K_2 \equiv & -4L^9 \sum_{i<j} \frac{(-1)^{i+j}}{|\xi_j|} \int_{|\xi_i|}^{|\xi_j|} dr \sum_{\ell,k=0}^{\infty} r^{k-\ell} \frac{\xi_i^\ell}{\xi_j^k} \\ & \times \int_0^\pi d\theta \, \sin\theta P_\ell P_k \left(r^3 - r^2 \cos\theta \left(\xi_i + \xi_j\right) + r\xi_i\xi_j\right) \\ = & -4L^9 \sum_{i<j} \frac{(-1)^{i+j}}{|\xi_j|} \int_{|\xi_i|}^{|\xi_j|} dr \sum_{\ell,k=0}^{\infty} r^{k-\ell} \frac{\xi_i^\ell}{\xi_j^k} \left[\frac{2}{2\ell+1} \delta_{\ell k} \left(r^3 + r\xi_i\xi_j\right) - r^2(\xi_i + \xi_j) X_{\ell k}\right] \end{aligned} \tag{A.1.16}$$

where again we have used (A.1.3) and (A.1.13). Performing the sum over k then integrating over r we find

$$\begin{aligned} K_2 = & -4L^9 \sum_{i<j} \frac{(-1)^{i+j}}{|\xi_j|} \sum_{\ell=0}^{\infty} \frac{2}{2\ell+1} \frac{\xi_i^\ell}{\xi_j^\ell} \left[1 - \frac{\ell+1}{2\ell+3} \left(1 + \frac{\xi_i}{\xi_j}\right)\right] \\ & \times \left(\frac{|\xi_j|^4 - |\xi_i|^4}{4} + \frac{|\xi_j|^2 - |\xi_i|^2}{2} \xi_i\xi_j\right) \end{aligned} \tag{A.1.17}$$

We can compute K_3 using the same method:

$$\begin{aligned} K_3 \equiv & -4L^9 \sum_{i<j} \frac{(-1)^{i+j}}{|\xi_i||\xi_j|} \int_0^{|\xi_i|} dr \sum_{\ell,k=0}^{\infty} \frac{r^{\ell+k}}{\xi_i^\ell \xi_j^k} \\ & \times \int_0^\pi d\theta \, \sin\theta P_\ell P_k \left(r^4 - r^3 \cos\theta \left(\xi_i + \xi_j\right) + r^2\xi_i\xi_j\right) \\ = & -4L^9 \sum_{i<j} \frac{(-1)^{i+j}}{|\xi_i||\xi_j|} \int_0^{|\xi_i|} dr \sum_{\ell,k=0}^{\infty} \frac{r^{\ell+k}}{\xi_i^\ell \xi_j^k} \left[\frac{2}{2\ell+1} \delta_{\ell k} \left(r^4 + r^2\xi_i\xi_j\right) - r^3(\xi_i + \xi_j) X_{\ell k}\right] \\ = & -4L^9 \sum_{i<j} \frac{(-1)^{i+j}}{|\xi_i||\xi_j|} \sum_{\ell=0}^{\infty} \frac{2}{2\ell+1} \frac{1}{\xi_i^\ell \xi_j^\ell} \left\{\left[1 - \frac{\ell+1}{2\ell+3} \left(\xi_i + \xi_j\right) \left(\frac{1}{\xi_i} + \frac{1}{\xi_j}\right)\right] \frac{|\xi_i|^{5+2\ell}}{5-2\ell} \right. \\ & \left. + \frac{|\xi_i|^{3+3\ell}}{3+2\ell} \xi_i\xi_j\right\} \end{aligned} \tag{A.1.18}$$

Now we combine the finite contributions to $J_{2,b}$. The infinite sums can be evaluated and

the following remarkably simple result is obtained:

$$K_1^{\text{lower}} + K_2 + K_3 = \frac{4L^9}{3} \sum_{i<j} (-1)^{i+j} \operatorname{sgn} \xi_j \, (\xi_i - \xi_j)^3 \tag{A.1.19}$$

Recall that we have assumed $|\xi_i| < |\xi_j|$. The ordering of the ξ_i in (2.1.13) implies that $\operatorname{sgn} \xi_j$ evaluates to $+1$ and since the sum is ordered we can write the finite contribution to $J_{2,b}$ as

$$-\frac{4L^9}{3} \sum_{i<j} (-1)^{i+j} |\xi_i - \xi_j|^3 \tag{A.1.20}$$

Note that this term cannot be expressed in terms of the moments m_k. Thus, our final result for $J_{2,b}$ is:

$$J_{2,b} = L^9 \left[\frac{64n}{3\varepsilon^6} - \frac{n(40 + 3m_2^2 - 8m_3)}{18\varepsilon^2} - \frac{64}{3\varepsilon^2} - \frac{4}{3} \sum_{i<j} (-1)^{i+j} |\xi_i - \xi_j|^3 + O\left(\varepsilon^2\right) \right] \tag{A.1.21}$$

Summing (A.1.7) and (A.1.21) we find

$$J_2 = L^9 \left[-\frac{64}{3\varepsilon^2} - \frac{4}{3} \sum_{i<j} (-1)^{i+j} |\xi_i - \xi_j|^3 + O\left(\varepsilon^2\right) \right] \tag{A.1.22}$$

A.2 Calculation of the holographic stress tensor

In this appendix we present some details of the KK reduction calculation as well as the calculation of the stress tensor using holographic renormalization. As mentioned in section 2.3, first one has to decompose the metric into the vacuum $AdS_7 \times S^4$ part and fluctuations, as in (2.3.2). In FG coordinates the vacuum metric is given by

$$g^{(0)}_{MN} \, dx^M dx^N = L^2 \left[\frac{4}{u^2} \left(du^2 + \left(1 + \frac{u^2}{2} + \frac{u^4}{16} \right) ds^2_{AdS_3} + \left(1 - \frac{u^2}{2} + \frac{u^4}{16} \right) ds^2_{S^3} \right) \right.$$
$$\left. + d\tilde{\theta}^2 + \sin^2 \tilde{\theta} ds^2_{\tilde{S}_3} \right]. \tag{A.2.1}$$

The metric fluctuations in terms of the functions $\alpha_i(u,\tilde{\theta})$ appearing in (2.1.21) are

$$h_{MN}\,dx^M dx^N = L^2\left[\frac{4}{u^2}\left\{\left(\alpha_1 - 1 - \frac{u^2}{2} - \frac{u^4}{16}\right)ds^2_{AdS_3} + \left(\alpha_2 - 1 + \frac{u^2}{2} - \frac{u^4}{16}\right)ds^2_{S^3}\right\}\right.$$
$$\left. + (\alpha_3 - 1)\,d\tilde{\theta}^2 + \left(\alpha_4 - \sin^2\tilde{\theta}\right)ds^2_{\tilde{S}_3}\right]. \tag{A.2.2}$$

Using these expressions, we calculate the seven-dimensional reduced metric (2.3.4) and the outcome is

$$ds^2_7 = \frac{4L^2}{u^2}\left[du^2 + \left(1 + \frac{u^2}{2} + \frac{u^4}{16} + \frac{1}{320}(16 + 3m_2^2 - 8m_3)u^6\right)ds^2_{AdS_3}\right.$$
$$\left. + \left(1 - \frac{u^2}{2} + \frac{u^4}{16} - \frac{1}{320}(16 + 3m_2^2 - 8m_3)u^6\right)ds^2_{S^3}\right] \tag{A.2.3}$$

Notice that substituting the vacuum moments in (A.2.3) one can retrieve the AdS_7 entries in (A.2.1). This is because the trace shift does not contribute to the reduced metric, i.e. $\bar{\pi}$ vanishes. Furthermore, a further FG map of (A.2.3) is not necessary since it is already in FG form:

$$ds^2_7 = \frac{4L^2}{u^2}\left(du^2 + g_{ij}\,dx^i dx^j\right) \tag{A.2.4}$$

where the six-dimensional metric g_{ij} is given by a power series in u:

$$g = g_{(0)} + g_{(2)}\,u^2 + g_{(4)}\,u^4 + g_{(6)}\,u^6 + h_{(6)}\,u^6\log u^2 + \ldots \tag{A.2.5}$$

To compute the holographic stress tensor, we simply read off the asymptotic metric coefficients $g_{(0)}$, $g_{(2)}$, $g_{(4)}$ and $g_{(6)}$ from (A.2.3) and substitute them into the $d = 6$ formula given in [30]. For completeness we present this fomula here:

$$\langle T_{ij}\rangle = \frac{3\,(2L)^5}{8\pi G_N^{(7)}}\left(g_{(6)ij} - A_{(6)ij} + \frac{1}{24}\,S_{ij}\right) \tag{A.2.6}$$

where the second and third terms are defined via

$$\begin{aligned} A_{(6)ij} = \frac{1}{3}\Big[& 2(g_{(2)}g_{(4)})_{ij} + (g_{(4)}g_{(2)})_{ij} - (g^3_{(3)})_{ij} + \frac{1}{8}g_{(2)ij}\left(\operatorname{tr} g^2_{(2)} - (\operatorname{tr} g_{(2)})^2\right) \\ & - \operatorname{tr} g_{(2)}\left(g_{(4)ij} - \frac{1}{2}(g^2_{(2)})_{ij}\right) - g_{(0)ij}\left(\frac{1}{8}\operatorname{tr} g^2_{(2)}\operatorname{tr} g_{(2)} - \frac{1}{24}(\operatorname{tr} g_{(2)})^3\right. \\ & \left.\left. -\frac{1}{6}\operatorname{tr} g^3_{(2)} + \frac{1}{2}\operatorname{tr}(g_{(2)}g_{(4)})\right)\right] \end{aligned} \tag{A.2.7}$$

$$\begin{aligned} S_{ij} = {} & \nabla^2 C_{ij} - 2R^k{}_{i\,j}{}^l C_{kl} + 4\left((g_{(2)}g_{(4)}) - (g_{(4)}g_{(2)})\right)_{ij} + \frac{1}{10}\left(\nabla_i\nabla_j B - g_{(0)ij}\nabla^2 B\right) \\ & + \frac{2}{5}g_{(2)ij}B + g_{(0)ij}\left(-\frac{2}{3}\operatorname{tr} g^3_{(2)} - \frac{4}{15}(\operatorname{tr} g_{(2)})^3 + \frac{3}{5}\operatorname{tr} g_{(2)}\operatorname{tr} g^2_{(2)}\right) \end{aligned} \tag{A.2.8}$$

with the quantities C_{ij} and B defined by

$$\begin{aligned} C_{ij} &= g_{(4)ij} - \frac{1}{2}(g^2_{(2)})_{ij} + \frac{1}{4}g_{(2)ij}\operatorname{tr} g_{(2)} + \frac{1}{8}g_{(0)ij}B \\ B &= \operatorname{tr} g^2_{(2)} - (\operatorname{tr} g_{(2)})^2 \end{aligned} \tag{A.2.9}$$

Note that the contraction of indices is performed with the inverse of $g_{(0)ij}$. A general formula for the trace of the stress tensor follows from these definitions:

$$\langle T^i{}_i\rangle = \frac{3\,(2L)^5}{8\pi G^{(7)}_N}\left(-\frac{1}{24}(\operatorname{tr} g_{(2)})^3 + \frac{1}{8}\operatorname{tr} g_{(2)}\operatorname{tr} g^2_{(2)} - \frac{1}{6}\operatorname{tr} g^3_{(2)} + \frac{1}{3}\operatorname{tr} g_{(2)}g_{(4)}\right) \tag{A.2.10}$$

Evaluating these formulae we find

$$\langle T_{ij}\rangle\, dx^i dx^j = \frac{2^4 L^5}{8\pi G^{(7)}_N}\,\frac{20 + 9m_2^2 - 24m_3}{160}\left(ds^2_{AdS_3} - ds^2_{S^3}\right) \tag{A.2.11}$$

Notice that the stress tensor is traceless, which reflects the fact there is no Weyl anomaly for $AdS_3 \times S^3$. After observing

$$\frac{1}{8\pi G^{(7)}_N} = \frac{\mathrm{Vol}(S^4_L)}{8\pi G^{(11)}_N}, \quad \mathrm{Vol}(S^4_L) = \frac{8\pi^2}{3}\,L^4 \tag{A.2.12}$$

and using the definitions (2.2.14), we then subtract off the contribution from the vacuum to obtain our final result:

$$\Delta\langle T_{ij}\rangle\, dx^i dx^j = \frac{N^3}{160\pi^3}\left(16 + 3m_2^2 - 8m_3\right)\left(ds^2_{AdS_3} - ds^2_{S^3}\right) \tag{A.2.13}$$

A.3 Four-form field strength

In this appendix we present the formula for the four-form field strength

$$F = (f_1)^3 g_{1m}\,\omega_{AdS_3} \wedge e^m + (f_2)^3 g_{2m}\,\omega_{S^3} \wedge e^m + (f_3)^3 g_{3m}\,\omega_{\tilde{S}^3} \wedge e^m \tag{A.3.1}$$

where ω_X denotes the volume form for a unit-radius space X. The g_{Im} are related to derivatives of potentials b_I via

$$\begin{aligned}
(f_1)^3 g_{1w} &= -\partial_w b_1/L^3 = 2(j_w^+ + j_w^-) \\
(f_2)^3 g_{2w} &= -\partial_w b_2/L^3 = -2(j_w^+ - j_w^-) \\
(f_3)^3 g_{3w} &= -\partial_w b_3/L^3 = \frac{1}{8}\, j_w^3
\end{aligned} \tag{A.3.2}$$

Since the four-form field strength is related to the three-form potentials by $F_{(I)} = dC_{(I)}$, it follows from (A.3.2) that the potentials take the following form:

$$\begin{aligned}
C_{(1)} &= b_1 \frac{1}{z^3} dz \wedge dt \wedge dl \\
C_{(2)} &= b_2 \sin^2\theta_1 \sin\theta_2\; d\theta_1 \wedge \theta_2 \wedge d\theta_3 \\
C_{(3)} &= b_3 \sin^2\psi_1 \sin\psi_2\; d\psi_1 \wedge d\psi_2 \wedge d\psi_3
\end{aligned} \tag{A.3.3}$$

Next we review the the expressions for the fields j in (A.3.2) found in [77]. The currents

can be expressed in a compact way by defining

$$J_w = \frac{h}{L^3(G+\bar{G})}\left[\bar{G}\left(G - 3\bar{G} + 4G\bar{G}^2\right)\partial_w G + G\left(G+\bar{G}\right)\partial_w \bar{G}\right] \tag{A.3.4}$$

and are given by

$$\begin{aligned} j_w^+ &= 2i\, J_w \left((G-\bar{G})^2 - 4G^3\bar{G}\right) W^{-4} \\ j_w^- &= 2\, G J_w \left(-2G\bar{G} + 3\bar{G}^2 - G^2 + 4G^2\bar{G}^2\right) W^{-4} \\ j_w^3 &= 3\partial_w h\, \frac{W^2}{G(1-G\bar{G})} - 2J_w\, \frac{(1+G^2)}{G(1-G\bar{G})^2} \end{aligned} \tag{A.3.5}$$

It is then straightforward to verify that the potentials are given by

$$\begin{aligned} b_1 &= \frac{2(G+\bar{G})h}{2G\bar{G} + i(G-\bar{G})} + 2\tilde{h} - 2\Phi \\ b_2 &= -\frac{2(G+\bar{G})h}{2G\bar{G} - i(G-\bar{G})} + 2\tilde{h} + 2\Phi \\ b_3 &= -\frac{(G+\bar{G})h}{4(G\bar{G}-1)} - \Phi \end{aligned} \tag{A.3.6}$$

Here, $\tilde{h}$ is the dual harmonic function to h and satisfies

$$i\partial_w h = \partial_w \tilde{h} \tag{A.3.7}$$

With $h = -iL^3(w-\bar{w})$ as in (2.1.11), one obtains

$$\tilde{h} = L^3(w+\bar{w}) \tag{A.3.8}$$

Also, Φ is defined via

$$\bar{G}\partial_w h = \partial_w \Phi \tag{A.3.9}$$

Using $\partial_w h = -iL^3$ and G given by (2.1.12) we solve (A.3.9) to find

$$\Phi = L^3 \sum_j (-1)^j \sqrt{(w-\xi_j)(\bar{w}-\xi_j)} \tag{A.3.10}$$

Note that Φ is real, hence the only thing that could be added is a constant, corresponding to an ambiguity in the definition of the b_I.

A.4 Calculation of the real line contribution to the on-shell action

In this appendix we present details on the calculation of the contribution from the real line to the on-shell action. To do this we have to expand the metric factors and b_I in a power series in y around $y = 0$. The important point is that the expansion of $G, \bar{G}$ differs in different intervals. Let us define

$$\begin{aligned} \mathcal{I}_0 &= [-\infty, \xi_1] \cup [\xi_2, \xi_3] \cup \cdots \cup [\xi_{2n}, +\infty] \\ \mathcal{I}_+ &= [\xi_1, \xi_2] \cup [\xi_3, \xi_4] \cup \cdots \cup [\xi_{2n-1}, \xi_{2n}] \end{aligned} \tag{A.4.1}$$

For the Taylor series expansion of G we have

$$G = \begin{cases} 0 + g_1(x)y + ig_2(x)y^2 + g_3(x)y^3 + \ldots & x \in \mathcal{I}_0 \\ i + g_1(x)y + ig_2(x)y^2 + g_3(x)y^3 + \ldots & x \in \mathcal{I}_+ \end{cases} \tag{A.4.2}$$

where

$$\begin{aligned} g_1(x) &= \sum_j (-1)^j \frac{1}{2} \frac{1}{|x-\xi_j|} \\ g_2(x) &= \sum_j (-1)^j \frac{1}{4} \frac{\text{sign}(x-\xi_j)}{|x-\xi_j|^2} \\ g_3(x) &= \sum_j (-1)^{j+1} \frac{1}{4} \frac{1}{|x-\xi_j|^3} \end{aligned} \tag{A.4.3}$$

For the calculation of b_I we also need the Taylor series expansion of Φ defined in (A.3.10):

$$\Phi = L^3 \left(\phi_0(x) + \phi_2(x) y^2 + \phi_4(x) y^4 + \ldots \right) \tag{A.4.4}$$

where

$$\begin{aligned} \phi_0(x) &= \sum_j (-1)^j |x - \xi_j| \\ \phi_2(x) &= \sum_j (-1)^j \frac{1}{2} \frac{1}{|x - \xi_j|} \\ \phi_4(x) &= \sum_j (-1)^{j+1} \frac{1}{8} \frac{1}{|x - \xi_j|^3} \end{aligned} \tag{A.4.5}$$

Note that $g_1 = \phi_2$ and $g_3 = 2\phi_4$ which will be important in the expansion of the action. The combinations of metric functions appearing in (2.4.9) can be expanded as follows:

$$\left(\frac{f_2 f_3}{f_1} \right)^3 = \begin{cases} \frac{L^3 (g_1^2 - g_2)^2}{g_1^2 + g_2} y^3 + O(y^5) & x \in \mathcal{I}_0 \\ \\ -\frac{L^3 (g_1^2 + g_2)^2}{2(g_1^2 + 2g_2)} y^3 + O(y^5) & x \in \mathcal{I}_+ \end{cases} \tag{A.4.6}$$

and

$$\left(\frac{f_1 f_3}{f_2} \right)^3 = \begin{cases} -\frac{L^3 (g_1^2 + g_2)^2}{g_1^2 - g_2} y^3 + O(y^5) & x \in \mathcal{I}_0 \\ \\ \frac{4L^3}{g_1^4 + 3g_1^2 g_2 + 2g_2^2} \frac{1}{y^3} + O(\frac{1}{y}) & x \in \mathcal{I}_+ \end{cases} \tag{A.4.7}$$

and

$$\left(\frac{f_1 f_2}{f_3} \right)^3 = \begin{cases} -\frac{8L^3}{(g_1^4 - g_2^2)} \frac{1}{y^3} + O(\frac{1}{y}) & x \in \mathcal{I}_0 \\ \\ -\frac{4L^3 (g_1^2 + 2g_2)^2}{g_1^2 + g_2} y^3 + O(y^5) & x \in \mathcal{I}_+ \end{cases} \tag{A.4.8}$$

The expansion of b_I with $I = 1, 2, 3$ works the same way, but there are some cancellations due to the relations of the expansion coefficients for G and Φ mentioned above. We find

$$b_1 = \begin{cases} L^3 \left(\frac{4g_1}{g_1^2 - g_2} - 2\phi_0 + 4x + O(y^2) \right) & x \in \mathcal{I}_0 \\ \\ L^3 \left(\frac{4g_1}{g_1^2 + g_2} - 2\phi_0 + 4x + O(y^2) \right) & x \in \mathcal{I}_+ \end{cases} \tag{A.4.9}$$

Since the subleading term is of order y^2 as $y \to 0$ we find that $\partial_y(b_1^2)$ is of order y. Also note that the metric factor (A.4.6) is of order y^3 as $y \to 0$. Thus we find that the contribution to the action coming from b_1 vanishes at $y = 0$ and hence does not contribute.

The Taylor expansion of b_2 is given by

$$b_2 = \begin{cases} L^3 \left(-\frac{4g_1}{g_1^2 + g_2} + 2\phi_0 + 4x + O(y^2) \right) & x \in \mathcal{I}_0 \\ \\ L^3 \left((2\phi_0 + 4x) + (g_1^3 + 3g_1 g_2 - g_3) y^4 + O(y^6) \right) & x \in \mathcal{I}_+ \end{cases} \tag{A.4.10}$$

It is important to note that for $x \in \mathcal{I}_+$ we find that $\partial_y(b_2)^2$ will behave as y^3 as $y \to 0$ and together with the behavior of the metric factor (A.4.7) produces a finite contribution to the action.

Similarly the Taylor expansion for b_3 is given by

$$b_3 = \begin{cases} L^3 \left(-\phi_0 + \left(g_1^3 + \frac{g_3}{2} \right) y^4 + O(y^5) \right) & x \in \mathcal{I}_0 \\ \\ L^3 \left(-\frac{g_1}{g_1^2 + 2g_2} - \phi_0 + O(y^2) \right) & x \in \mathcal{I}_+ \end{cases} \tag{A.4.11}$$

In a similar manner as for b_2 we note that for $x \in \mathcal{I}_0$ the $\partial_y(b_3)^2$ term will be of order y^3 which together with the behavior of the metric factor (A.4.8) will produce a finite contribution to the action at $y = 0$.

Summarizing we find that

$$\begin{aligned}
&\lim_{y\to 0}\frac{f_2^3 f_3^2}{2f_1^3}\partial_y(b_1^2)=0, \qquad x\in\mathbb{R}\\
&\lim_{y\to 0}\frac{f_1^3 f_3^3}{2f_2^3}\partial_y(b_2^2)=\begin{cases} 0 & x\in\mathcal{I}_0\\ \frac{32L^9(g_1^3+3g_1g_2-g_3)(\phi_0+2x)}{(g_1^2+g_2)(g_1^2+2g_2)} & x\in\mathcal{I}_+\end{cases}\\
&\lim_{y\to 0}\frac{f_1^3 f_2^3}{2f_3^3}\partial_y(b_3^2)=\begin{cases} \frac{16L^9(2g_1^3+g_3)\phi_0}{(g_1^2-g_2)(g_1^2+g_2)} & x\in\mathcal{I}_0\\ 0 & x\in\mathcal{I}_+\end{cases}
\end{aligned} \tag{A.4.12}$$

The integration region $\mathcal{I}_0$ is cut off by the large r_c cutoff and includes the intervals $[-r_c,\xi_1]$ and $[\xi_{2n},r_c]$ that are responsible for r_c divergent terms. Using the large $|x|$ expansion one can show using the Taylor series expansions of (A.4.12) for large arguments that the contribution from the integral is given from the large integration limits $x_{c,+}$ and $x_{c,-}$ by

$$\begin{aligned}
&\int_{\xi_{2n}}^{x_{c,+}} dx\frac{f_1^3 f_2^3}{2f_3^3}\partial_y(b_3^2)|_{y=0}=L^9\left[-16x_{c,+}^3+12m_2x_{c,+}^2+(16-9m_2^2+16m_3)x_{c,+}\right]+\text{finite}\\
&\int_{x_{c,-}}^{\xi_1} dx\frac{f_1^3 f_2^3}{2f_3^3}\partial_y(b_3^2)|_{y=0}=L^9\left[-16|x_{c,-}|^3-12m_2|x_{c,-}|^2+(16-9m_2^2+16m_3)|x_{c,-}|\right]+\text{finite}
\end{aligned} \tag{A.4.13}$$

Using the fact that $x_{c,+}=r_c(0,\varepsilon)$ and $x_{c,-}=r_c(\pi,\varepsilon)$ together with the relation of the radial cut-off to the FG cut-off parameter ε given in (2.1.26), one can extract the contributions of the x-integral that are divergent with respect to the cut-off ε as follows:

$$S_{(x)}^{\text{div}}=+\frac{L^9}{48\pi G_N^{(11)}}\,\text{Vol}(S^3)^2\,\text{Vol}(AdS_3)\left(-\frac{256}{\varepsilon^6}+\frac{80-12m_2^2+32m_3}{\varepsilon^2}\right) \tag{A.4.14}$$

Appendix B

Surface defect Calculations

B.1 Fefferman-Graham coordinates

This section complements the discussion of the FG mapping procedure in section 3.2. We describe the gauge choice for the one-form V and give the results of the FG coordinate map.

B.1.1 Gauge choice

As mentioned in section 3.2 we are interested to choose ω such that $V_\rho = 0$. In particular, we first need to expand the function

$$\omega = \sum_{n=0}^{\infty} \frac{\omega^{(n)}(\theta, \alpha)}{\rho^n} \tag{B.1.1}$$

where $\alpha = \psi + \phi$ and demand that $V_\rho = 0$ at each order in the ρ^{-1} expansion. This is a gauge choice that kills all $d\rho\, dY$ cross terms with $Y \in \{\psi, \theta, \phi\}$ in the asymptotic expansion of the metric[1].Then we fix $\omega^{(0)}$ by demanding that the $d\theta\, d\psi$ and $d\psi\, d\phi$ cross terms vanish

[1]Note that ds_X^2 defined in (3.2.2) has no $d\rho\, dY$ cross terms.

at zeroth order for all M. Considering the expansion of the one-form (3.2.9) at large ρ:

$$V_I = \sum_{n=1}^{\infty} \frac{V_I^{(n)}(\theta, \alpha)}{\rho^n} \tag{B.1.2}$$

The result for ω is given in terms of $V_I^{(n)}$ coefficients in (3.2.15). Substituting the explicit expressions for the coefficients it can be written as

$$\begin{aligned}
\omega = & -\frac{M-1}{2}\,\alpha + \frac{1}{2\sin\theta\,\rho}\sum_{i=1}^{M}\left(x_{i2}\cos\alpha - x_{i1}\sin\alpha\right) \\
& - \frac{1}{4\sin^2\theta\,\rho^2}\sum_{i=1}^{M}\left[\left(x_{i1}^2 - x_{i2}^2\right)\sin 2\alpha - 2x_{i1}x_{i2}\cos 2\alpha\right] \\
& - \frac{1}{6\sin^3\theta\,\rho^3}\sum_{i=1}^{M}\left[\left(x_{i1}^3 - 3x_{i1}x_{i2}^2\right)\sin 3\alpha + \left(x_{i2}^3 - 3x_{i1}^2x_{i2}\right)\cos 3\alpha\right] \\
& + \frac{1}{8\rho^4}\left\{\frac{1}{\sin^4\theta}\sum_{i=1}^{M}\left[4\left(x_{i1}^3x_{i2} - x_{i1}x_{i2}^3\right)\cos 4\alpha - \left(x_{i1}^4 - 6x_{i1}^2x_{i2}^2 + x_{i2}^4\right)\sin 4\alpha\right]\right. \\
& \left. + \sin^2\theta\sum_{i=1}^{M}\left[-8y_i^2x_{i1}x_{i2}\cos 2\alpha + 4\left(y_i^2x_{i1}^2 - y_i^2x_{i2}^2\right)\sin 2\alpha\right]\right\} + O\left(\rho^{-5}\right)
\end{aligned} \tag{B.1.3}$$

This is the gauge choice which eliminates the V_ρ component and brings the metric in a manifestly asymptotically $AdS_5 \times S^5$ form.

B.1.2 The coordinate map

In this subsection we give the results of the FG mapping. We express them in terms of the expansion coefficients of the functions F_a appearing in (3.2.16). The coefficients relevant to our calculation come from the expansion of F_ρ:

$$F_\rho = \sum_{n=1}^{\infty} \frac{F_\rho^{(n)}(\theta, \alpha)}{\rho^n} \tag{B.1.4}$$

In what follows we express the relevant coefficients in terms of the moments:

$$
\begin{aligned}
4F_\rho^{(2)} &= (1-3\cos 2\theta)\left[1+2\left(m_{220}+m_{202}\right)-m_{400}\right] \\
&\quad + 12\left[\cos 2\alpha\left(m_{220}-m_{202}\right)+2m_{211}\sin 2\alpha\right]\sin^2\theta \\
F_\rho^{(3)} &= 3\left(\sin\theta-\sin 3\theta\right)\left[\left(m_{212}+m_{230}-m_{410}\right)\cos\alpha+\left(m_{221}+m_{203}-m_{401}\right)\sin\alpha\right] \\
&\quad + 4\sin^3\theta\left[\left(-3m_{212}+m_{230}\right)\cos 3\alpha-\left(-3m_{221}+m_{203}\right)\sin 3\alpha\right] \\
32F_\rho^{(4)} &= -4\cos^4\theta+\left(5-12\cos 2\theta+15\cos 4\theta\right)\left(2m_{202}+2m_{220}-m_{400}\right) \\
&\quad - 16\left(1+5\cos 2\theta\right)\sin^2\theta\sin 2\alpha\left[3m_{211}+8\left(m_{213}+m_{231}\right)-12m_{411}\right] \\
&\quad - 8\left(1+5\cos 2\theta\right)\sin^2\theta\cos 2\alpha\left[3\left(m_{220}-m_{202}\right)+8\left(m_{240}-m_{204}\right)\right] \\
&\quad - 8\left(1+5\cos 2\theta\right)\sin^2\theta\cos 2\alpha\left[12\left(m_{402}-m_{420}\right)\right] \\
&\quad - 640\sin 4\alpha\sin^4\theta\left(m_{213}-m_{231}\right) \\
&\quad + 24\left(3-4\cos 2\theta+5\cos 4\theta-40\cos 4\alpha\sin^4\theta\right)m_{222} \\
&\quad + 4\left(9-12\cos 2\theta+15\cos 4\theta+40\cos 4\alpha\sin^4\theta\right)\left(m_{204}+m_{240}\right) \\
&\quad - 4\left(3-4\cos 2\theta+5\cos 4\theta\right)\left[6\left(m_{402}+m_{420}\right)-m_{600}\right] \\
&\quad - \Big(12\sin^2\theta\left[\cos 2\alpha\left(m_{202}-m_{220}\right)-2\sin 2\alpha\, m_{211}\right] \\
&\qquad - \left(1-3\cos 2\theta\right)\left(2m_{202}+2m_{220}-m_{400}\right)\Big)^2
\end{aligned}
\tag{B.1.5}
$$

The FG mapping, as described in section 3.2, gives the following results for the FG

coordinates:

$$
\begin{aligned}
u &= \frac{1}{\rho}\left[1+\frac{F_\rho^{(2)}-1}{4\rho^2}+\frac{F_\rho^{(3)}}{6\rho^3}+\frac{16(F_\rho^{(4)}-F_\rho^{(2)}+1)-(\partial_\theta F_\rho^{(2)})^2-(\partial_\phi F_\rho^{(2)})^2\csc^2\theta}{128\rho^4}+O\left(\rho^{-5}\right)\right]\\
\tilde{\psi} &= \psi-\frac{\partial_\psi F_\rho^{(2)}}{16\rho^4}-\frac{\partial_\psi F_\rho^{(3)}}{30\rho^5}+O\left(\rho^{-6}\right)\\
\tilde{\theta} &= \theta-\frac{\partial_\theta F_\rho^{(2)}}{8\rho^2}-\frac{\partial_\theta F_\rho^{(3)}}{18\rho^3}+\frac{1}{256\rho^4}\left[-8\partial_\theta F_\rho^{(4)}+3\partial_\phi F_\rho^{(2)}\,\partial_\theta\partial_\phi F_\rho^{(2)}\csc^2\theta\right.\\
&\quad\left.-(\partial_\phi F_\rho^{(2)})^2\cot\theta\csc^2\theta+\partial_\theta F_\rho^{(2)}\left(12-4F_\rho^{(2)}+16F_4^{(2)}+3\partial_\theta^2 F_\rho^{(2)}\right)\right]+O\left(\rho^{-5}\right)\\
\tilde{\phi} &= \phi-\frac{\partial_\phi F_\rho^{(2)}}{8\sin^2\theta\,\rho^2}-\frac{\partial_\phi F_\rho^{(3)}}{18\sin^2\theta\,\rho^3}+\frac{1}{256\sin^2\theta\,\rho^4}\left[-8\partial_\phi F_\rho^{(4)}+3\partial_\theta F_\rho^{(2)}\,\partial_\theta\partial_\phi F_\rho^{(2)}\right.\\
&\quad\left.+\partial_\phi F_\rho^{(2)}\left(12-4F_\rho^{(2)}+16F_5^{(2)}+3\partial_\phi^2 F_\rho^{(2)}\csc^2\theta-4\partial_\theta F_\rho^{(2)}\cot\theta\right)\right]+O\left(\rho^{-5}\right)
\end{aligned}
\tag{B.1.6}
$$

B.2 Holographic entanglement entropy

In this section we present some details of the holographic entanglement entropy calculation performed in section 3.3. To compute the integrals (3.3.13) involved in the area functional we performed a change of variables (3.3.14) which brought the integrals to a form matching the vacuum integrals (3.3.16). To set the limits of integration over $\bar{\rho}$ we need to express the FG cut-off in the new coordinates as $\bar{\rho}_c(\bar{\theta},\bar{\alpha},\varepsilon)$.

The first step is to express $\{\rho,\theta,\alpha\}$ coordinates in terms of $\{\bar{\rho},\bar{\theta},\bar{\alpha}\}$. Combining (3.2.11, 3.3.14, 3.3.17) we can write the change of variables as

$$
\begin{aligned}
\sqrt{\rho^2+1}\cos\theta &= y_i\sqrt{\bar{\rho}^2+1}\cos\bar{\theta}\\
\rho\sin\theta\cos(\alpha) &= y_i\bar{\rho}\sin\bar{\theta}\cos\bar{\alpha}+r_i^2\cos^2\beta_i\\
\rho\sin\theta\sin(\alpha) &= y_i\bar{\rho}\sin\bar{\theta}\sin\bar{\alpha}+r_i^2\sin^2\beta_i
\end{aligned}
\tag{B.2.1}
$$

where we have defined $x_{i1}=r_i\cos\beta_i$ and $x_{i2}=r_i\sin\beta_i$. We begin with solving the first equation in terms of ρ. Then, we combine the last two equations to eliminate α and we

substitute ρ. This gives an equation for $\sin\theta$ in terms of the barred variables:

$$\sin^4\theta + A\,\sin^2\theta + B = 0 \tag{B.2.2}$$

with

$$\begin{aligned} A &= -1 + r_i^2 + 2\bar{\rho}\, r_i\, y_i \cos\left(\bar{\alpha} - \beta_i\right)\sin\bar{\theta} + \frac{y_i^2\left(1 + \cos 2\bar{\theta} + 2\bar{\rho}^2\right)}{2} \\ B &= -r_i^2 - 2\bar{\rho}\, r_i\, y_i \cos\left(\bar{\alpha} - \beta_i\right)\sin\bar{\theta} + \frac{\bar{\rho}^2\, y_i^2\left(\cos 2\bar{\theta} - 1\right)}{2} \end{aligned} \tag{B.2.3}$$

Since $\theta \in [0, \pi/2]$ we choose the solution for which $\sin\theta$ is real and positive. We get the rest by plugging this solution into the equations (B.2.1) . Specifically, ρ is found by plugging $\sin\theta$ into the first equation while $\sin\bar{\alpha}$ and $\cos\bar{\alpha}$ are found using the other two equations. Since we only need the asymptotic behavior we give the results expanded at large $\bar{\rho}$:

$$\begin{aligned} \rho^2 &= y_i^2\bar{\rho}^2 + 2r_i y_i \cos(\bar{\alpha} + \beta_i)\sin\bar{\theta}\bar{\rho} + \frac{1}{2}\left(y_i^2 + 2r_i^2 - 1 + (y_i^2 - 1)\cos 2\bar{\theta}\right) + O\left(\frac{1}{\bar{\rho}}\right) \\ \sin^2\theta &= \sin^2\bar{\theta} + \frac{2r_i\cos(\bar{\alpha} + \beta_i)\cos^2\bar{\theta}\sin\bar{\theta}}{y_i\bar{\rho}} \\ &\quad + \frac{\cos^2\bar{\theta}\left(1 - y_i^2 + (y_i^2 + 2r_i^2 - 1)\cos 2\bar{\theta} - 4r_i^2\cos(2\bar{\alpha} + 2\beta_i)\sin^2\bar{\theta}\right)}{2y_i^2\bar{\rho}^2} + O\left(\frac{1}{\bar{\rho}^3}\right) \\ \sin\alpha &= \sin\bar{\alpha} + \frac{r_i\csc\bar{\theta}(\cos\beta_i - \cos(\bar{\alpha} + \beta_i)\sin\bar{\alpha})}{y_i\bar{\rho}} \\ &\quad + \frac{r_i^2\csc^2\bar{\theta}\left(-4\cos\beta_i\cos(\bar{\alpha} + \beta_i) + \sin\bar{\alpha} + 3\cos(2\bar{\alpha} + 2\beta_i)\sin\bar{\alpha}\right)}{4y_i^2\bar{\rho}^2} + O\left(\frac{1}{\bar{\rho}^3}\right) \\ \cos\alpha &= \cos\bar{\alpha} - \frac{r_i\csc\bar{\theta}(\cos\beta_i + \cos(2\bar{\alpha} + \beta_i) - 2\sin\beta_i)}{2y_i\bar{\rho}} \\ &\quad + \frac{r_i^2\csc^2\bar{\theta}\left(-4\sin\beta_i\cos(\bar{\alpha} + \beta_i) + \cos\bar{\alpha} + 3\cos(2\bar{\alpha} + 2\beta_i)\cos\bar{\alpha}\right)}{4y_i^2\bar{\rho}^2} + O\left(\frac{1}{\bar{\rho}^3}\right) \end{aligned} \tag{B.2.4}$$

To find the cut-off $\bar{\rho}_c(\bar{\theta}, \bar{\alpha}, \varepsilon)$ we substitute (B.2.4) in the expression for the FG coordinate

u, which can be found in (B.1.6), to get u in terms of the barred coordinates.

$$\begin{aligned} u = \frac{1}{y_i\bar{\rho}} - \frac{r_i\cos(\bar{\alpha}+\beta_i)\sin\bar{\theta}}{y_i^2\bar{\rho}^2} - \frac{1}{8y_i^3\bar{\rho}^3}\Big[1 + 4r_i^2 + 2y_i^2 + 2(y_i^2-1)\cos 2\bar{\theta} \\ + 2m_{220} + 2m_{202} - m_{400} - 3\sin^2\bar{\theta}\left(1 + 2r_i^2 + 2r_i^2\cos(2\bar{\alpha}+2\beta_i)\right. \\ \left. +2m_{220} + 2m_{202} - m_{400} + 4\sin 2\bar{\alpha}\, m_{211} + 2\cos 2\bar{\alpha}(m_{220} - m_{202})\right)\Big] + O\left(\frac{1}{\bar{\rho}^4}\right) \end{aligned} \tag{B.2.5}$$

Solving this asymptotically for $\bar{\rho}$ and setting $u = \varepsilon$ we find the cut-off surface in barred coordinates.

$$\begin{aligned} \bar{\rho}_c(\varepsilon,\bar{\theta},\bar{\alpha}) = \frac{1}{y_i\varepsilon} - \frac{r_i\cos(\bar{\alpha}+\beta_i)\sin\bar{\theta}}{y_i} + \frac{1}{8y_i}\Big[-1 - 4r_i^2 - 2y_i^2 - 2(y_i^2-1)\cos 2\bar{\theta} \\ - 2m_{220} - 2m_{202} + m_{400} + \sin^2\bar{\theta}\left(3 + 2r_i^2 + 2r_i^2\cos(2\bar{\alpha}+2\beta_i)\right. \\ \left. +6m_{220} + 6m_{202} - 3m_{400} + 12\sin 2\bar{\alpha}\, m_{211} + 6\cos 2\bar{\alpha}(m_{220} - m_{202})\right)\Big]\varepsilon + O\left(\varepsilon^2\right) \end{aligned} \tag{B.2.6}$$

B.3 Coordinate systems and maps

In this section we collect useful formulae for the various coordinate systems and their maps along with information about our setup in these systems. In particular we relate $AdS_3 \times S^1$ to $S^1 \times H^3$ with an intermediate transformation to $\mathbb{R}^4$. In the latter space the picture of our setup becomes more clear (see figure 3.1).

The metrics on the 4D Euclidean spaces we consider are the following:

$$\begin{aligned} AdS_3 \times S^1 \qquad & ds^2_{AdS_3\times S^1} = \frac{dt^2 + dl^2 + dz^2}{z^2} + d\psi^2 \\ \text{spherical} \qquad & ds^2_{\mathbb{R}^4} = dt^2 + dx^2 + x^2\left(d\vartheta^2 + \sin^2\vartheta\, d\psi^2\right) \\ \text{hyperboloid} \qquad & ds^2_{S^1\times H^3} = d\tau^2 + R^2\left(d\rho^2 + \sinh^2\rho\left(d\vartheta^2 + \sin^2\vartheta\, d\psi^2\right)\right) \end{aligned} \tag{B.3.1}$$

They are conformally related to each other as follows:

$$ds^2_{AdS_3\times S^1} = z^{-2}\, ds^2_{\mathbb{R}^4}, \quad ds^2_{\mathbb{R}^4} = \bar{\Omega}^2\, ds^2_{S^1\times H^3}, \quad ds^2_{AdS_3\times S^1} = \Omega^2\, ds^2_{S^1\times H^3} \tag{B.3.2}$$

where

$$\bar{\Omega} = (\cosh\rho + \cos(\tau/R))^{-1}, \quad \Omega = (R\sinh\rho\sin\vartheta)^{-1} \tag{B.3.3}$$

The coordinate maps corresponding to these three transformations are given by

$$\begin{aligned}
AdS_3\times S^1 \text{ to spherical:} &\quad l = x\cos\vartheta, \quad z = x\sin\vartheta \\
\text{spherical to hyperboloid:} &\quad t = R\,\bar{\Omega}\sin(\tau/R), \quad x = R\,\bar{\Omega}\sinh\rho \\
AdS_3\times S^1 \text{ to hyperboloid:} &\quad t = R\,\bar{\Omega}\sin(\tau/R), \quad l = R\,\bar{\Omega}\sinh\rho\cos\vartheta, \quad z = R\,\bar{\Omega}\sinh\rho\sin\vartheta
\end{aligned} \tag{B.3.4}$$

where the last transformation comes from combining the first two.

For easy reference we quote the location Σ of the surface defect and the location $\partial\mathcal{A}$ of the entangling surface in the various coordinate charts:

	Σ	$\partial\mathcal{A}$
$AdS_3\times S^1$	fills t, fills $l, z=0$	$t=0, l^2+z^2=R^2$
spherical	fills t, fills $x, \vartheta=0,\pi$	$t=0, x=R$
hyperboloid	fills τ, fills $\rho, \vartheta=0,\pi$	$\rho\to\infty$

It can be seen, in all coordinate charts, that the surface defect intersects the entangling surface exactly at two points.

B.4 Asymptotic expansion comparison with [1]

For calculating holographic observables one has to expand the supergravity solution in an asymptotic form. In this section we quote the way the asymptotic expansion was performed in [1] and compare with ours.

Defining $\Phi = f/y$ the equation for f, (3.2.3), can be written as the six-dimensional Laplace equation for Φ with $SO(4)$ invariant sources. In [1] the authors write Φ as the vacuum part and a deviation:

$$\Phi = \Phi^{(0)} + \Delta\Phi \tag{B.4.1}$$

Then, they expand the deviation $\Delta\Phi$ in $SO(4)$-invariant spherical harmonics. The coefficients of this expansion are denoted by $\Delta\Phi_{\Delta,k}$, where Δ, k are eigenvalues characterizing the spherical harmonics (for more details on the spherical harmonics see appendix A in [1]).

As an example, we quote their result for the one-point function of the stress tensor which was found using holography:

$$\langle T_{\mu\nu}\rangle_\Sigma \, dx^\mu dx^\nu = \frac{N^2}{2\pi^2}\left(\frac{1}{16} - \frac{1}{12\sqrt{3}}\,\Delta\Phi_{2,0}\right)\left(ds^2_{AdS_3} - 3\,d\psi^2\right) \tag{B.4.2}$$

One can see that this matches (3.4.21, 3.4.22), when a definition for $\Delta\Phi_{2,0}$ is given in terms of the moments. For completeness we give all the coefficients corresponding to spherical harmonics with eigenvalue $\Delta = 2$ in terms of the moments:

$$\begin{aligned}\Delta\Phi_{2,0} &= 4\sqrt{3}\left(m_{220} + m_{202} + \frac{1 - m_{400}}{2}\right)\\ \Delta\Phi_{2,\pm 2} &= 6e^{\mp 2i\psi}\left(m_{220} - m_{202} \pm 2i m_{211}\right)\end{aligned} \tag{B.4.3}$$

B.5 Holographic expectation value

In this appendix we compute the integrals involved in the expectation value of the surface defect (3.4.1). Specifically, these are the bulk contribution given in (3.4.6) and the Gibbons-Hawking term in (3.4.4).

B.5.1 Bulk term

Let us start with the evaluation of the bulk term. The method described in [110, 111] led us to (3.4.11) the integrand of which we expressed as (3.4.13). We begin with carrying out the integration over AdS_3, S^3 and S^1, which is trivial. Then, the bulk term can be expressed in terms of two integrals over the base space X:

$$S_{\text{IIB,bulk}} = -\frac{4}{\kappa^2}\,\text{Vol}\,(AdS_3)\,\text{Vol}\left(S^3\right)\text{Vol}\left(S^1\right)\left[-\frac{1}{2}\,J_1 + J_2\right] \tag{B.5.1}$$

where we have defined:

$$J_1 = \int_X dx_1\,dx_2\,dy\,fy \tag{B.5.2}$$

$$J_2 = \int_X dx_1\,dx_2\,dy\,\partial_I u_I \tag{B.5.3}$$

Making use of the integral (3.3.7) appearing in the entanglement entropy calculation we can write

$$J_1 = \int_X dx_1\,dx_2\,dy\,\left[\left(f-\frac{1}{2}\right)y + \frac{1}{2}\,y\right] \tag{B.5.4}$$

$$= \frac{\pi}{4\varepsilon^2} + \frac{\pi}{24}\left[1 - 4\left(m_{220}+m_{202}+m_{400}\right)\right] + \frac{1}{2}\int_X dx_1\,dx_2\,dy\,y \tag{B.5.5}$$

where we have dropped terms that vanish as $\varepsilon \to 0$. The integral in the second line can be

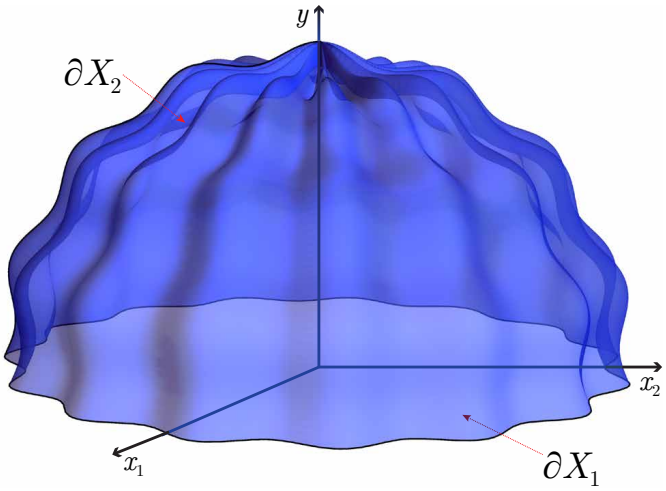

Figure B.1: The base space X boundary components: the blue wiggled dome noted as ∂X_2 is the large ρ cut-off and the lowest flat surface noted as ∂X_1 is the boundary at the x_1, x_2 plane.

evaluated directly by changing to $\{\rho, \theta, \alpha\}$ coordinates (the relevant map is given in (3.2.11)):

$$\begin{aligned}\int_X dx_1\, dx_2\, dy\, y &= \int d\rho\, d\theta\, d\alpha\, \rho \left(\rho^2 + \sin^2\theta\right) \cos\theta \sin\theta \\ &= \int_0^{\pi/2} d\theta \int_0^{2\pi} d\alpha\ \frac{1}{4}\rho^2 \left(\rho^2 + 2\sin^2\theta\right) \cos\theta \sin\theta \Big|_0^{\rho_c(\varepsilon,\theta,\alpha)} \\ &= \frac{\pi}{4\varepsilon^4} + \frac{\pi}{16\varepsilon^2}\left(1 + 2m_{220} + 2m_{202} - m_{400}\right) + Y_1 \end{aligned} \tag{B.5.6}$$

where the term Y_1 reads:

$$\begin{aligned} Y_1 \equiv \frac{\pi}{768}\big[&-7 + 12m_{220} + 12m_{202} - 6m_{400} \\ &- 288\left(m_{220}^2 + m_{202}^2\right) + 144 m_{220} m_{202} - 720 m_{211}^2 + 108\left(m_{220} + m_{202}\right) m_{400} - 27 m_{400}^2 \\ &+48\left(m_{240} + m_{204}\right) + 96\left(m_{222} - m_{402} - m_{420}\right) + 16 m_{600}\big] \end{aligned} \tag{B.5.7}$$

Next we evaluate J_2 by turning it into an integral over the boundary of X. Switching to

covariant notation in which g_{IJ} is a metric on X we have

$$J_2 = \int_X d^3x\,\sqrt{g}\,\nabla_I\,u^I \tag{B.5.8}$$

$$= \int_{\partial X} d^2x\,\sqrt{\gamma}\,n_I\,u^I \tag{B.5.9}$$

where n is the outward-pointing unit normal vector and γ the induced metric on ∂X. This surface consists of two components (see figure B.1):

$$\partial X_1 = \left\{\,(x_1, x_2, y)|\, y = 0, x_1^2 + x_2^2 \leq \rho_c(\varepsilon, \pi/2, \alpha)^2\right\} \tag{B.5.10}$$

$$\partial X_2 = \left\{\,(\rho, \theta, \alpha)|\, \rho = \rho_c(\varepsilon, \theta, \alpha), \theta \in [0, \pi/2], \alpha \in [0, 2\pi]\right\} \tag{B.5.11}$$

The contribution to J_2 from ∂X_1 vanishes. This can be easily seen by expanding (3.4.12) for small y and take the $y \to 0$ limit. For the remaining contribution we work in $\{\rho, \theta, \alpha\}$ coordinates. The metric on X is

$$ds_X^2 = \frac{\rho^2 + \sin^2\theta}{\rho^2 + 1}\,d\rho^2 + \left(\rho^2 + \sin^2\theta\right)d\theta^2 + \rho^2\sin^2\theta\,d\alpha^2 \tag{B.5.12}$$

The unit vector normal to the surface $\rho - \rho_c(\varepsilon, \theta, \alpha) = 0$ has the following components in this chart:

$$n_\rho = \frac{1}{\mathcal{D}}, \quad n_\theta = -\frac{\partial_\theta\rho_c(\varepsilon, \theta, \alpha)}{\mathcal{D}}, \quad n_\alpha = -\frac{\partial_\alpha\rho_c(\varepsilon, \theta, \alpha)}{\mathcal{D}} \tag{B.5.13}$$

$$\mathcal{D} \equiv \sqrt{\frac{[\partial_\alpha\rho_c(\varepsilon, \theta, \alpha)]^2}{\rho^2\sin^2\theta} + \frac{\rho^2 + 1 + [\partial_\theta\rho_c(\varepsilon, \theta, \alpha)]^2}{\rho^2 + \sin^2\theta}} \tag{B.5.14}$$

The induced metric and pullback components are given by

$$\gamma_{ab} = g_{IJ}\,e_a^I\,e_b^J \quad \text{with} \quad e_a^I = \begin{pmatrix} \partial_\theta\rho_c(\varepsilon, \theta, \alpha) & \partial_\alpha\rho_c(\varepsilon, \theta, \alpha) \\ 1 & 0 \\ 0 & 1 \end{pmatrix} \tag{B.5.15}$$

where $a \in \{\theta, \alpha\}$. We are now ready to evaluate J_2:

$$\begin{aligned} J_2 &= \int_0^{\pi/2} d\theta \int_0^{2\pi} d\alpha \, \sqrt{\gamma} \, \frac{y^3}{4\,(4f^2-1)} \, g^{IJ} \, n_I \, \partial_J f \\ &= -\frac{\pi}{16\varepsilon^4} + \frac{\pi}{64\varepsilon^2} \left(1 + 2m_{220} + 2m_{202} - m_{400}\right) + Y_2 \end{aligned} \tag{B.5.16}$$

where

$$\begin{aligned} Y_2 \equiv \frac{\pi}{3072} \, [&-51 - 100m_{220} - 100m_{202} + 50m_{400} \\ &+ 72\left(m_{220}^2 + m_{202}^2\right) + 144m_{211}^2 - 36\left(m_{220} + m_{202}\right) m_{400} + 9m_{400}^2 \\ &+48\left(m_{240} + m_{204}\right) + 96\left(m_{222} - m_{402} - m_{420}\right) + 16m_{600}] \end{aligned} \tag{B.5.17}$$

Putting everything together we get

$$S_{\text{IIB,bulk}} = \frac{\pi}{2\kappa^2} \, \text{Vol}\left(AdS_3\right) \text{Vol}\left(S^3\right) \text{Vol}\left(S^1\right) \left[\frac{1}{\varepsilon^4} + \frac{1}{\varepsilon^2} + \frac{3}{8} - m_{400} + \frac{2}{\pi}\left(Y_1 - 4Y_2\right)\right] \tag{B.5.18}$$

Plugging in the explicit expressions for Y_1 and Y_2 we notice that the moments of weight six drop out. The result is given in (3.4.14, 3.4.15).

B.5.2 Gibbons-Hawking term

To compute the Gibbons-Hawking term (3.4.4) we use a similar method to that used in the previous subsection for the total derivative on X, but now in the full ten-dimensional spacetime. The unit vector normal to the surface $\rho - \rho_c(\varepsilon, \theta, \alpha) = 0$ has the following non-trivial components

$$n_\rho = \frac{1}{\mathcal{D}\sqrt{\frac{2y}{\sqrt{4f^2-1}}}}, \quad n_\theta = -\frac{\partial_\theta \rho_c(\varepsilon,\theta,\alpha)}{\mathcal{D}\sqrt{\frac{2y}{\sqrt{4f^2-1}}}}, \quad n_\alpha = -\frac{\partial_\alpha \rho_c(\varepsilon,\theta,\alpha)}{\mathcal{D}\sqrt{\frac{2y}{\sqrt{4f^2-1}}}} \tag{B.5.19}$$

where $\mathcal{D}$ is defined in (B.5.14). The induced metric and non-trivial pullback components are given by

$$\gamma_{ab} = g_{MN}\, e_a^M\, e_b^N \tag{B.5.20}$$

$$e_\theta^\rho = \partial_\theta \rho_c(\varepsilon,\theta,\alpha), \quad e_\alpha^\rho = \partial_\alpha \rho_c(\varepsilon,\theta,\alpha), \quad e_b^a = \delta_b^a \tag{B.5.21}$$

where now a runs over all coordinates except ρ. The extrinsic curvature can be computed from the Lie derivative along n:

$$K_{ab} = \frac{1}{2}\left(\mathcal{L}_n\, g\right)_{MN} e_a^M\, e_b^N \tag{B.5.22}$$

$$= \frac{1}{2}\left(n^P\, \partial_P g_{MN} + g_{PN}\, \partial_M n^P + g_{MP}\, \partial_N n^P\right) e_a^M\, e_b^N \tag{B.5.23}$$

and its trace is simply $K \equiv \gamma^{ab}\, K_{ab}$ (whose small ε expansion leads with order 4). The result is

$$S_{\rm GH} = \frac{\pi}{2\kappa^2}\, \mathrm{Vol}\left(AdS_3\right) \mathrm{Vol}\left(S^3\right) \mathrm{Vol}\left(S^1\right) \left(\frac{4}{\varepsilon^4} + \frac{1}{\varepsilon^2}\right) \tag{B.5.24}$$

The moments appearing in the boundary integrand drop out when the integration over the angles $\{\theta, \alpha\}$ is performed.

Note that there is in principle a contribution from the other component of the boundary at $y = 0$, but again this vanishes. Specifically, expanding the Gibbons-Hawking integrand for small y we get $\sqrt{\gamma}\, K = O\left(y^2\right)$ which vanishes in the $y \to 0$ limit.

Appendix C

5d SCFTs Calculations

C.1 Type IIB on-shell action as boundary term

To recall how the type IIB supergravity action can be written as a boundary term on-shell, we start from the action in the form [133]

$$S_{\text{IIB}} = \frac{1}{2\kappa^2}\int d^{10}x\sqrt{-g}\left(R - \frac{\partial_\mu\bar{\tau}\partial^\mu\tau}{2\left(\text{Im}\tau\right)^2} - \frac{\mathcal{M}_{ij}}{2}F_3^i\cdot F_3^j - \frac{1}{4}|\tilde{F}_5|^2\right) - \frac{\epsilon_{ij}}{8\kappa^2}\int C_4\wedge F_3^i\wedge F_3^j\ , \tag{C.1.1}$$

where the dot product is defined as $Q_p\cdot F_p = \frac{1}{p!}g^{\mu_1\nu_1}...g^{\mu_p\nu_p}Q_{\mu_1...\mu_p}F_{\nu_1...\nu_p}$ and $\kappa^2 = 8\pi G_{\text{N}}$ with Newton's constant G_{N}. In the main part we will not use the short hand κ^2 to avoid confusion with the composite quantity defined in (4.1.3). The field strengths are defined as

$$F_3^i = dC_2^i\ , \qquad F_5 = dC_4\ , \qquad \tilde{F}_5 = F_5 - \frac{1}{2}C_2^2\wedge F_3^1 + \frac{1}{2}C_2^1\wedge F_3^2, \tag{C.1.2}$$

with $i = 1, 2$ where $i = 1$ and $i = 2$ correspond to the NS-NS and R-R 2-forms, respectively. The 2×2 matrix $\mathcal{M}$ is given by

$$\mathcal{M}_{ij} = \frac{1}{\mathrm{Im}\tau} \begin{bmatrix} |\tau|^2 & -\mathrm{Re}\tau \\ -\mathrm{Re}\tau & 1 \end{bmatrix} . \tag{C.1.3}$$

As shown in [66], on-shell this action reduces to a boundary term. For $C_4 = 0$, which applies for all configurations considered here, this boundary term reduces to

$$S_{\mathrm{IIB}} = \frac{1}{2\kappa^2} \int d\left(-\frac{1}{4} \mathcal{M}_{ij} C_2^i \wedge \star F_3^j \right) . \tag{C.1.4}$$

To translate this expression to our conventions for the supergravity fields, we combine the two real 2-forms C_2^i into one complex 2-form, $C_2 = C_2^1 + iC_2^2$, with field strength $F_3 = dC_2$, and redefine the fields as follows,

$$B = \frac{1 + i\tau}{1 - i\tau} , \qquad\qquad f^2 = \left(1 - |B|^2\right)^{-1} . \tag{C.1.5}$$

In terms of f, B and C_2, and eliminating κ^2 in favor of G_{N}, the boundary term (C.1.4) becomes

$$\begin{aligned} S_{\mathrm{IIB}} = -\frac{1}{64\pi G_{\mathrm{N}}} \int d\Big(& \frac{1}{2} f^2 (1 + |B|^2) \left(\bar{C}_2 \wedge \star dC_2 + C_2 \wedge \star d\bar{C}_2 \right) \\ & - f^2 \bar{B} C_2 \wedge \star dC_2 - f^2 B \bar{C}_2 \wedge \star d\bar{C}_2 \Big) . \end{aligned} \tag{C.1.6}$$

For the configurations we are interested in, there is no non-trivial dependence on the AdS_6 coordinates. We can therefore Wick rotate between Lorentzian and Euclidean signature purely within the AdS_6 part, which only enters through the volume form and at most accounts for a sign in the on-shell action. That sign can be fixed directly in Euclidean signature, where we want $\mathcal{Z} = \int Dg \exp(-S)$ with S positive semi-definite, such that $F = -\ln \mathcal{Z}$

is non-negative. For AdS there are the usual subtleties with divergences and holographic renormalization, and we will discuss this in more detail in app. C.2. We will demand the leading divergent term in the regularized free energy to be positive, and this corresponds to

$$S^{\mathrm{E}}_{\mathrm{IIB}} = \frac{1}{64\pi G_{\mathrm{N}}} \int d \left(\frac{1}{2} f^2 (1 + |B|^2)\, \bar{C}_2 \wedge \star dC_2 - f^2 \bar{B} C_2 \wedge \star dC_2 + \mathrm{c.c.} \right) \ . \tag{C.1.7}$$

C.2 Holographic renormalization

Holographic renormalization of the gravity theory on an asymptotically-AdS space becomes considerably more involved if the geometry does not reduce to a simple product form in the near-boundary limit. In general, the entire ten-dimensional geometry has to be considered with a nine-dimensional cut-off surface limiting the range of the radial coordinate in the asymptotic part of the geometry. There is a substantial amount of freedom in choosing this cut-off surface, which by the usual AdS/CFT lore corresponds to the freedom to choose a regularization scheme on the field theory side. In many cases one can restrict the choice of the cut-off surface by symmetry requirements. E.g., for $\mathrm{AdS}_5 \times \mathrm{S}^5$, one would require the cut-off surface to respect the S^5 isometries, which essentially reduces the problem of finding counterterms to the AdS_5 factor. For our geometries the analogous symmetry argument restricts the location of the cut-off on the AdS_6 radial coordinate to be independent of the location on S^2. The dependence on the location on Σ, however, is not restricted by that requirement.

For definiteness, we will choose global coordinates on Euclidean AdS_6 such that the metric takes the form

$$g_{\mathrm{AdS}_6} = du^2 + \sinh u^2 g_{\mathrm{S}^5} \ , \tag{C.2.1}$$

with $u \in [0, \infty)$. The cut-off surface should provide an upper bound on the range of u. The perhaps most natural choice is to pick a small $\epsilon \in \mathbb{R}^+$ and require $u < \mathrm{arcsinh}(1/\epsilon)$. The cut-off surface is then the nine-dimensional surface defined by $u = \mathrm{arcsinh}(1/\epsilon)$. This regulator

is invariant under the isometries of the S^5 inside AdS_6 and under the isometries of S^2, corresponding to spacetime isometries and R-symmetry in the dual field theory, respectively. However, any cut-off surface of the form $u = \text{arcsinh}(1/\epsilon(w))$, with $\epsilon(w)$ small throughout Σ, satisfies these requirements as well, and we are indeed free to choose any of them.

The value of the regularized on-shell action will certainly depend on the choice of regulator, as it usually does. The freedom in choosing a cut-off surface is enhanced here compared to the simpler cases with highly symmetric bulk geometries (where the freedom essentially boils down to rescalings of the cut-off), but the fact that there is ambiguity is by no means a new feature of the solutions considered here. More importantly, after proper holographic renormalization the universal parts of any physical quantity considered still have to be independent of the choice of regulator. We can therefore pick the simplest one, where ϵ is constant over Σ, as long as we only ask for physically meaningful (universal) quantities.

Moreover, since we have an even-dimensional AdS space with odd-dimensional field theory, there are no finite counterterms from the metric sector: the volume form on AdS_6 scales like ϵ^{-5}, and all other covariant quantities constructed from the induced metric on the cut-off surface (including the GHY term) have an expansion in even powers of ϵ. That means the covariant boundary terms scale as odd powers of ϵ and do not produce finite contributions. We have not explicitly verified that this holds for the other fields as well, but since they are related by supersymmetry we expect the corresponding covariant counterterms to scale with odd powers of ϵ as well. There is therefore no ambiguity in choosing a renormalization scheme, and we can read off the universal part directly, e.g. as the finite part of the free energy, without going through the proper procedure of holographic renormalization.

With the cut-off $u < \text{arcsinh}(1/\epsilon)$, the holographic renormalization indeed reduces to a pure AdS_6 problem, with the regularized volume of AdS_6 given by

$$\text{Vol}_{AdS_6} = \text{Vol}_{S^5} \int_0^{\text{arcsinh}\,\frac{1}{\epsilon}} \sinh^5 u du = \text{Vol}_{S^5} \left(\frac{1}{5\epsilon^5} - \frac{1}{6\epsilon^3} + \frac{3}{8\epsilon} - \frac{8}{15} + \mathcal{O}(\epsilon) \right) . \qquad \text{(C.2.2)}$$

As argued above, the universal part can be extracted immediately and is given by

$$\mathrm{Vol}_{\mathrm{AdS}_6,\mathrm{ren}} = -\frac{8}{15}\,\mathrm{Vol}_{\mathrm{S}^5} \ . \tag{C.2.3}$$

Bibliography

[1] N. Drukker, J. Gomis, and S. Matsuura, "Probing N=4 SYM With Surface Operators," *JHEP* **10** (2008) 048, 0805.4199.

[2] S. A. Gentle, M. Gutperle, and C. Marasinou, "Entanglement entropy of Wilson surfaces from bubbling geometries in M-theory," *JHEP* **08** (2015) 019, 1506.00052.

[3] S. A. Gentle, M. Gutperle, and C. Marasinou, "Holographic entanglement entropy of surface defects," *JHEP* **04** (2016) 067, 1512.04953.

[4] M. Gutperle, C. Marasinou, A. Trivella, and C. F. Uhlemann, "Entanglement entropy vs. free energy in IIB supergravity duals for 5d SCFTs," *JHEP* **09** (2017) 125, 1705.01561.

[5] L. Susskind, "The World as a hologram," *J. Math. Phys.* **36** (1995) 6377–6396, hep-th/9409089.

[6] J. M. Maldacena, "The Large N limit of superconformal field theories and supergravity," *Int. J. Theor. Phys.* **38** (1999) 1113–1133, hep-th/9711200. [Adv. Theor. Math. Phys.2,231(1998)].

[7] G. 't Hooft, "A Planar Diagram Theory for Strong Interactions," *Nucl. Phys.* **B72** (1974) 461.

[8] J. D. Brown and M. Henneaux, "Central Charges in the Canonical Realization of Asymptotic Symmetries: An Example from Three-Dimensional Gravity," *Commun. Math. Phys.* **104** (1986) 207–226.

[9] D. A. Lowe and L. Thorlacius, "AdS / CFT and the information paradox," *Phys. Rev.* **D60** (1999) 104012, hep-th/9903237.

[10] A. Almheiri, D. Marolf, J. Polchinski, and J. Sully, "Black Holes: Complementarity or Firewalls?," *JHEP* **02** (2013) 062, 1207.3123.

[11] E. D'Hoker and D. Z. Freedman, "Supersymmetric gauge theories and the AdS / CFT correspondence," in *Strings, Branes and Extra Dimensions: TASI 2001: Proceedings*, pp. 3–158, 2002. hep-th/0201253.

[12] J. D. Bekenstein, "Black holes and entropy," *Phys. Rev.* **D7** (1973) 2333–2346.

[13] S. W. Hawking, "Particle Creation by Black Holes," *Commun. Math. Phys.* **43** (1975) 199–220. [,167(1975)].

[14] S. Ryu and T. Takayanagi, "Holographic derivation of entanglement entropy from AdS/CFT," *Phys. Rev. Lett.* **96** (2006) 181602, hep-th/0603001.

[15] S. Ryu and T. Takayanagi, "Aspects of Holographic Entanglement Entropy," *JHEP* **08** (2006) 045, hep-th/0605073.

[16] B. Swingle", "Entanglement renormalization and holography," *Physical Review D* **86** (2012), no. 6.

[17] M. Van Raamsdonk, "Comments on quantum gravity and entanglement," 0907.2939.

[18] M. Van Raamsdonk, "Building up spacetime with quantum entanglement," *Gen. Rel. Grav.* **42** (2010) 2323–2329, 1005.3035. [Int. J. Mod. Phys.D19,2429(2010)].

[19] J. Maldacena and L. Susskind, "Cool horizons for entangled black holes," *Fortsch. Phys.* **61** (2013) 781–811, 1306.0533.

[20] D. Harlow, "TASI Lectures on the Emergence of the Bulk in AdS/CFT," 1802.01040.

[21] D. Mateos, "String Theory and Quantum Chromodynamics," *Class. Quant. Grav.* **24** (2007) S713–S740, 0709.1523.

[22] S. A. Hartnoll, C. P. Herzog, and G. T. Horowitz, "Building a Holographic Superconductor," *Phys. Rev. Lett.* **101** (2008) 031601, 0803.3295.

[23] J. McGreevy, "Holographic duality with a view toward many-body physics," *Adv. High Energy Phys.* **2010** (2010) 723105, 0909.0518.

[24] J. D. Bekenstein, "A Universal Upper Bound on the Entropy to Energy Ratio for Bounded Systems," *Phys. Rev.* **D23** (1981) 287.

[25] R. Grimm, M. Sohnius, and J. Wess, "Extended Supersymmetry and Gauge Theories," *Nucl. Phys.* **B133** (1978) 275–284.

[26] O. Aharony, O. Bergman, D. L. Jafferis, and J. Maldacena, "N=6 superconformal Chern-Simons-matter theories, M2-branes and their gravity duals," *JHEP* **10** (2008) 091, 0806.1218.

[27] S. S. Gubser, I. R. Klebanov, and A. M. Polyakov, "Gauge theory correlators from noncritical string theory," *Phys. Lett.* **B428** (1998) 105–114, hep-th/9802109.

[28] E. Witten, "Anti-de Sitter space and holography," *Adv. Theor. Math. Phys.* **2** (1998) 253–291, hep-th/9802150.

[29] M. Henningson and K. Skenderis, "The Holographic Weyl anomaly," *JHEP* **07** (1998) 023, hep-th/9806087.

[30] S. de Haro, S. N. Solodukhin, and K. Skenderis, "Holographic reconstruction of space-time and renormalization in the AdS / CFT correspondence," *Commun. Math. Phys.* **217** (2001) 595–622, hep-th/0002230.

[31] K. Skenderis, "Lecture notes on holographic renormalization," *Class. Quant. Grav.* **19** (2002) 5849–5876, hep-th/0209067.

[32] J. L. Cardy, "Conformal Invariance and Surface Critical Behavior," *Nucl. Phys.* **B240** (1984) 514–532.

[33] D. M. McAvity and H. Osborn, "Conformal field theories near a boundary in general dimensions," *Nucl. Phys.* **B455** (1995) 522–576, cond-mat/9505127.

[34] E. D'Hoker, J. Estes, M. Gutperle, D. Krym, and P. Sorba, "Half-BPS supergravity solutions and superalgebras," *JHEP* **12** (2008) 047, 0810.1484.

[35] E. D'Hoker, J. Estes, and M. Gutperle, "Interface Yang-Mills, supersymmetry, and Janus," *Nucl. Phys.* **B753** (2006) 16–41, hep-th/0603013.

[36] A. Karch and L. Randall, "Locally localized gravity," *JHEP* **05** (2001) 008, hep-th/0011156. [,140(2000)].

[37] A. Karch and L. Randall, "Open and closed string interpretation of SUSY CFT's on branes with boundaries," *JHEP* **06** (2001) 063, hep-th/0105132.

[38] O. DeWolfe, D. Z. Freedman, and H. Ooguri, "Holography and defect conformal field theories," *Phys. Rev.* **D66** (2002) 025009, hep-th/0111135.

[39] E. D'Hoker, J. Estes, and M. Gutperle, "Exact half-BPS Type IIB interface solutions. I. Local solution and supersymmetric Janus," *JHEP* **06** (2007) 021, 0705.0022.

[40] E. D'Hoker, J. Estes, and M. Gutperle, "Exact half-BPS Type IIB interface solutions. II. Flux solutions and multi-Janus," *JHEP* **06** (2007) 022, 0705.0024.

[41] S. Gukov and E. Witten, "Gauge Theory, Ramification, And The Geometric Langlands Program," hep-th/0612073.

[42] J. Gomis and S. Matsuura, "Bubbling surface operators and S-duality," *JHEP* **06** (2007) 025, 0704.1657.

[43] H. Lin, O. Lunin, and J. M. Maldacena, "Bubbling AdS space and 1/2 BPS geometries," *JHEP* **10** (2004) 025, hep-th/0409174.

[44] O. J. Ganor, "Six-dimensional tensionless strings in the large N limit," *Nucl. Phys.* **B489** (1997) 95–121, hep-th/9605201.

[45] E. D'Hoker, J. Estes, M. Gutperle, and D. Krym, "Exact Half-BPS Flux Solutions in M-theory. I: Local Solutions," *JHEP* **08** (2008) 028, 0806.0605.

[46] E. D'Hoker, J. Estes, M. Gutperle, and D. Krym, "Exact Half-BPS Flux Solutions in M-theory II: Global solutions asymptotic to AdS(7) x S**4," *JHEP* **12** (2008) 044, 0810.4647.

[47] P. Calabrese and J. L. Cardy, "Entanglement entropy and quantum field theory," *J. Stat. Mech.* **0406** (2004) P06002, hep-th/0405152.

[48] T. Nishioka, S. Ryu, and T. Takayanagi, "Holographic Entanglement Entropy: An Overview," *J. Phys.* **A42** (2009) 504008, 0905.0932.

[49] T. Nishioka, "Entanglement entropy: holography and renormalization group," 1801.10352.

[50] H. Casini, M. Huerta, and R. C. Myers, "Towards a derivation of holographic entanglement entropy," *JHEP* **05** (2011) 036, 1102.0440.

[51] V. E. Hubeny, M. Rangamani, and T. Takayanagi, "A Covariant holographic entanglement entropy proposal," *JHEP* **07** (2007) 062, 0705.0016.

[52] S.-J. Rey and J.-T. Yee, "Macroscopic strings as heavy quarks in large N gauge theory and anti-de Sitter supergravity," *Eur. Phys. J.* **C22** (2001) 379–394, hep-th/9803001.

[53] J. M. Maldacena, "Wilson loops in large N field theories," *Phys. Rev. Lett.* **80** (1998) 4859–4862, hep-th/9803002.

[54] J. Gomis and F. Passerini, "Holographic Wilson Loops," *JHEP* **08** (2006) 074, hep-th/0604007.

[55] J. Gomis and F. Passerini, "Wilson Loops as D3-Branes," *JHEP* **01** (2007) 097, hep-th/0612022.

[56] H.-C. Chang and A. Karch, "Entanglement Entropy for Probe Branes," *JHEP* **01** (2014) 180, 1307.5325.

[57] K. Jensen and A. O'Bannon, "Holography, Entanglement Entropy, and Conformal Field Theories with Boundaries or Defects," *Phys. Rev.* **D88** (2013), no. 10 106006, 1309.4523.

[58] J. Estes, K. Jensen, A. O'Bannon, E. Tsatis, and T. Wrase, "On Holographic Defect Entropy," *JHEP* **05** (2014) 084, 1403.6475.

[59] E. D'Hoker, J. Estes, and M. Gutperle, "Gravity duals of half-BPS Wilson loops," *JHEP* **06** (2007) 063, 0705.1004.

[60] O. Lunin, "On gravitational description of Wilson lines," *JHEP* **06** (2006) 026, hep-th/0604133.

[61] S. Yamaguchi, "Bubbling geometries for half BPS Wilson lines," *Int. J. Mod. Phys.* **A22** (2007) 1353–1374, hep-th/0601089.

[62] A. Lewkowycz and J. Maldacena, "Exact results for the entanglement entropy and the energy radiated by a quark," *JHEP* **05** (2014) 025, 1312.5682.

[63] V. Pestun, "Localization of gauge theory on a four-sphere and supersymmetric Wilson loops," *Commun. Math. Phys.* **313** (2012) 71–129, 0712.2824.

[64] A. Kapustin, B. Willett, and I. Yaakov, "Exact Results for Wilson Loops in Superconformal Chern-Simons Theories with Matter," *JHEP* **03** (2010) 089, 0909.4559.

[65] S. A. Gentle and M. Gutperle, "Entanglement entropy of Wilson loops: Holography and matrix models," *Phys. Rev.* **D90** (2014), no. 6 066011, 1407.5629.

[66] T. Okuda and D. Trancanelli, "Spectral curves, emergent geometry, and bubbling solutions for Wilson loops," *JHEP* **09** (2008) 050, 0806.4191.

[67] J. Gomis, S. Matsuura, T. Okuda, and D. Trancanelli, "Wilson loop correlators at strong coupling: From matrices to bubbling geometries," *JHEP* **08** (2008) 068, 0807.3330.

[68] E. Witten, "Some comments on string dynamics," in *Future perspectives in string theory. Proceedings, Conference, Strings'95, Los Angeles, USA, March 13-18, 1995*, pp. 501–523, 1995. hep-th/9507121.

[69] A. Strominger, "Open p-branes," *Phys. Lett.* **B383** (1996) 44–47, hep-th/9512059.

[70] D. E. Berenstein, R. Corrado, W. Fischler, and J. M. Maldacena, "The Operator product expansion for Wilson loops and surfaces in the large N limit," *Phys. Rev.* **D59** (1999) 105023, hep-th/9809188.

[71] R. Corrado, B. Florea, and R. McNees, "Correlation functions of operators and Wilson surfaces in the d = 6, (0,2) theory in the large N limit," *Phys. Rev.* **D60** (1999) 085011, hep-th/9902153.

[72] B. Chen, W. He, J.-B. Wu, and L. Zhang, "M5-branes and Wilson Surfaces," *JHEP* **08** (2007) 067, 0707.3978.

[73] B. Chen and J.-B. Wu, "Wilson-Polyakov surfaces and M-theory branes," *JHEP* **05** (2008) 046, 0802.2173.

[74] H. Mori and S. Yamaguchi, "M5-branes and Wilson surfaces in AdS_7/CFT_6 correspondence," *Phys. Rev.* **D90** (2014), no. 2 026005, 1404.0930.

[75] O. Lunin, "1/2-BPS states in M theory and defects in the dual CFTs," *JHEP* **10** (2007) 014, 0704.3442.

[76] D. Bak, M. Gutperle, and S. Hirano, "A Dilatonic deformation of AdS(5) and its field theory dual," *JHEP* **05** (2003) 072, hep-th/0304129.

[77] C. Bachas, E. D'Hoker, J. Estes, and D. Krym, "M-theory Solutions Invariant under $D(2,1;\gamma) \oplus D(2,1;\gamma)$," *Fortsch. Phys.* **62** (2014) 207–254, 1312.5477.

[78] K. Skenderis and M. Taylor, "Kaluza-Klein holography," *JHEP* **05** (2006) 057, hep-th/0603016.

[79] K. Pilch, P. van Nieuwenhuizen, and P. K. Townsend, "Compactification of $d = 11$ Supergravity on S(4) (Or $11 = 7 + 4$, Too)," *Nucl. Phys.* **B242** (1984) 377–392.

[80] P. van Nieuwenhuizen, "The Complete Mass Spectrum of $d = 11$ Supergravity Compactified on S(4) and a General Mass Formula for Arbitrary Cosets M(4)," *Class. Quant. Grav.* **2** (1985) 1.

[81] M. Gunaydin, P. van Nieuwenhuizen, and N. P. Warner, "General Construction of the Unitary Representations of Anti-de Sitter Superalgebras and the Spectrum of the S**4 Compactification of Eleven-dimensional Supergravity," *Nucl. Phys.* **B255** (1985) 63–92.

[82] R. G. Leigh and M. Rozali, "The Large N limit of the (2,0) superconformal field theory," *Phys. Lett.* **B431** (1998) 311–316, hep-th/9803068.

[83] P. Kraus, F. Larsen, and R. Siebelink, "The gravitational action in asymptotically AdS and flat space-times," *Nucl. Phys.* **B563** (1999) 259–278, hep-th/9906127.

[84] C. R. Graham and E. Witten, "Conformal anomaly of submanifold observables in AdS / CFT correspondence," *Nucl. Phys.* **B546** (1999) 52–64, hep-th/9901021.

[85] M. Henningson and K. Skenderis, "Weyl anomaly for Wilson surfaces," *JHEP* **06** (1999) 012, hep-th/9905163.

[86] A. Gustavsson, "Conformal anomaly of Wilson surface observables: A Field theoretical computation," *JHEP* **07** (2004) 074, hep-th/0404150.

[87] A. Kapustin and E. Witten, "Electric-Magnetic Duality And The Geometric Langlands Program," *Commun. Num. Theor. Phys.* **1** (2007) 1–236, hep-th/0604151.

[88] S. Gukov and E. Witten, "Rigid Surface Operators," *Adv. Theor. Math. Phys.* **14** (2010), no. 1 87–178, 0804.1561.

[89] H. Lin and J. M. Maldacena, "Fivebranes from gauge theory," *Phys. Rev.* **D74** (2006) 084014, hep-th/0509235.

[90] A. Lewkowycz and J. Maldacena, "Generalized gravitational entropy," *JHEP* **08** (2013) 090, 1304.4926.

[91] A. Karch and C. F. Uhlemann, "Generalized gravitational entropy of probe branes: flavor entanglement holographically," *JHEP* **05** (2014) 017, 1402.4497.

[92] C. Holzhey, F. Larsen, and F. Wilczek, "Geometric and renormalized entropy in conformal field theory," *Nucl. Phys.* **B424** (1994) 443–467, hep-th/9403108.

[93] N. R. Constable, J. Erdmenger, Z. Guralnik, and I. Kirsch, "Intersecting D-3 branes and holography," *Phys. Rev.* **D68** (2003) 106007, hep-th/0211222.

[94] A. Gadde and S. Gukov, "2d Index and Surface operators," *JHEP* **03** (2014) 080, 1305.0266.

[95] B. McClain, F. Yu, and Y. S. Wu, "Covariant quantization of chiral bosons and OSp(1,1—2) symmetry," *Nucl. Phys.* **B343** (1990) 689–704.

[96] C. Wotzasek, "The Wess-Zumino term for chiral bosons," *Phys. Rev. Lett.* **66** (1991) 129–132.

[97] I. Martin and A. Restuccia, "Duality symmetric actions and canonical quantization," *Phys. Lett.* **B323** (1994) 311–315.

[98] F. P. Devecchi and M. Henneaux, "Covariant path integral for chiral p forms," *Phys. Rev.* **D54** (1996) 1606–1613, hep-th/9603031.

[99] I. Bengtsson and A. Kleppe, "On chiral p forms," *Int. J. Mod. Phys.* **A12** (1997) 3397–3412, hep-th/9609102.

[100] N. Berkovits, "Manifest electromagnetic duality in closed superstring field theory," *Phys. Lett.* **B388** (1996) 743–752, hep-th/9607070.

[101] N. Berkovits, "Local actions with electric and magnetic sources," *Phys. Lett.* **B395** (1997) 28–35, hep-th/9610134.

[102] P. Pasti, D. P. Sorokin, and M. Tonin, "On Lorentz invariant actions for chiral p forms," *Phys. Rev.* **D55** (1997) 6292–6298, hep-th/9611100.

[103] G. Dall'Agata, K. Lechner, and D. P. Sorokin, "Covariant actions for the bosonic sector of d = 10 IIB supergravity," *Class. Quant. Grav.* **14** (1997) L195–L198, hep-th/9707044.

[104] G. Dall'Agata, K. Lechner, and M. Tonin, "D = 10, N = IIB supergravity: Lorentz invariant actions and duality," *JHEP* **07** (1998) 017, hep-th/9806140.

[105] G. Dall'Agata, K. Lechner, and M. Tonin, "Action for IIB supergravity in 10-dimensions," hep-th/9812170. [Lect. Notes Phys.525,416(1999)].

[106] A. Sen, "Covariant Action for Type IIB Supergravity," *JHEP* **07** (2016) 017, 1511.08220.

[107] M. Henneaux and C. Teitelboim, "Dynamics of Chiral (Selfdual) P Forms," *Phys. Lett.* **B206** (1988) 650–654.

[108] J. H. Schwarz and A. Sen, "Duality symmetric actions," *Nucl. Phys.* **B411** (1994) 35–63, hep-th/9304154.

[109] D. M. Belov and G. W. Moore, "Type II Actions from 11-Dimensional Chern-Simons Theories," hep-th/0611020.

[110] S. B. Giddings, S. Kachru, and J. Polchinski, "Hierarchies from fluxes in string compactifications," *Phys. Rev.* **D66** (2002) 106006, hep-th/0105097.

[111] O. DeWolfe and S. B. Giddings, "Scales and hierarchies in warped compactifications and brane worlds," *Phys. Rev.* **D67** (2003) 066008, hep-th/0208123.

[112] K. Skenderis and M. Taylor, "Anatomy of bubbling solutions," *JHEP* **09** (2007) 019, 0706.0216.

[113] L.-Y. Hung, R. C. Myers, M. Smolkin, and A. Yale, "Holographic Calculations of Renyi Entropy," *JHEP* **12** (2011) 047, 1110.1084.

[114] W. Nahm, "Supersymmetries and their Representations," *Nucl. Phys.* **B135** (1978) 149.

[115] V. G. Kac, "Lie Superalgebras," *Adv. Math.* **26** (1977) 8–96.

[116] O. Aharony and A. Hanany, "Branes, superpotentials and superconformal fixed points," *Nucl. Phys.* **B504** (1997) 239–271, hep-th/9704170.

[117] O. Aharony, A. Hanany, and B. Kol, "Webs of (p,q) five-branes, five-dimensional field theories and grid diagrams," *JHEP* **01** (1998) 002, hep-th/9710116.

[118] O. DeWolfe, A. Hanany, A. Iqbal, and E. Katz, "Five-branes, seven-branes and five-dimensional E(n) field theories," *JHEP* **03** (1999) 006, hep-th/9902179.

[119] E. D'Hoker, M. Gutperle, A. Karch, and C. F. Uhlemann, "Warped $AdS_6 \times S^2$ in Type IIB supergravity I: Local solutions," *JHEP* **08** (2016) 046, 1606.01254.

[120] E. D'Hoker, M. Gutperle, and C. F. Uhlemann, "Holographic duals for five-dimensional superconformal quantum field theories," *Phys. Rev. Lett.* **118** (2017), no. 10 101601, 1611.09411.

[121] E. D'Hoker, M. Gutperle, and C. F. Uhlemann, "Warped $AdS_6 \times S^2$ in Type IIB supergravity II: Global solutions and five-brane webs," 1703.08186.

[122] Y. Lozano, E. Ó Colgáin, D. Rodríguez-Gómez, and K. Sfetsos, "Supersymmetric AdS_6 via T Duality," *Phys. Rev. Lett.* **110** (2013), no. 23 231601, 1212.1043.

[123] Y. Lozano, E. Ó Colgáin, and D. Rodríguez-Gómez, "Hints of 5d Fixed Point Theories from Non-Abelian T-duality," *JHEP* **05** (2014) 009, 1311.4842.

[124] F. Apruzzi, M. Fazzi, A. Passias, D. Rosa, and A. Tomasiello, "AdS_6 solutions of type II supergravity," *JHEP* **11** (2014) 099, 1406.0852. [Erratum: JHEP05,012(2015)].

[125] H. Kim, N. Kim, and M. Suh, "Supersymmetric AdS_6 Solutions of Type IIB Supergravity," *Eur. Phys. J.* **C75** (2015), no. 10 484, 1506.05480.

[126] H. Kim and N. Kim, "Comments on the symmetry of AdS_6 solutions in String/M-theory and Killing spinor equations," 1604.07987.

[127] J. B. Gutowski and G. Papadopoulos, "On supersymmetric AdS6 solutions in 10 and 11 dimensions," 1702.06048.

[128] J. H. Schwarz, "Covariant Field Equations of Chiral N=2 D=10 Supergravity," *Nucl. Phys.* **B226** (1983) 269.

[129] P. S. Howe and P. C. West, "The Complete N=2, D=10 Supergravity," *Nucl. Phys.* **B238** (1984) 181–220.

[130] D. L. Jafferis and S. S. Pufu, "Exact results for five-dimensional superconformal field theories with gravity duals," *JHEP* **05** (2014) 032, 1207.4359.

[131] F. Benini, S. Benvenuti, and Y. Tachikawa, "Webs of five-branes and N=2 superconformal field theories," *JHEP* **09** (2009) 052, 0906.0359.

[132] J. Källén, J. Qiu, and M. Zabzine, "The perturbative partition function of supersymmetric 5D Yang-Mills theory with matter on the five-sphere," *JHEP* **08** (2012) 157, 1206.6008.

[133] J. Polchinski, *String theory. Vol. 2: Superstring theory and beyond*. Cambridge University Press, 2007.